2011

The Geological Society of America
Field Guide 24
2011

Structural geology of the subprovince boundaries in the Archean Superior Province of northern Minnesota and adjacent Ontario

Robert L. Bauer*
Department of Geological Sciences, University of Missouri, Columbia, Missouri 65211, USA

Dyanna M. Czeck*
Department of Geosciences, University of Wisconsin–Milwaukee, P.O. Box 413, Milwaukee, Wisconsin 53201, USA

Peter J. Hudleston*
Department of Earth Sciences, University of Minnesota, Minneapolis, Minnesota 55455, USA

Basil Tikoff*
Department of Geoscience, University of Wisconsin–Madison, 1215 W. Dayton Street, Madison, Wisconsin 53706, USA

ABSTRACT

The geometric, kinematic, and deformational features along the subprovince boundaries of the Archean Superior Province are keys to understanding the tectonic amalgamation of the province. This field trip investigates the structural geology along two of the subprovince boundaries—the Wabigoon-Quetico and Quetico-Vermilion—of the Superior Craton. These boundaries separate the relatively high-grade gneisses of the Quetico Belt from typical low-grade granite-greenstone terranes to its north (Wabigoon) and south (Wawa). Both boundaries are characterized by different styles of transpressional deformation and strike-slip tectonism. Along the Wabigoon-Quetico boundary, deformation is recorded by a variety of structures controlled by competence contrast of heterogeneous lithologies at a variety of scales: from weak greenstones surrounding more competent gneiss domes to deformed polymictic conglomerates. Along the Quetico-Vermilion boundary, we will emphasize the role of plutonism and pluton geometry on subsequent deformation. Lastly, we characterize multiple deformation episodes in the Vermilion district in Minnesota.

*Bauer—BauerR@missouri.edu; Czeck—dyanna@uwm.edu; Hudleston—hudle001@umn.edu; corresponding author, Tikoff—basil@geology.wisc.edu.

Bauer, R.L., Czeck, D.M., Hudleston, P.J., Tikoff, B., 2011, Structural geology of the subprovince boundaries in the Archean Superior Province of northern Minnesota and adjacent Ontario, *in* Miller, J.D., Hudak, G.J., Wittkop, C., and McLaughlin, P.I., eds., Archean to Anthropocene: Field Guides to the Geology of the Mid-Continent of North America: Geological Society of America Field Guide 24, p. 203–241, doi:10.1130/2011.0024(10).

GEOLOGIC SETTING

The Superior Province (Fig. 1) is the largest contiguous Archean terrane in the world. It is almost exclusively composed of Archean rocks with only minor Proterozoic dike swarms and Proterozoic or Phanerozoic cover. The Superior Province was, by and large, stabilized crust by the end of the Archean, affected to only a minor extent by Proterozoic deformation along its boundaries and internally by the Kapuskasing uplift zone. The central part of the Superior Province remained unaffected by post-Archean deformation, making it an important region for the study of middle to late Archean deformation and tectonic processes.

The Superior Province can be divided into subprovinces on the basis of lithostratigraphy, structural boundaries, and metamorphic grade (e.g., Card and Ciesielski, 1986; Percival et al., 2006; Percival and Helmstaedt, 2006). The subprovinces are generally of three types: granite-greenstone (volcanic-plutonic), metasedimentary, and high-grade gneiss. On this trip, we will investigate a part of the central Superior Province, which consists of approximately east-west–trending alternating bands of greenstone subprovinces (containing both metavolcanic and plutonic rocks) and relatively high-grade metasedimentary subprovinces.

The subprovinces were likely assembled by repeated island arc–microcontinent collisions. Several pieces of evidence are consistent with the island-arc accretion model. First, the rocks can be interpreted as arc sequence subprovinces (metavolcanic rocks of the greenstone belts) and their corresponding accretionary prism subprovinces (metasedimentary rocks) (Langford and Morin, 1976; Hoffman, 1989; Percival and Williams, 1989; Card, 1990; Hoffman, 1990). Second, the ages in the greenstone belts are generally similar along strike but differ systematically across strike (Hoffman, 1989). Third, the deformation characteristics found across the province are best explained by contractional deformation. With all evidence, a history of subduction and overall accretion against an evolving tectonic margin to the north was likely responsible for the juxtaposition of Superior Province subprovinces (Langford and Morin, 1976; Percival and Williams, 1989; Card, 1990; Percival et al., 2006).

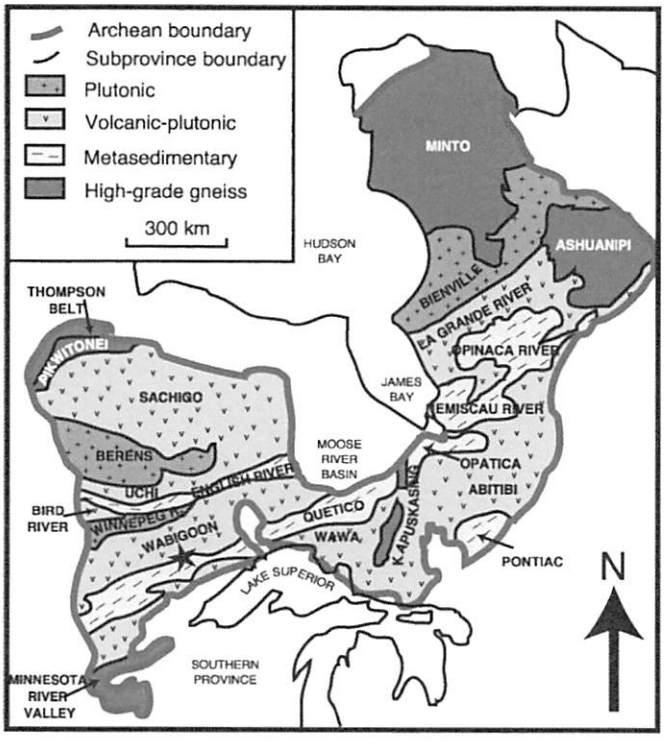

Figure 1. Map of Superior Province, based on divisions by Card and Ciesielski (1986).

On this trip, we will observe structures formed at two of the subprovince boundaries: the boundaries between the Quetico metasedimentary subprovince and its neighboring greenstone belts, the Wabigoon to the north and the Wawa to the south. Throughout the Superior Province, subprovince boundaries are commonly faulted or at least unconformable. The Wabigoon-Quetico and Quetico-Wawa boundaries are zones with localized deformation and major strike-slip features. Oblique collision between the Wabigoon and Wawa volcanic-plutonic terranes during the Neoarchean ca. 2.69–2.7 Ga (Stockwell, 1982; Davis et al., 1989; Fralick and Davis, 1999) most likely formed the tectono-metamorphic features of the two boundary zones (e.g., Poulsen, 1986; Percival and Williams, 1989). The metavolcanic granite-greenstone subprovinces (Wabigoon, Wawa) were island arcs that collided owing to ongoing subduction, and the metasedimentary subprovince (Quetico) is composed of sedimentary basin deposits between the arcs (Percival, 1989; Blackburn et al., 1991; Williams, 1991). We will view the Wabigoon-Quetico boundary in northwestern Ontario within the Rainy Lake District. Although most of the Superior Province lies in Canada, the Quetico metasedimentary subprovince and the Wawa volcanic-plutonic subprovince extend into northern Minnesota, and we will view their boundary along the Vermilion fault system within Minnesota's Vermilion District greenstone belt (Wawa subprovince) and adjacent regions of the Vermilion Granitic Complex (Quetico subprovince).

Rainy Lake Zone

The Rainy Lake District (Fig. 2) lies on the western part of the boundary between the Wabigoon granite-greenstone terrane to the north and the Quetico metasedimentary terrane to the south. The Quetico contains mostly amphibolite-facies metasedimentary rocks, and the Wabigoon contains mostly greenschist-facies metavolcanic rocks. The Rainy Lake region itself contains rather complicated geologic relationships. It consists of a series of lithostratigraphic terranes that were assembled along structurally controlled, stratigraphically discordant boundaries during the deformational events (e.g., Poulsen et al. 1980). The boundary between the Wabigoon and Quetico subprovinces in this region is divided among two major dextral strike-slip faults and several interconnected minor faults (Poulsen, 1986), now with mostly ductile shear zone fabrics (Czeck, 2001).

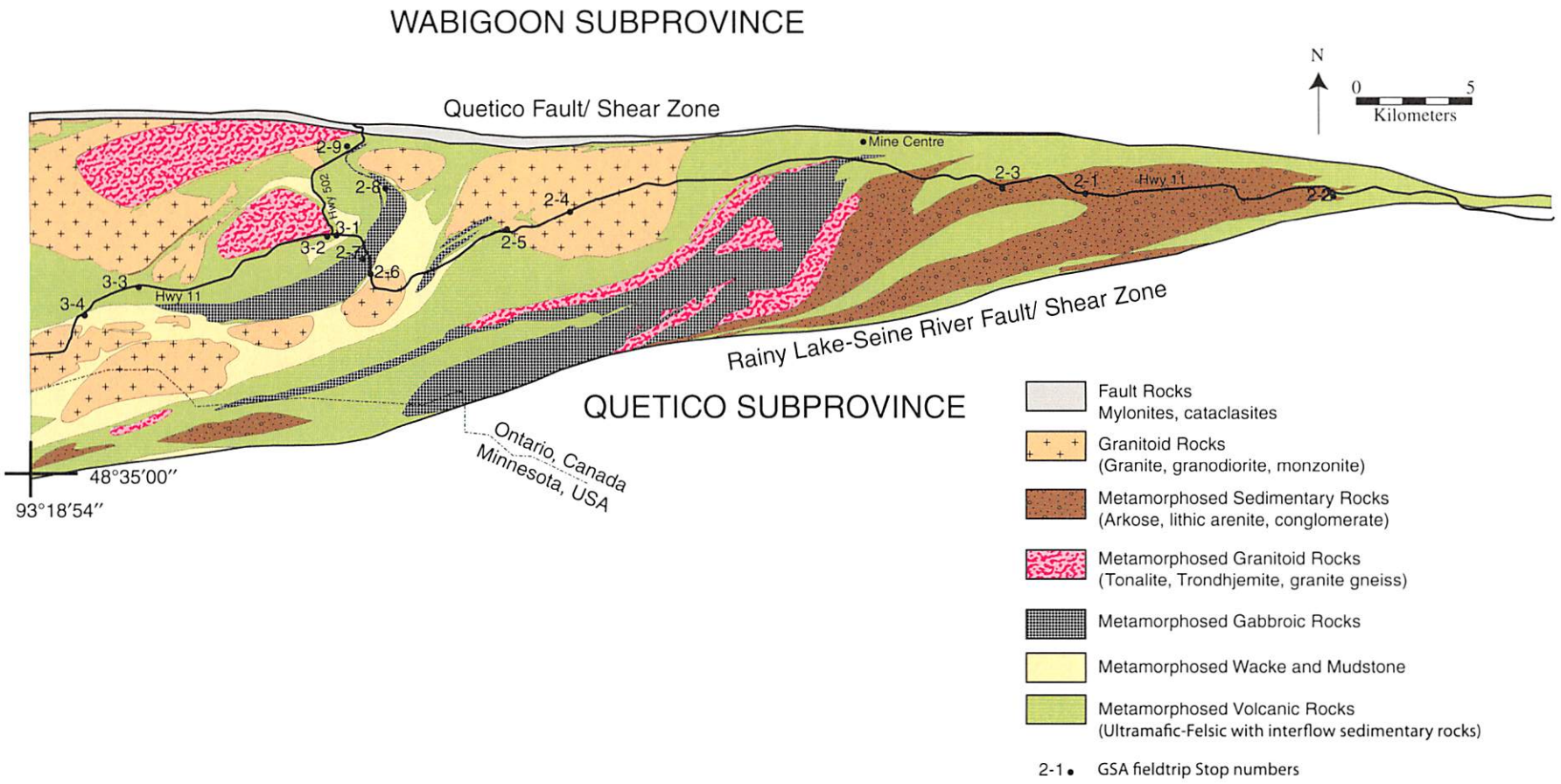

Figure 2. Simplified geologic map of the Rainy Lake region, combined and modified from Wood et al. (1980a, 1980b), Davis et al. (1989), Stone et al. (1997a, 1997b), and Poulsen (2000c).

The two major structures bounding the area are the Quetico and the Rainy Lake–Seine River faults, which have most likely behaved as both dextral faults and ductile shear zones during their deformation histories (Fig. 2). The two faults and/or shear zones converge to the east into a single structure and delineate a wedge-shaped area between them (Poulsen, 1986, 2000a, 2000b, 2000c). Poulsen (1986) recognized the Rainy Lake boundary area as a complex transpressive deformation zone. Within the wedge, a complex pattern of anastomosing subvertical shear zones and faults wraps around gneissic domes and granitoid plutons (Poulsen, 1986, 2000a, 2000b, 2000c; Druguet et al., 2008). Flattening fabrics, combined with the evidence for dextral shearing, indicate an overall dextral transpressive tectonic regime with subhorizontal NW-SE shortening (Poulsen, 1986; Tabor and Hudleston, 1991; Borradaile and Dehls, 1993; Borradaile et al., 1993; Poulsen, 2000a, 2000b; Czeck and Hudleston, 2003; Druguet et al., 2008; Czeck et al., 2009).

The main lithological units in the Rainy Lake district can be summarized on the basis of dates obtained by Davis et al. (1989) and Fralick and Davis (1999), as follows:

1. Tholeiitic and calc-alkaline metavolcanic rocks that form interlayered sequences with ultramafic to felsic compositions, although basalts and andesites are most common. Crystallization ages range from 2728 ± 4 to 2725 ± 2 Ma.
2. Metagabbroic rocks (including metadiabases and metaanorthosites) found as sills and larger intrusions of variable dimensions, generally showing compositional and textural layering. They are generally ca. 2728–2727 Ma, and include the Grassy Portage Sill (2727 ± 2 Ma).
3. Gneisses, mostly synvolcanic orthogneisses ca. 2725 Ma, which vary compositionally from granitic to tonalitic, include the core of the Rice Bay Dome.
4. Quetico turbiditic metasedimentary rocks, found to the south of the Rainy Lake–Seine River fault. The youngest analyzed detrital zircon is 2699 ± 1 Ma.
5. Coutchiching Group metasedimentary rocks between the two bounding faults (Quetico and Rainy Lake–Seine River). They are bracketed in age between 2704 ± 3 and 2692 ± 2 Ma by detrital zircon and a cross-cutting intrusion. They contain metagraywackes and metapelites, especially biotite schists, and locally contain porphyroblasts of garnet, andalusite, and staurolite.
6. Seine River metasedimentary group. Syn- and postdepositional with the nearby Coutchiching metasedimentary rocks. The depositional age is bracketed between 2693 ± 1 and 2692 ± 1 Ma (Fralick and Davis, 1999). Formed as one of the Superior Province's molasse basin-fill units (Corcoran and Mueller, 2007), and includes the Seine River conglomerates (Wood, 1980; Frantes, 1987; Czeck, 2001; Czeck and Fralick, 2002; Czeck and Hudleston, 2003; Fissler, 2006; Czeck et al., 2009).
7. "Algoman" calc-alkaline granitoid rocks. These are relatively unmetamorphosed and poorly deformed granite, granodiorite, and quartz monzonite rocks that form several individual plutons of similar age (including the Ottertail pluton at 2686 ± 2 Ma). They were previously interpreted as postkinematic, and their crystallization age was used as a constraint for the end of regional deformation (Davis et al., 1989; Poulsen, 2000a). However, Czeck et al. (2006) demonstrated that they formed syntectonically, late within the Archean transpressional event.

The complex juxtaposition of varied lithologic units accounts for intriguing and diverse geologic structures. Within the Rainy Lake wedge, the structural styles and strain intensities were largely controlled by the rheological contrasts of adjacent rock types. In the field, we will see these rheologic contrasts at a variety of scales, from centimeter-scale pebbles with contrasting strengths in deformed conglomerates, to kilometer-scale strong plutonic rocks surrounded by weaker volcanic rocks.

Many authors have found evidence for a three-phase deformational history (Poulsen, 1986; Davis et al., 1989; Tabor and Hudleston, 1991; Poulsen, 2000a; Druguet et al., 2008) associated with the late Archean oblique convergence, similar to the deformational histories found along boundaries throughout the central Superior Province. The structures may be similar in style and sequence to neighboring regions, but the phases are unlikely to temporally correlate across subprovince boundaries, and may not even correlate within the Rainy Lake region owing to the dynamic nature of the tectonic setting.

The three phases of deformation are as follows:

1. Early "stacking," consisting of faulting, recumbent folding, and a weak regional schistosity.
2. Ductile transpressional deformation, resulting in the majority of strain accumulation, the strong pervasive deformational fabrics, and prograde greenschist to amphibolite facies metamorphism.
3. Localization of structures during exhumation and retrograde metamorphism.

D_1 is characterized by early recumbent folding that produced the inversion of the stratigraphic sequence leading to the present-day juxtaposition of adjacent right-way-up and overturned folds (Poulsen et al., 1980; Borradaile, 1982; Poulsen, 2000a). S_1 is generally weak and subparallel to the layering in the metavolcanic and metasedimentary rocks and is well developed in the gneiss domes. Significant thrust or oblique faulting likely juxtaposed the allochthonous units found within the Rainy Lake wedge during D_1, but owing to a general lack of marker units there is less direct evidence for thrusting compared with the D_1 folding. However, finite strain magnitudes within this and other Archean belts are generally too low to be consistent with the now largely steeply dipping units having been predominantly deformed by folding (e.g., Schultz-Ela, 1988; Hudleston and Schwerdtner, 1997).

As the crust was "stacked" in D_1, rocks that were once near the surface became buried. In these rocks, D_1 deformation was followed by D_2 deformation, which is characterized by folding and dextral shearing within a transpressional regime. F_2 folds resulted in regional subparallel subvertical bedding, and S_2 foliation with a mean ENE-WSW strike. The Seine River Group was

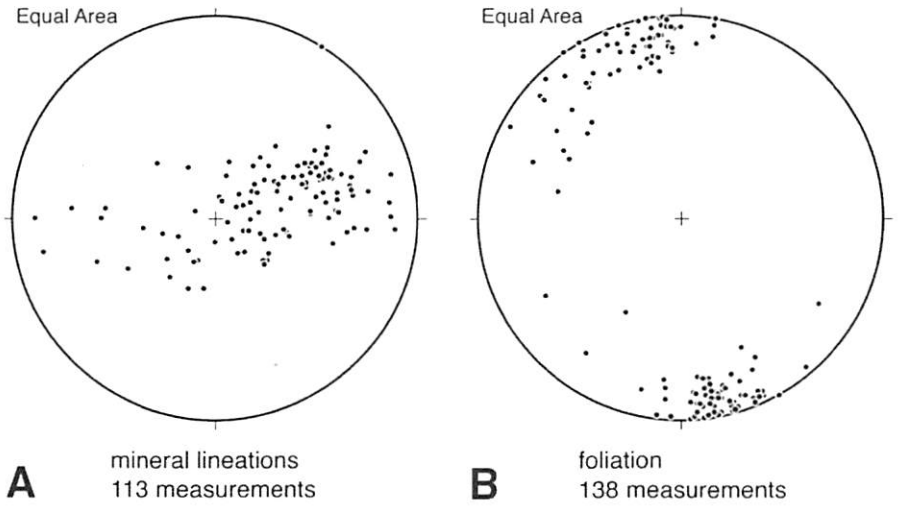

Figure 3. Equal-area stereonets, representing structural fabric in the Rainy Lake region, from Czeck and Hudleston (2003). (A) Stretching (mineral) lineations. (B) Poles to foliation.

deposited in a fault-related basin during early D_2 (Poulsen, 1986, 2000a), which explains the strong D_2 fabrics and minor amounts of internal folding (Czeck, 2001; Czeck and Hudleston, 2003; Czeck et al., 2009). The transition of D_1 to D_2 was not necessarily contemporaneous across the Rainy Lake region, and the vertical bedding in the Seine is likely a result of initial internal stacking followed by D_2 deformation. The Algoman plutons, including the Ottertail pluton, were emplaced and cooled during late stages of D_2 (Czeck et al., 2006). Many leucocratic dikes and quartzofeldspathic veins were emplaced throughout D_2 deformation (Druguet et al., 2008).

D_2 was responsible for the penetrative foliation and lineation fabrics and much of the recorded strain throughout the region. In general, the foliation is subvertical (Fig. 3B), and where strain can be measured, such as within the Seine conglomerates, strain is largely of a flattening type (Czeck, 2001; Czeck and Hudleston, 2003; Fissler, 2006; Czeck et al., 2009). Dextral shear-sense indicators in the form of asymmetric folds, conglomerate strain shadows, clast tiling, and other features are often observed on subhorizontal planes regardless of lineation orientation (Czeck and Hudleston, 2003).

Most of these fabric features along the boundary are consistent with a type of ductile transpression first described by Sanderson and Marchini (1984). This style of transpression is a mathematical description of a specialized case of "transpression" that in its simplest form just means oblique convergence (Harland, 1971). The style of transpression described by Sanderson and Marchini (1984) involves homogeneous deformation consisting of orthogonal simple shear and pure shear components with constant volume in a vertically bounded zone (Fig. 4A). Such an idealized scenario has since been termed *monoclinic transpression* (e.g., Lin et al., 1998) and is perhaps most likely to correspond with strain in deep, vertical ductile shear zones during oblique convergence. The structural fabrics for this model include vertical foliations, flattening fabrics, and asymmetric shear-sense indicators on the horizontal plane (Fossen and Tikoff, 1993) (Fig.

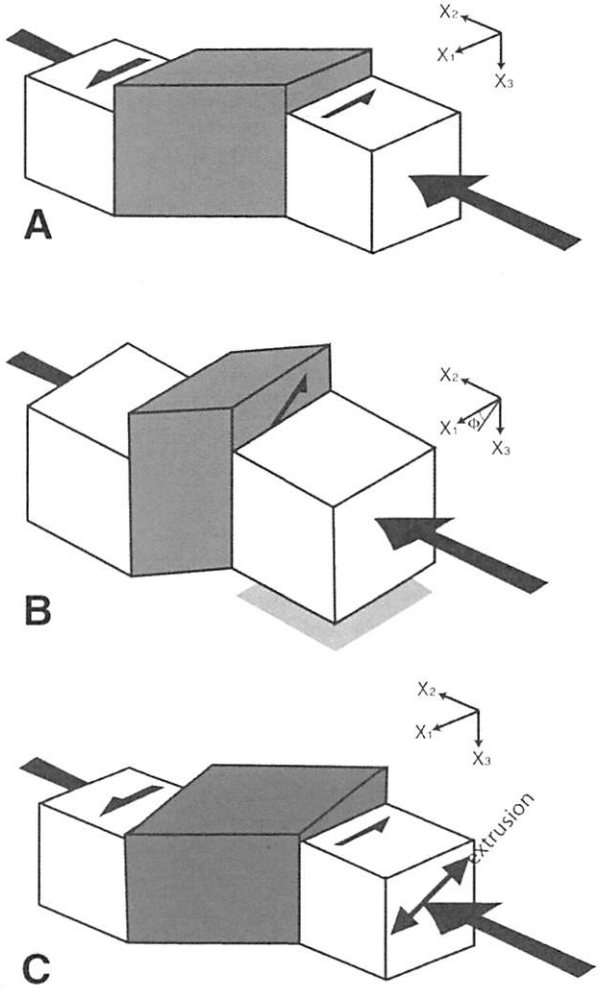

Figure 4. Transpression models. (A) Homogeneous monoclinic transpression (Sanderson and Marchini, 1984). (B) Triclinic transpression with oblique simple shear component (Lin et al., 1998). (C) Triclinic transpression model with horizontal simple shear component and oblique extrusion direction (Czeck and Hudleston, 2003, 2004).

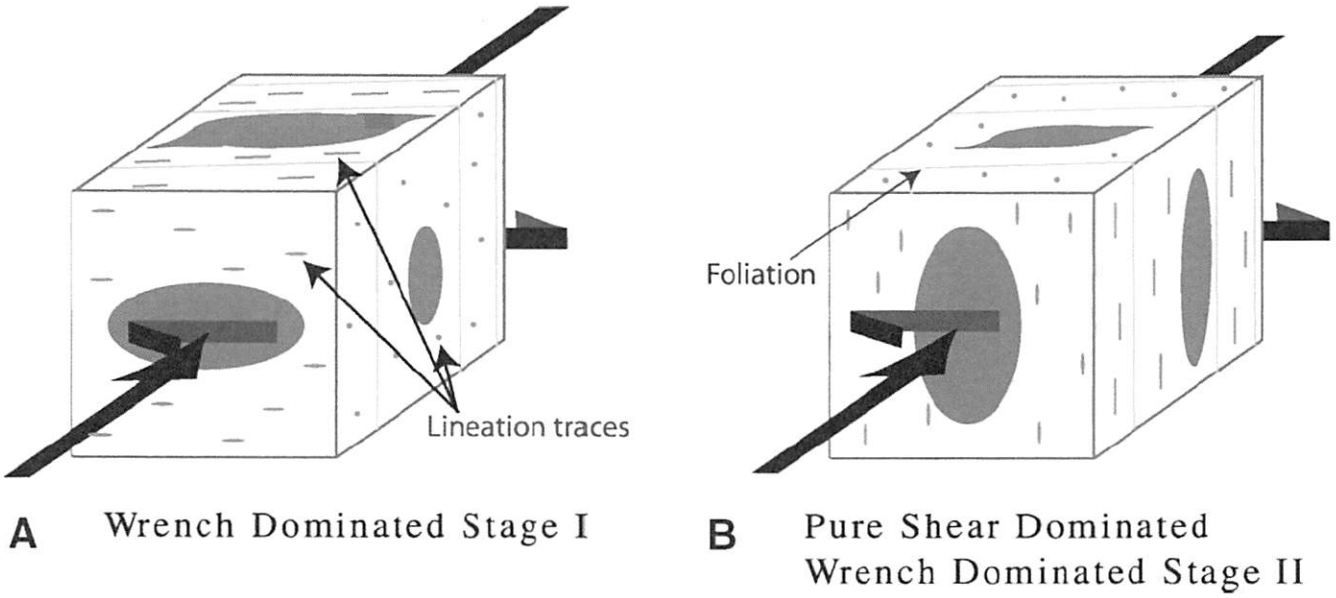

Figure 5. Schematic deformation fabrics and strain predicted for monoclinic transpression (Fossen and Tikoff, 1993). Planes shown are foliations, lines shown are stretching lineations, and schematic "pebble" indicates flattening strain and asymmetric strain shadows from Czeck and Hudleston (2003). Wrench-dominated transpression has horizontal lineations at low strains (A), and vertical lineations at high strains (B). Pure shear-dominated transpression has vertical lineations at all strain magnitudes (B). Only a detailed determination of strain magnitude or kinematic vorticity will allow one to distinguish between pure shear-dominated transpression and simple shear-dominated transpression at high strain.

5). The consistencies of fabrics observed along the Wabigoon-Quetico boundary with the homogeneous transpression model suggest that at least the Wabigoon-Quetico boundary as a whole has undergone quasi-homogeneous transpression.

The lineation orientation (Fig. 3A) is one major aspect of the structural fabric in the Rainy Lake region that does not mesh with the monoclinic transpression model, which predicts either vertical or horizontal lineations (Fossen and Tikoff, 1993) (Fig. 5). The orientations of the stretching lineations, as defined by the preferred orientation of metamorphic minerals, vary at the hectometric scale; they plunge between 0° and 90° in both east and west directions (Czeck and Hudleston, 2003). The subhorizontal asymmetric shear-sense indicators, combined with the greatly variable stretching lineation orientations, prove to be difficult to explain with most kinematic models. In shear zones that deformed via simple shear, we would expect to find asymmetric shear-sense indicators on the horizontal plane, but the lineations should be horizontal. In shear zones that deformed via homogeneous monoclinic transpression models (Sanderson and Marchini, 1984; Fossen and Tikoff, 1993), we would expect to find asymmetric shear-sense indicators on the horizontal plane, but the lineations should be only vertical or horizontal depending on the amount of pure shear versus simple shear and the strain magnitude. In many triclinic transpression models that can explain obliquely plunging lineations (Jiang and Williams, 1998; Jones and Holdsworth, 1998; Lin et al., 1998), the simple shear component is no longer horizontal, so the asymmetric shear-sense indicators should be found on a corresponding oblique plane (Fig. 4B). For these reasons, most kinematic models for shear zones are incompatible with structures found in the region. The best model proposed for D_2 that explains the subhorizontal asymmetric shear-sense indicators and the highly variable stretching-lineation orientations is a triclinic transpression with horizontal simple shear and variable extrusion direction (Czeck and Hudleston, 2003, 2004) (Figs. 4C and 6). In the original monoclinic transpression and in most subsequent triclinic models (Sanderson and Marchini, 1984; Fossen and Tikoff, 1993; Robin and Cruden, 1994; Dutton, 1997; Jones and Holdsworth, 1998; Lin et al., 1998), material was assumed to extrude vertically upward. This assumption is logical, because in general, one would expect the direction toward the Earth's surface to provide the least resistance for material movement. However, rocks at depth may have other boundary conditions imposed by anastomosing shear-zone geometries or large-scale rheology contrasts owing to a diverse lithologic assemblage that caused localized deviations in the extrusion direction. Certainly, the Rainy Lake region has both complex three-dimensional anastomosing shear zones and lithologies with strong competence contrasts that could account for local variation in the extrusion directions.

Domains of higher strain are localized in the relatively incompetent metavolcanic and metasedimentary rocks and channeled around the competent gneissic domes, metagabbros, and Algoman plutons. Two-dimensional strain was estimated using folded and boudined dikes, and the areas of lowest strain are located on the "strain shadow" flanks of the gneiss domes and plutons (Castaño, 2007; Druguet et al., 2008). As a result, the

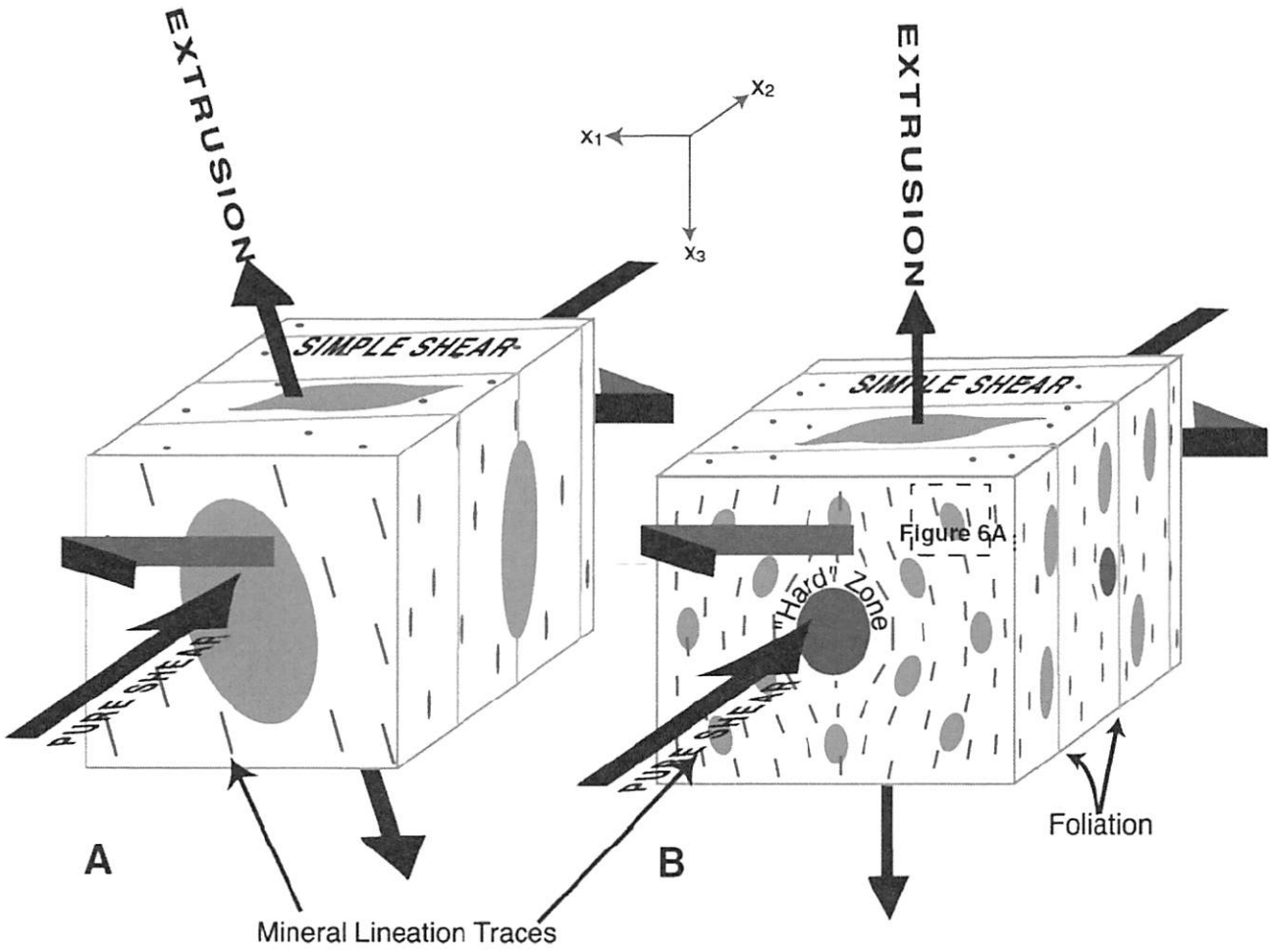

Figure 6. Schematic deformation fabrics and strain predicted for transpression with oblique extrusion; from Czeck and Hudleston (2003). Planes shown are foliations, lines shown are stretching lineations, and schematic "pebble" indicates flattening-strain and asymmetric-strain shadows. (A) Simple view of transpression with nonvertical extrusion. (B) Schematic view of transpression with overall bulk vertical extrusion and localized zones of nonvertical extrusion. Dark-colored ellipses represent schematic competent zones that influence local extrusion directions. The relative location of (A) is indicated.

dominant, composite $S_1 + S_2$ foliation displays a complex heterogeneous pattern both in orientation and intensity.

Dextral transpression continued as the rocks were exhumed, as evidenced by retrograde metamorphism and D_3 structures (Poulsen et al., 1980; Poulsen, 2000a). During D_3, strain localized along major mylonitized dextral shear zones and faults such as the Quetico and Rainy Lake–Seine River faults, narrow mesoscale shear zones, and crenulation bands. This late stage of deformation is more brittle-ductile in nature than D_2 and thus represents rock exhumation. Progressive D_2 to D_3 dextral transpressional deformation was likely controlled by the distribution of lithologic units with contrasting competence, the previous structure, and the emplacement of the Algoman plutons. Many of the late quartz veins may have been emplaced during D_3, but this inference needs to be more rigorously tested.

Some authors note that the final D_3 stage of deformation involved amplification of strike-slip motion along wrench zones (Bauer et al., 1992). The latest brittle faulting has largely been described as dextral strike-slip motion (Kennedy, 1984); however, some late-stage brittle faults associated with N-S shortening have been observed (Tabor and Hudleston, 1991). In all likelihood the last stages of deformation associated with the oblique convergence may have been strongly partitioned, with the major strike-slip faults accommodating the boundary-parallel motion, and the domains between the major faults accommodating the boundary-perpendicular motion (Tabor and Hudleston, 1991). Rb/Sr dating of one pseudotachylite sample from each of the boundaries was conducted by Peterman and Day (1989). The resulting age for the pseudotachylites from the Rainy Lake–Seine River fault and the Quetico fault are 1950 ± 20 and 1937 ± 46 Ma, respectively, leading to an intriguing hypothesis that these faults may have been reactivated during Proterozoic orogenesis south of the Superior Province. However, it should be noted that these dates do not match more recent dates for the

earliest onset of Paleoproterozoic orogenesis at ca. 1875 Ma (Schulz and Cannon, 2007).

Vermilion Fault System

In northeastern Minnesota the Vermilion Granitic Complex is the southwestern extension of the Quetico subprovince, and the Vermilion District is the southwestern extension of the Wawa subprovince (Southwick, 1972; Sims, 1972, 1976; Hudleston et al., 1988; Bauer and Bidwell, 1990) (Fig. 7). The local boundary between these two subprovinces is delineated by a series of faults that includes largely dextral strike slip along the Vermilion fault and south-side down dip slip on the Haley and Burntside Lake faults (Sims, 1976) (Figs. 7 and 8). The Vermilion fault is a major dextral structural feature that can be traced on the aeromagnetic and geologic maps of Minnesota (Chandler, 1991; Chandler and Lively, 2007; Jirsa et al., 2011, respectively) to the northwest corner of the state. Its trace cuts across the entire Vermilion Granitic Complex to the northwest and is interpreted to offset the projection of the Rainy Lake–Seine River fault and therefore the southwestern projection of the Quetico-Wabigoon subprovince boundary in Minnesota. Aeromagnetic data (Chandler and Lively, 2007) also clearly show that the Vermilion fault is cut by the Kenora-Kabetogama dikes (ca. 2.067 Ga; Schmitz et al., 2006). Along the southern margin of the Vermilion Granitic Complex the Vermilion fault extends into the Vermilion District, where it continues as the Wolf Lake and North Kawishiwi faults (Sims, 1976). A series of dextral strike-slip faults and shear zones that roughly parallel the Vermilion fault are concentrated in an anastomosing pattern in the central Vermilion District in the vicinity of the town of Ely (Fig. 8).

The boundary between the Quetico and Wawa subprovinces is generally considered to be the break across these various faults, which juxtapose amphibolite facies rocks of the Vermilion Granitic Complex on the north and the greenschist facies rocks of the Vermilion District greenstone belt on the south. Thus Sims (1976) marked the boundary from west to east by the Haley fault, the Vermilion fault, and the Burntside Lake fault (Figs. 7 and 8). Sims (1976) inferred south-side-down dip slip on both the Haley and the Burntside Lake faults based on the lower grade, greenschist-facies rocks on their south side. He estimated the offset on the Vermilion fault to be 16.8–19 km of dextral displacement on the basis of stratigraphic correlations across the fault, and he noted that reversing this offset would juxtapose the Haley and Burntside Lake faults, which he inferred were originally a single dip-slip (normal?) fault. As a result of this offset the western extension of the Vermilion fault (on its path toward the northwestern corner of Minnesota) cuts into the Vermilion Granitic Complex to form the northern boundary of the Wakemup block (Bauer, 1986), which is bounded on the south by the Haley fault (Figs. 7 and 8).

The focus for the southern (Minnesota) part of the trip will be on the Vermilion fault system and its relationship to deformation in adjacent parts of the Vermilion Granitic Complex on the north and the Vermilion District on the south. The following brief overview of the Vermilion Granitic Complex provides background for stops and discussion of the Wakemup Bay and Burntside Lake plutons.

Vermilion Granitic Complex

The Vermilion Granitic Complex (Southwick and Sims, 1980) (Fig. 7) is broadly composed of biotite schist from a graywacke protolith, schist-rich to granite-rich migmatite, and the Lac La Croix Granite (Southwick, 1972; Hudleston et al., 1988; Bauer et al., 1992). This complex is bounded to the north by biotite schist of the Kabetogama Peninsula (Fig. 7) and to the south by the Vermilion District (Figs. 7 and 8). The biotite schist becomes more migmatitic to the south from the Kabetogama Peninsula and to the north from the Vermilion fault system, where it is considered to be the high-grade equivalent of the greenschist-facies metagraywacke of the adjacent Vermilion District (Sims, 1972). The migmatite leucosomes are composed of pink leucogranite that is indistinguishable from Lac La Croix Granite (Southwick, 1972; Bauer, 1986). The biotite schist contains detrital zircons as young as 2700 Ma, and monazite ages of the pink Lac La Croix biotite granite indicate an age of 2665 ± 2 Ma (Percival and Williams, 1989).

Two major tonalite-trondhjemite bodies and numerous lenses of tonalite-trondhjemite occur in the southern Vermilion Granitic Complex. The Wakemup Bay tonalite (Figs. 7 and 9) is an elliptically shaped body that occupies the core of a major antiformal structure north of the Haley fault (Bauer, 1986). The Burntside trondhjemite (Green and Schulz, 1982) occurs as a lenticular intrusive body parallel to the Burntside Lake fault (Fig. 10). Both of these plutons vary in composition from trondhjemite to tonalite to granodiorite and locally contain a foliation approximately parallel to the boundaries of the intrusion. Veins of trondhjemite have intruded the supracrustal rocks to form a locally complex intrusion migmatite, and veins from both of these plutons are folded by both the F_2 and F_3 fold phases that affected the migmatite (cf. Bauer, 1986, and discussion below).

The biotite schist in the southern part of the Vermilion Granitic Complex, adjacent to the Vermilion District, contains local staurolite- and sillimanite-bearing mineral assemblages indicative of middle amphibolite-facies metamorphic conditions (Bauer, 1986). However, the metamorphic record along the northern boundary of the Vermilion Granitic Complex is more complex. Just south of the Kabetogama Peninsula, kyanite occurs locally in assemblages with garnet + muscovite + staurolite, but

Figure 7. Generalized geologic map of the Vermilion Granitic Complex and adjacent areas in northern Minnesota. The Minnesota-Ontario boundary is approximately defined by Rainy Lake, Namakan Lake, the Loon River, and Lac La Croix. Geology adapted from Southwick (1972), Sims and Southwick (1985), and Day et al. (1990). See Figure 8 for explanation of map units. RLSR—Rainy Lake–Seine River.

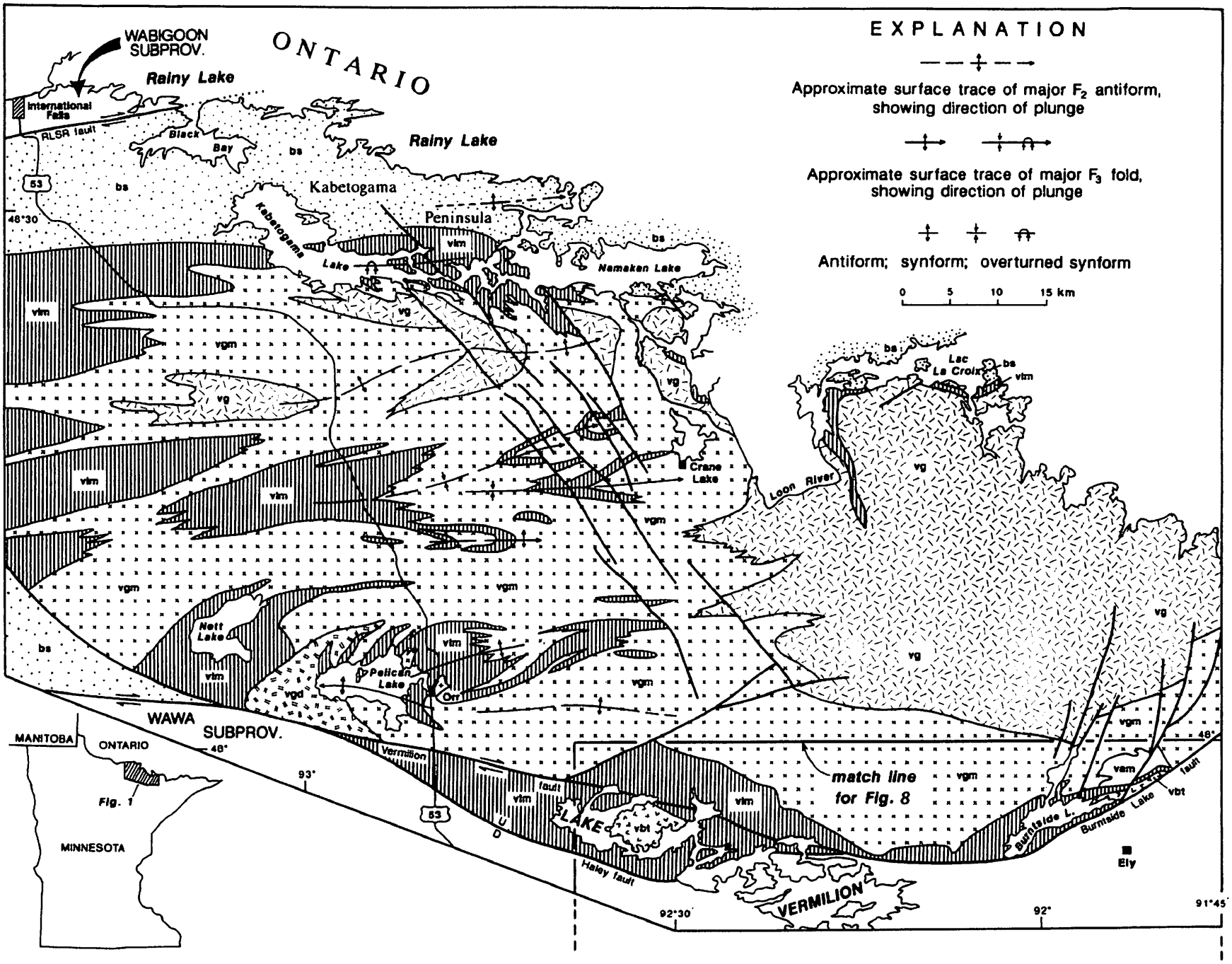
EXPLANATION
Approximate surface trace of major F_2 antiform, showing direction of plunge
Approximate surface trace of major F_3 fold, showing direction of plunge
Antiform; synform; overturned synform
0 5 10 15 km
WABIGOON SUBPROV.
ONTARIO
Rainy Lake
International Falls
RLSR fault
Black Bay
Kabetogama Peninsula
Kabetogama Lake
Namakan Lake
Crane Lake
Loon River
Lac La Croix
Nett Lake
Pelican Lake
WAWA SUBPROV.
Vermilion fault
SLATE
Haley fault
VERMILION
Burntside L.
Burntside Lake
Ely
match line for Fig. 8
MANITOBA
ONTARIO
MINNESOTA
Fig. 1
bs
vim
vgm
vg
vgd
vbt
vam
53
48°30'
48°
93°
92°30'
92°
91°45'

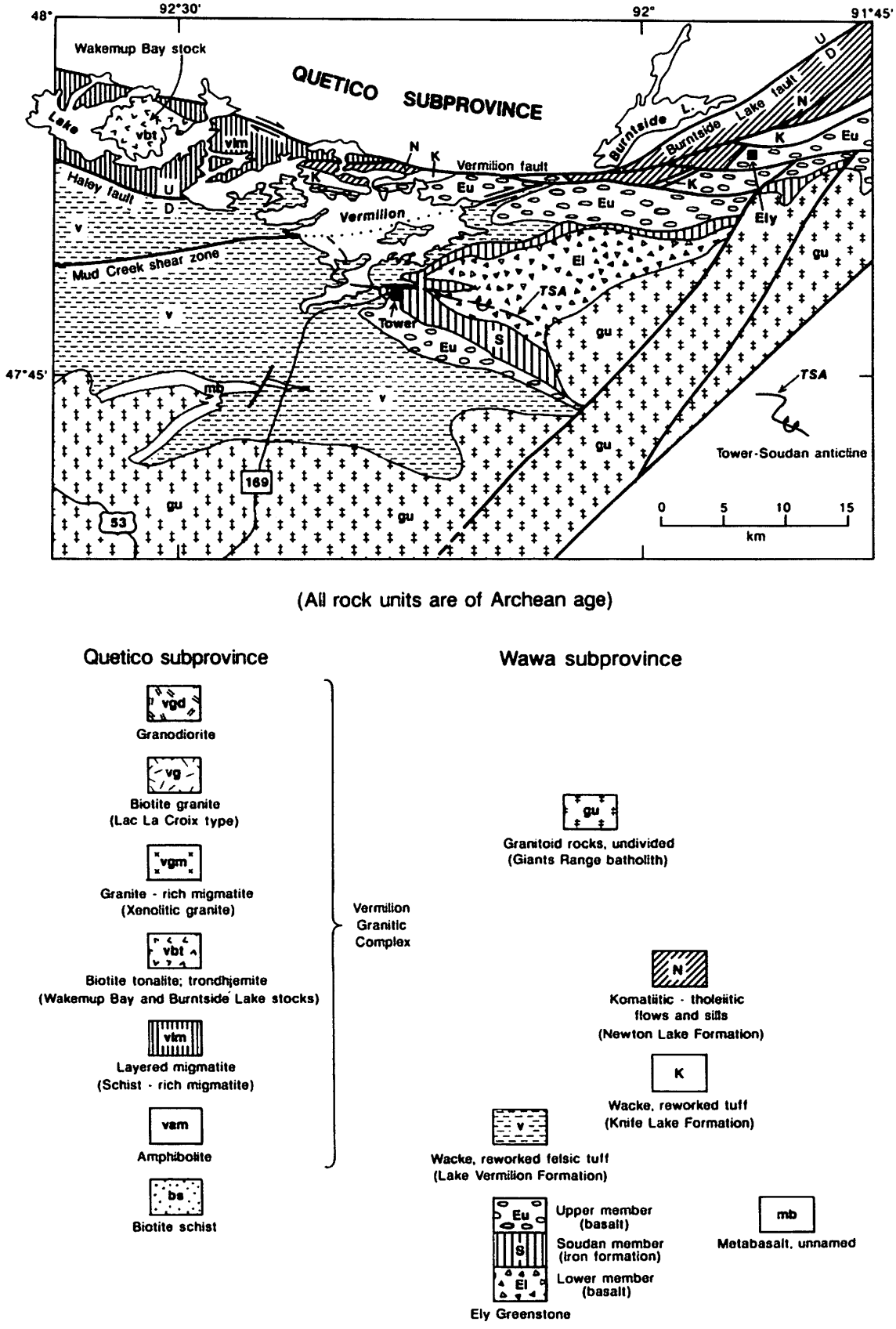

Figure 8. Generalized geologic map of the Vermilion District (Wawa subprovince), northeastern Minnesota, showing stop localities for Day 4. Geology adapted from Sims and Southwick (1985). See Figure 7 for match line to the adjacent Vermilion Granitic Complex features discussed in the text.

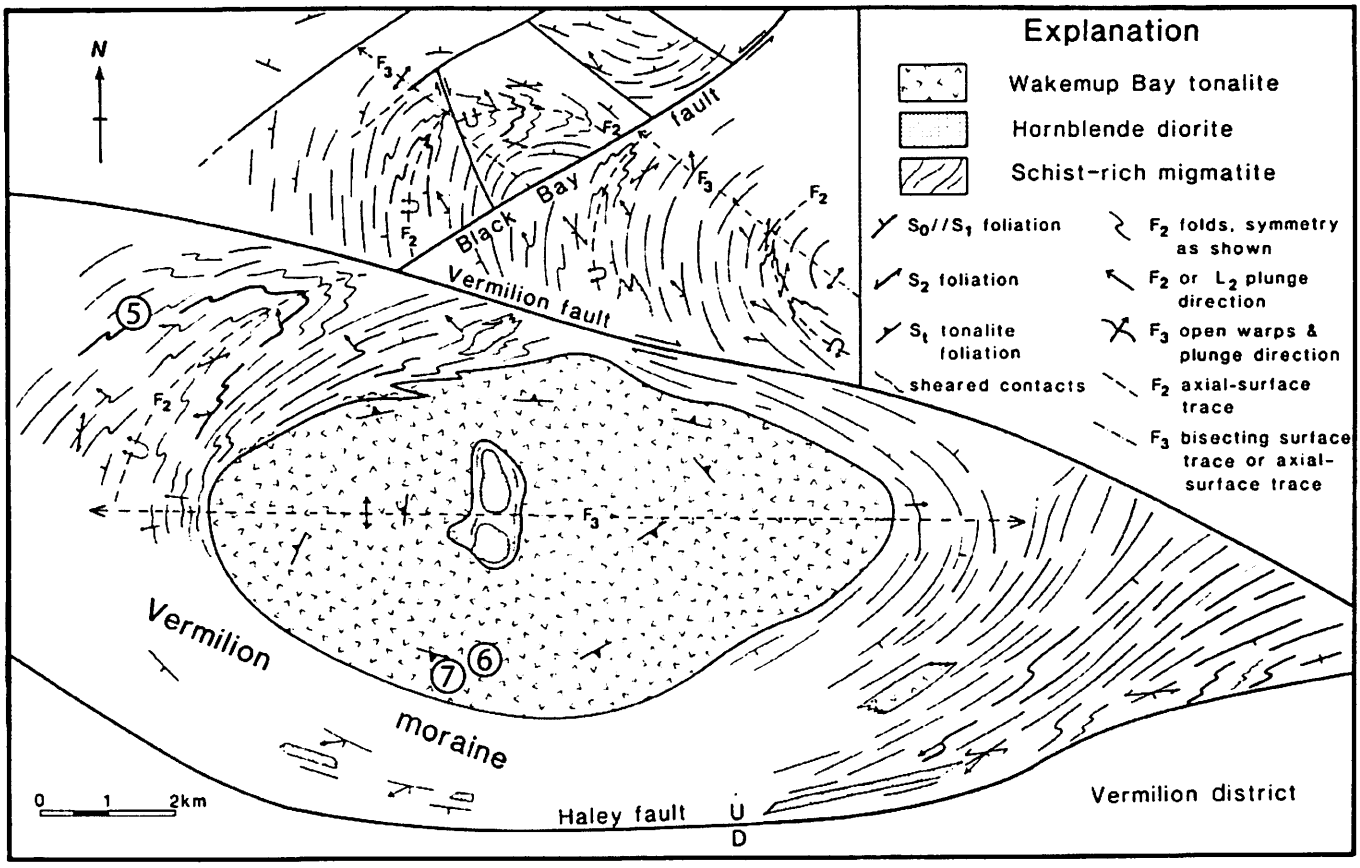

Figure 9. Generalized geologic map of Wakemup Bay block, showing stop locations for Part 2 of Day 3. The form lines are parallel to bedding and a bedding-parallel S_1 foliation, and outline the F_2 and F_3 folds discussed in the text.

kyanite is replaced by sillimanite, still within the staurolite zone, within 5 km south of the peninsula (Tabor, 1988). Farther south into the Vermilion Granitic Complex, within more migmatitic zones adjacent to arcuate satellitic plutons of the granite (Fig. 7), metamorphic assemblages progressively grade from muscovite + K-feldspar to K-feldspar without muscovite in sillimanite-bearing rocks. Locally, cordierite replacing staurolite in assemblages with muscovite + biotite (± garnet ± sillimanite) (Bauer and Tabor, 1990) is indicative of late decompression (cf. Pattison et al., 1999, 2002). The replacement reactions occur in the schist adjacent to F_3, pluton-cored folds (Fig. 7), discussed below, and are interpreted to be a response to uplift and decompression during F_3 folding.

Vermilion District and Adjacent Areas

The Vermilion District, ~160 km long and 10–30 km wide, is bounded to the south by the Giants Range Batholith, to the east by the Saganaga Granite, and to the north by the Vermilion Granitic Complex (Sims and Southwick, 1985) (Fig. 8). The most common rock units include low-grade metasedimentary and metavolcanic rocks, including basaltic to dacitic volcanic rocks associated with pyroclastic, volcaniclastic, and epiclastic deposits (Sims, 1976). In contrast to the Vermilion Granitic Complex, the Vermilion District contains a coherent stratigraphy. The oldest unit in the sequence, the Ely Greenstone, is subdivided into a lower member of tholeiitic pillow lavas that is overlain successively by the Soudan Iron Formation member and the Upper Ely member, which comprises a second sequence of pillowed to massive tholeiitic basalt flows and locally interlayered iron formation. In the western Vermilion District (Fig. 8), the Ely Greenstone is interlayered with a sequence of dacite tuff, dacite porphyry, and volcaniclastic sedimentary rocks of the Lake Vermilion Formation. At approximately the same stratigraphic level in the central Vermilion District (Fig. 8), volcanogenic graywacke and slate of the Knife Lake Group are interlayered with and overlie rocks of the Upper Ely member. To the east and northeast, the Knife Lake Group thickens considerably and is continuous with metasediments in adjacent parts of Canada. The Giants Range Batholith is a large composite granitic body that includes components that span the prominent D_2 deformation, which produced most of the strain in the Vermilion District (discussed below). Boerboom and Zartman (1993) obtained U-Pb ages for the pre- to syn-D_2 Britt granodiorite and the syn- to post-D_2 Shannon Lake Granite that bracket D_2 deformation in the Vermilion District to the interval between 2685 and 2669 Ma.

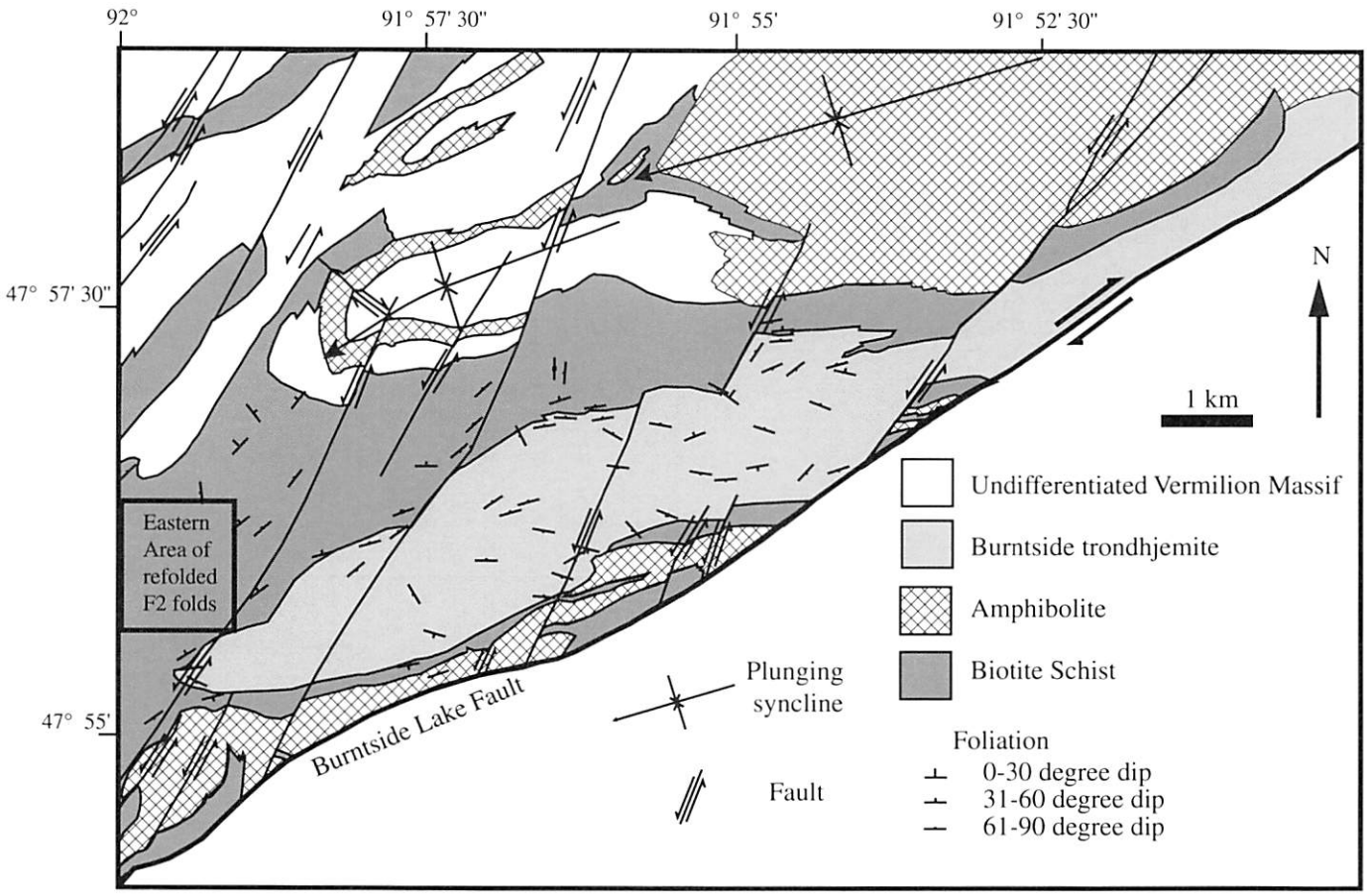

Figure 10. Generalized geologic map of the Burntside Lake area.

Deformation

Deformational events along the southern margin of the Vermilion Granitic Complex and its boundary with the Vermilion District are similar in many respects to the deformation along its northern boundary with the Rainy Lake zone. Flattening fabrics, combined with the evidence for dextral shearing, indicate an overall dextral transpressive tectonic regime produced by subhorizontal NW-SE shortening (Hudleston et al., 1987). However, much of the simple shear strain is strongly partitioned into the Vermilion District south of the boundary, and much of the pure-shear component of the shortening produced folding in the Vermilion Granitic Complex. The southern boundary of this complex, similar to the Rainy Lake zone, includes an early phase of recumbent folding (D_1) followed by metamorphism and a strong strain- and fabric-forming event (D_2). Early recumbent folding (F_1) and a weak, nearly bedding-parallel S_1 foliation were folded by upright F_2 folds along and across the southern Vermilion Granitic Complex boundary with the Vermilion District. Downward facing strata produced by this deformational sequence is evident in F_2 folds across the Haley fault (Bauer, 1985) and to the southwest, in the western extension of the Vermilion District (Jirsa et al., 1992), where they are recognized as early recumbent nappe-like folds in the Lake Vermilion Formation. Despite the D_1 designation for this earliest deformational event, and its similarity to D_1 in the Rainy Lake zone, it is unlikely that this deformation was synchronous across the two subprovince boundaries.

Upright folding of the overturned and upright limbs of F_1 folds produced moderately to gently plunging F_2 folds with east-west–trending axial planes. F_2 folds in the Vermilion Granitic Complex commonly contain an axial planar S_2 foliation, which is rarely a crenulation foliation where S_1 is well developed. The strongest D_2 fabric elements, however, are L_2 stretching lineations subparallel to F_2 fold hinges along both the southern and northern margins of this complex. During the D_2 event, ductile dextral shear was concentrated in steeply dipping east-west–trending shear zones in the Vermilion District, similar to those along the Rainy Lake–Seine River fault in the Rainy Lake zone. In the northern Vermilion District, shear was strongly concentrated in relatively incompetent, steeply dipping metasedimentary and tuffaceous units interlayered with more competent greenstone units (Bauer and Bidwell, 1990). Concentrated zones of ductile shear are not evident within the Vermilion Granitic

Complex away from its boundary regions. However, emplacement of syntectonic satellite plutons of the Lac La Croix Granite reoriented F_2 folds that were then refolded by large regional F_3 folds during continued regional north-south shortening (Bauer et al., 1992). The F_2 and F_3 folds on all scales are nearly coaxial, resulting in common type-3 fold interference patterns. Large, relatively open F_3 folds are common across the Vermilion Granitic Complex and are responsible for the large fold patterns and axial traces mapped by Southwick and Ojakangas (1979) and shown in Figure 7. F_3 folds include the folds that appear to have been intruded by the Lac La Croix Granite, south of Kabetogama and Namakan Lakes, and the Wakemup Bay pluton in the northwestern part of Lake Vermilion (Figs. 7 and 8). However, it is also clear that decimeter- to meter-scale layers of the Lac La Croix Granite are folded by upright F_3 folds in the migmatites to the west of the main batholith. Such observations are consistent with syntectonic emplacement of the granite during both the F_2 and F_3 fold events. If, as suggested by Bauer (1986) and Bauer et al. (1992), F_3 folds formed in response to continued north-south shortening following reorientation of F_2 folds during intrusion, the formation of F_2 and F_3 folds could have overlapped in time during shortening across the Vermilion Granitic Complex.

The U-Pb monazite age of 2665 ± 2 Ma for the syn- to late-D_2 Lac La Croix Granite (Percival and Williams, 1989), and the D_2 bracket between 2685 and 2669 Ma, based on the U-Pb zircon ages (Boerboom and Zartman, 1993), suggest that D_2 deformation began somewhat earlier in the Vermilion District than in the Vermilion Granitic Complex. However, north-south shortening across the Vermilion Granitic Complex, to include the F_3 folding, may well have persisted longer in the higher grade, less competent rocks of this complex.

Finally, late-stage faults at a high angle to the subprovince boundary (longitudinal faults of Sims, 1972) cross-cut all of the folds and commonly display left-lateral offset (Fig. 8).

DAY 1: MINNEAPOLIS TO FORT FRANCES, ONTARIO

DAY 2: RAINY LAKE ZONE, ONTARIO

Rainy Lake Zone

Many of the stop descriptions are modified from a previous field guide (Czeck and Poulsen, 2010). All stops are in the Rainy Lake district (Fig. 2), which is a complex zone of allochthonous units at the boundary between the Wabigoon and Quetico subprovinces.

Stops are shown in Figure 2, and localities are described by UTM coordinates based on NAD 83, UTM Zone 15U.

Stop 2-1: Moderately Strained Seine Metaconglomerates
From Fort Frances, Ontario, drive east along Highway 11 for ~68 km (42.3 mi) to Mine Centre. From Mine Centre, continue driving east on Highway 11 for 15.2 km (9.4 mi) to Horsecollar Junction. Outcrop along north side of Highway 11 across from junction. (15U 0542130E, 5398538N)

The Seine Group was deposited in a fluvial system (e.g., Lawson, 1913; Wood, 1980; Czeck and Fralick, 2002) and contains metamorphosed interbedded conglomerates and sandstones. The lithofacies found within the Seine match various environments of braided stream systems including channels and bars. Conglomerate-dominated, longitudinal bar-channel sequences are the most common; however, sandier channel sequences are not rare and dominate higher levels in the group (Czeck and Fralick, 2002).

There are several late-stage sequences similar to the Seine in the Superior Province, many bearing a striking resemblance to one another. They are known as Timiskaming-type sequences and have long been recognized as having formed in a dynamic tectonic environment (e.g., Lawson, 1913; Pettijohn, 1943). All of these conglomerates are found along major wrench zones, leading to the conclusion that these conglomerates were deposited synkinematically in wrench-related basins (Poulsen, 1986; Poulsen, 2000a).

Within the Seine conglomerates throughout the region, asymmetric shear-sense indicators are prevalent. In general, these are either in the form of asymmetric strain shadows at the ends of clasts, wrapped foliation indicating rotation of the most rigid clasts, or clast tiling. All of these shear-sense indicators suggest dextral shear and are most evident on the subhorizontal plane, *regardless of lineation orientation,* which varies on a hectometric scale. The best model proposed for the deformation in the metaconglomerates that explains the subhorizontal asymmetric shear-sense indicators, the dominant flattening fabrics, and the highly variable stretching-lineation orientations is a transpression with horizontal simple shear and a variable extrusion direction (Czeck and Hudleston, 2003, 2004). The specific clast strain, combined with the other structural evidence, should allow for a more rigorous test to this model.

The metaconglomerates within the Seine Group provide an excellent opportunity to observe competence contrasts and their effects on deformation. The deformation here is typical of much of the Seine: The granitoid clasts are fairly undeformed, and the volcanic clasts display significant flattening. Minor amounts of quartzite, banded iron formation, and other lithologic clast types are also observable.

Czeck et al. (2009) used the clast shapes on the three-dimensional road outcrops to calculate strain within the Seine's various clast populations using the R_f/ϕ method for two-dimensional strain (Ramsay, 1967; Dunnet, 1969; Lisle, 1985), a bootstrap statistical technique (McNaught, 2002; Mulchrone, 2005; Yonkee, 2005), and best-fit three-dimensional ellipsoid calculations (Launeau and Robin, 2003, 2005) (Fig. 11). In most cases the calculated long axes of the strain ellipsoid match the mineral lineation, and short axes are normal to the foliation, indicating that primary clast fabrics have not significantly affected the results. The strain magnitude is strongly dependent on lithology and varies greatly and nonsystematically throughout the

region. In general, the mafic and felsic volcanic clast populations have similar strain magnitudes at a particular outcrop, and granitoid clasts have consistently smaller strain magnitudes. The regional-scale variations in strain magnitude cannot be linked to changes in the concentrations of clast types within the outcrops (Fissler, 2006), but are likely related to spatial proximity to the minor shear zones. Of the 26 outcrops evaluated, 19 have an overall flattening strain, 5 exhibited a constrictional strain, and 2 exhibited plane-strain. Flattening dominates throughout the field area, whereas constriction exists in the western and easternmost stations. Strain magnitude does not correlate with strain shape.

At this particular outcrop, strain magnitude is typical of many of the sites and long/short strain axes ratios were ~2:1 for granitoid clasts, 6:1 for mafic volcanic clasts, and 4:1 for felsic

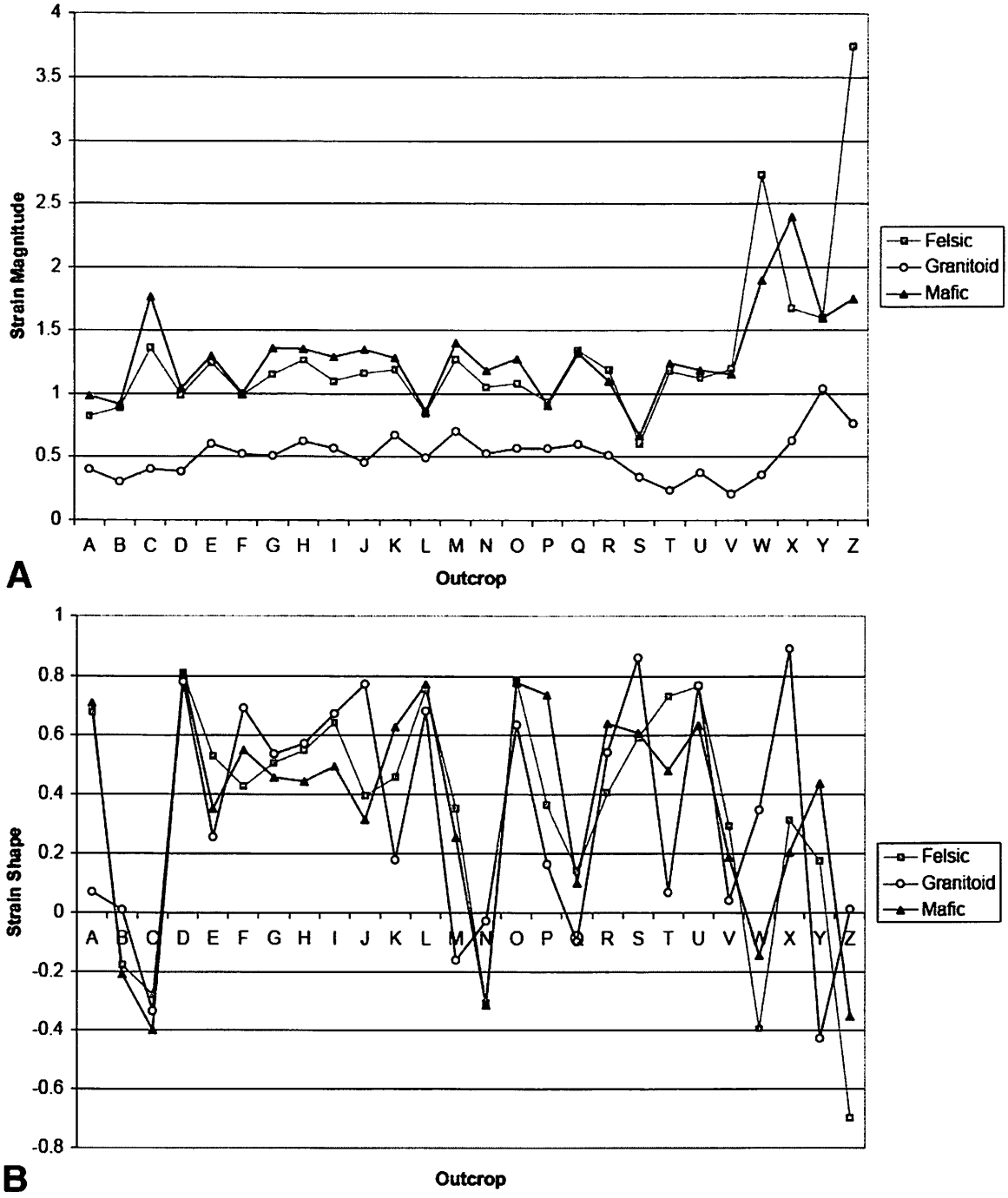

Figure 11. Plots indicating (A) strain magnitudes ($\bar{\varepsilon}_1$) and (B) strain shapes (v) from west to east across the Seine outcrop (stations A–Z). From Czeck et al. (2009).

volcanic clasts. The strain results plot in the flattening field. Czeck et al. (2009) also used detailed finite strain measurements of the clasts to calculate effective viscosity contrasts using established methods (Treagus and Treagus, 2002). The two volcanic clast populations have similar effective viscosities, regardless of strain magnitude, with ratios of felsic/mafic ranging from 0.27 to 2.12 and an average ratio of 1.19. The granitoid clasts are significantly more competent than the mafic clasts, with effective viscosity ratios ranging from 2.35 to 12.39 and an average ratio of 5.61. The results are consistent with a qualitative competence hierarchy of granitoid > felsic ≥ mafic, although the quantitative effective viscosity ratios change with strain magnitude. For small strains, granitoid >> felsic ≥ mafic. For large strains, granitoid > felsic ≥ mafic. The variations in these ratios throughout the field area indicate that the effective viscosity contrast between clast types is strain dependent and possibly deformation-path dependent (Czeck et al., 2009).

Stop 2-2: Highly Strained Seine Metaconglomerates

Continue east along Highway 11 for 18.7 km (11.6 mi). Outcrop is along north side of Highway 11. (15U 0559619E, 5398914N)

The Seine metaconglomerates at this locality are extremely deformed (among the highest strain found within this unit), reflected in the strained shapes of both the volcanic and plutonic clasts. Many clasts are deformed beyond recognition, giving the rock a striped appearance. Is it possible to reliably estimate strain in a rock that is this deformed? Most likely, all strain estimates are minimum estimates, because only the least deformed clasts can be measured. Czeck et al. (2009) estimated strain for the various clast types at this outcrop and found the most disparate strain measurements in their study. Long/short strain axes ratios were ~3:1 for granitoid clasts, 11:1 for mafic volcanic clasts, and 136:1 for felsic volcanic clasts! The errors for the best-fit ellipsoids were high, leading to doubts as to the veracity of these results (don't put much faith in these numbers!).

The lineation plunges ~44°E. Although this lineation orientation is the approximate "average" stretching lineation for the Seine, it cannot be thought of as "typical" because the lineation orientations are so inconsistent. This outcrop is a key locality for demonstrating that the lineation orientation is not directly related to the amount of strain (Czeck, 2001; Fissler, 2006; Czeck et al., 2009). This is important because most transpression models predict subvertical-vertical lineations in highly strained outcrops, and outcrops such as this one allow us to rule out many kinematic models. Again, the dextral asymmetric indicators are most prominent on the subhorizontal plane, which allows us to rule out many triclinic transpression models. The combination of subhorizontal asymmetric shear indicators and variable lineation orientations makes a deformation model of quasi-homogeneous transpression with a variable extrusion direction most likely (Czeck and Hudleston, 2003, 2004).

This outcrop also displays some crenulation cleavage. In general, crenulations formed in the Seine when the clasts are strained enough to create a layering effect. Therefore, crenulations formed relatively late within the strain history, probably during D_3. Crenulations of both dextral and sinistral senses can be observed, indicating that there was likely still a significant pure shear component to the strain at the time of crenulation formation.

The extensive silica veining and carbonate alteration in this rock suggest that fluids infiltrated the rock during deformation. The relative timing of the carbonate fluid and quartz veins is ambiguous in thin section, suggesting that they were at least, at times, coeval (Czeck, 2001). Fluid flow in shear zones is often associated with the possibility of preferential volume loss of soluble material, although the largely constrictional strains measured here (Czeck et al., 2009) are not consistent with typical volume-loss apparent strains, which fall in the flattening field (Ramsay and Graham, 1970). There was probably a symbiotic relationship between fluid localization and enhanced deformation. With such instances of fluid infiltration in highly deformed zones, one might ask the "chicken versus egg" question of whether the fluid caused the high deformation through softening of the rock, or whether the high deformation caused paths for fluids to infiltrate. We will leave the "chicken versus egg" question open for discussion.

Stop 2-3: Two-Dimensional Horizontal View of Seine Metaconglomerates

Return west on Highway 11 for 24.4 km (15.2 mi). Turn south onto Forest Tour Road (dirt track heavily overgrown with weeds). Continue along Forest Tour "Road" for 0.7 km (0.4 mi). (15U 0536866E, 5398509N)

This outcrop allows us to see a large two-dimensional view of the Seine metaconglomerates with many beautiful examples of clast tiling, asymmetric strain shadows, and other kinematic indicators.

Many sandy beds and channels, locally with graded bedding, can be located within this outcrop. Is it possible to determine stratigraphic facing here? As a note of historical interest, A.C. Lawson recognized cross-beds in the Seine sandstones as early as 1911, only a year or so after their significance as a "way-up" indicator was appreciated in younger, flat-lying rocks elsewhere. Lawson's work in the Seine appears to have been the first use of observed reversals in stratigraphic facing to define traces of folds in a Precambrian setting.

Stop 2-4: Ottertail Pluton

Return to Highway 11 and continue driving west for ~32.2 km (20 mi). Outcrop lies on both sides of Highway 11. (15U 0510221E, 5397524N)

The Ottertail pluton is one of the calc-alkaline granitoids of the Algoman type according to Lawson (1913) that range in composition from diorite to granite. They are compositionally distinct from the older orthogneisses in the area, such as the Rice Bay Dome, which typically have a tonalitic composition

(Poulsen, 2000a). All of the Algoman-type intrusions have relatively discrete discordant boundaries and are generally semi-elliptical in map view. Although the Ottertail is obviously relatively late, as judged simply by looking at the map, the details of how late is a bit more complicated and requires a look at both its margins and interior.

The Ottertail itself is mostly granite to granodiorite. The granites are two-feldspar subsolvus granites, containing both K-feldspar and plagioclase along with quartz, hornblende, and biotite. Across its extent it has a heterogeneous composition and grain size distribution (Czeck et al., 2006).

Here we are in the center of the Ottertail pluton with its typical granitic chemistry. The rocks appear largely unmetamorphosed in outcrop but in fact were subjected to low-grade, locally hydrous metamorphism. Chlorite is the primary metamorphic mineral present, which formed by retrograde metamorphic reactions of biotite and hornblende (Czeck et al., 2006). Trace evidence of other metamorphic minerals, including epidote, clinozoisite, and zoisite, are typically present (Czeck et al., 2006).

The pluton is not highly deformed, but a range of deformation microstructures can be observed throughout to varying degrees. The amount of grain-scale deformation varies non-systematically throughout the pluton. In most samples, quartz microstructures, such as undulose extinction and subgrain formation, indicate that some solid-state deformation accommodated by dislocation creep mechanisms was active (Czeck et al., 2006). In the samples with the most deformation microstructures, a weak to moderate S-C fabric, quartz ribbons, fractured feldspars, and kinked biotites have also been observed (Czeck et al., 2006). Variations in the microstructural assemblages are most likely due to strain localization or possibly different cooling histories. The microstructures indicate that the granite was emplaced and cooled enough to deform in the solid state (in at least some parts) during deformation.

Anisotropy of magnetic susceptibility (AMS) analyses were conducted for the Ottertail pluton. For those not familiar with this technique, AMS is a nondestructive method commonly used to obtain three-dimensional average rock fabric (Borradaile, 1988; Grégoire et al., 1998). The distribution and shape of the iron-bearing minerals in a rock dominate the strength of the anisotropy and the shape of the AMS ellipsoid. In a rock in which magnetite is the primary magnetic carrier, the shape and distribution of magnetite grains control the AMS ellipsoid where the long axis of the magnetite grain typically aligns with the long axis of the AMS ellipsoid (e.g., Borradaile and Henry, 1997). If the grains are equidimensional and distributed homogeneously throughout the rock, the AMS ellipsoid is spherical. The greater the distribution heterogeneity of the grains, the greater the AMS ellipsoid deviates from a sphere. The three axes of the AMS ellipsoid are k1, k2, and k3, with k1 > k2 > k3. The k1–k2 plane (pole to k3) is the magnetic foliation plane, and the k1 is the magnetic lineation direction. Well-defined planar AMS fabrics within the Ottertail pluton are roughly coincident with the steep foliations measured in the surrounding rocks, indicating that the AMS fabrics were most likely caused by regional deformation (Czeck et al., 2006).

Gravity inversion analysis indicates that the pluton is shallow, with a maximum depth of ~4.5 km (Czeck et al., 2006). The shallow nature of the pluton supports the conclusion that the steep internal fabrics are unlikely to be purely flow from a feeder zone, but rather a result of the regional strain. The pluton was likely syntectonic, late in D_2. Its geometry is consistent with intrusion into a transpressional setting, possibly into shallow rhombochasms created by en echelon P shears related to the major shear zones or along oblique thrusts (e.g., Tikoff and Teyssier, 1992).

Stop 2-5: Ottertail Pluton Margin

Return to Highway 11 and continue driving west for ~2.8 km (1.7 mi). Outcrop lies on both sides of Highway 11. (15U 0508292E, 5396632N)

At this stop, we will view breccias that are common at the margins of the Ottertail (Poulsen, 2000a). The breccia-like character implies hydraulic fracturing at the pluton edge. The xenolithic blocks within the breccia are foliated country-rock remnants that were likely deformed during D_1 and D_2. The strong foliation within these blocks suggests that a significant part of D_2 deformation occurred prior to intrusion of the pluton.

The Ottertail pluton's composition near the boundaries has significantly higher percentages of chlorite, biotite, and hornblende, presumably input from the country rock. Much of the chlorite is a retrograde reaction product of either biotite or hornblende. Together, the percentages of these three minerals range from 2% to 15% in the center of the pluton, grading to 34%–58% along the eastern and western margins (Czeck et al., 2006). Feldspars are more sericitized in these boundary regions (Czeck et al., 2006).

Stop 2-6: Pseudoboudins

Return west on Highway 11 for 11.7 km (7.3 mi). Turn southwest on dirt road and park. Outcrop is on a dirt road turnoff (south side of highway). Also note a small outcrop on north side of Highway 11. (15U 0497963E, 5393628N)

At this outcrop of pelitic-psammitic schists, we can see fine examples of segmented pegmatite veins resembling boudin trains. Some of these segmented veins are indeed boudins, and they can be distinguished on the basis of (1) clearly defined edges, typically with straight sides formed by fractures that are oriented at high angles to the host rock fabric, and (2) clear fabric deflection of the host rock into the boudin neck regions. However, within other segmented veins we can see distinct examples of apparent boudinage or "pseudoboudinage" (Bons et al., 2004; Bons and Druguet, 2007; Druguet et al., 2008) (Fig. 12). In pseudoboudinage, a string of pegmatite beads is oriented at a low angle to the foliation and layering. Although resembling boudinage, this structure more likely formed by irregular inflation and collapse during vein intrusion (Bons et al., 2004) or intrusion into

dilational jogs (Bons and Druguet, 2007). This interpretation is based on (1) the irregular "cauliflower" shape of the individual segments, and (2) the large amount of extension required to form these structures by boudinage, an amount that is incompatible with strain determined from nearby boudins (Druguet et al., 2008). Subsequent vein-parallel tectonic extension may have produced further separation between segments. Good examples of boudinage and pseudoboudinage can be seen at the outcrop off the south side of the highway. Good examples of folded and boudinaged veins can be seen at the small outcrop on the north side of the highway.

Stop 2-7: Shear Zones within the Grassy Portage Sill: Moderate Strain

Return west on Highway 11 for 1.6 km (1 mi) to the point at which a major power line intersects Highway 11. Park off road and observe rocks on south side of Highway 11. (15U 0497603E, 5395098N)

The Grassy Portage intrusion is a large metamorphosed, layered gabbroic sill, which is exposed ~20 km along its strike. It has been overturned so that it dips steeply to the northwest (Poulsen, 2000a). Within the sill, layering is formed by variations in mineralogy and chemistry, both regionally (kilometer scale) and locally (centimeter scale) (Poulsen, 2000a). Compositions range from melagabbro to anorthosite (Poulsen, 2000a). The margins have been exploited for disseminated chalcopyrite and pyrrhotite mineralization (Poulsen, 2000a).

Within the sill the anorthositic rocks are usually found as lenticular pods within the gabbros that range in size up to 50 cm maximum diameter. They have adcumulate textures of fine-grained andesine (Poulsen, 2000a).

Here, we observe small centimeter-scale shear zones within the coarser grained gabbros, with both dextral and sinistral offsets indicated by fabric deflection. Most of the shear zones are steep-subvertical, but they have curved intersecting geometries that intersect as shallow planes.

Stop 2-8: Shear Zones within the Grassy Portage Sill: High Strain

Continue west along Highway 11 for 2.8 km (1.7 mi) to the junction with Highway 502. Turn right and drive north along Highway 502 for 2.2 km (1.4 mi). Turn east along Baseline Road and drive for ~4.9 km (3 mi). Outcrop is a small mound on north side of road. Other outcrops are across road within recently forested logging trails. (15U 0498897E, 5399146N)

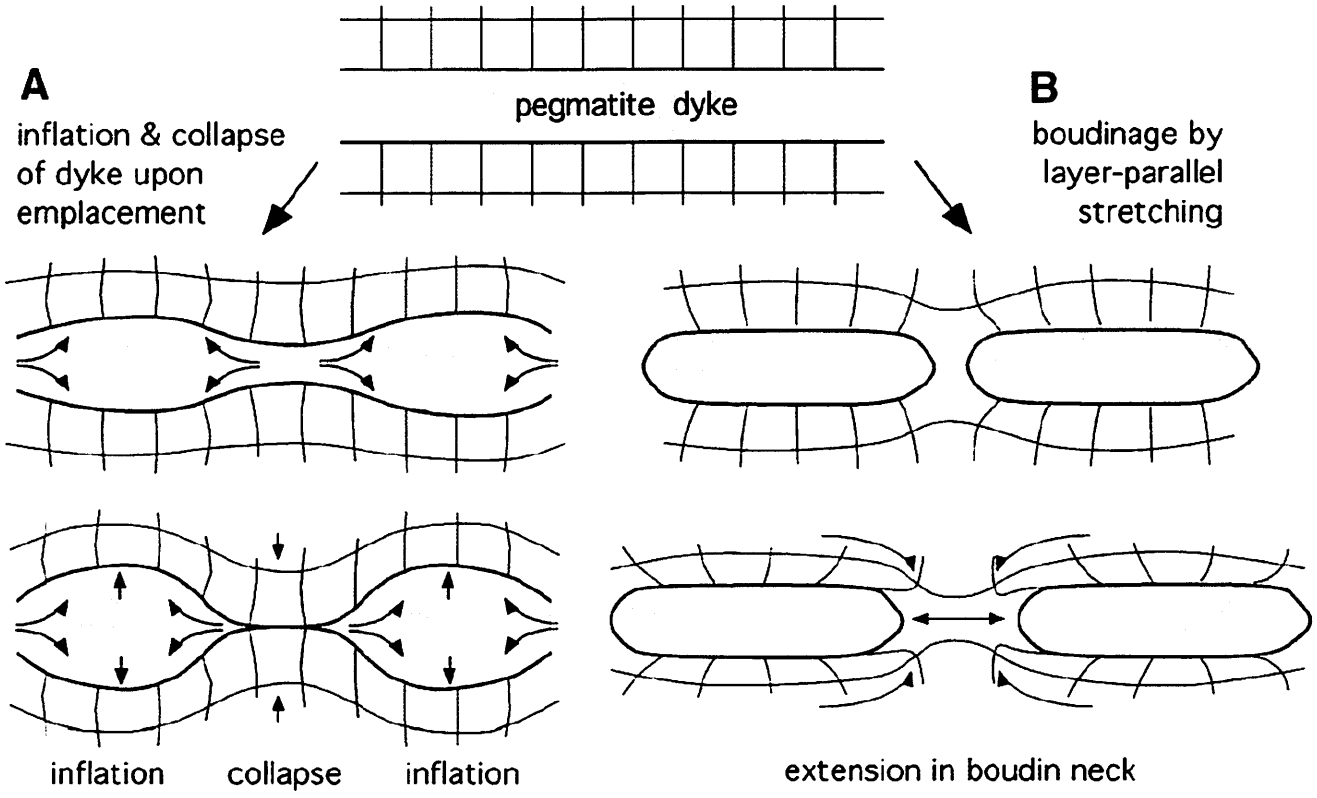

Figure 12. Schematic illustration of geometrical differences between apparent boudinage and actual boudinage from Bons et al. (2004). (A) Collapse and inflation of a pegmatite dike upon emplacement, without any dike-parallel stretching. (B) Boudinage of a solidified pegmatite dike, resulting from dike-parallel stretching.

Here, we observe the sill along its base (northwest margin) on a subhorizontal glaciated surface. This lower portion of the sill is dominated by compositions of gabbroic and anorthositic rocks that either may have formed by gravitational setting or autointrusion (Poulsen, 2000a). The metagabbroic rocks range from leucogabbro to gabbro in composition and contain hornblende and plagioclase with minor amounts of chlorite and biotite (Poulsen, 2000a). Most of the gabbros have a poikilitic texture with hornblende megacrysts, but some have an equigranular texture.

At this particular outcrop the pods have adcumulate textures but are composed of fine-grained zoisite. The zoisite textures indicate that they were formed by hydrous alteration of plagioclase, as evidenced by some relict plagioclase grains with quartz and minor amounts of calcite (Carreras et al., 2010).

The metagabbros contain a wavy pre-shearing weak foliation formed by aligned and linked amphiboles, which strikes ~110° with steep-subvertical dip. The orientation of this local foliation is consistent with the prevailing foliation in the immediate

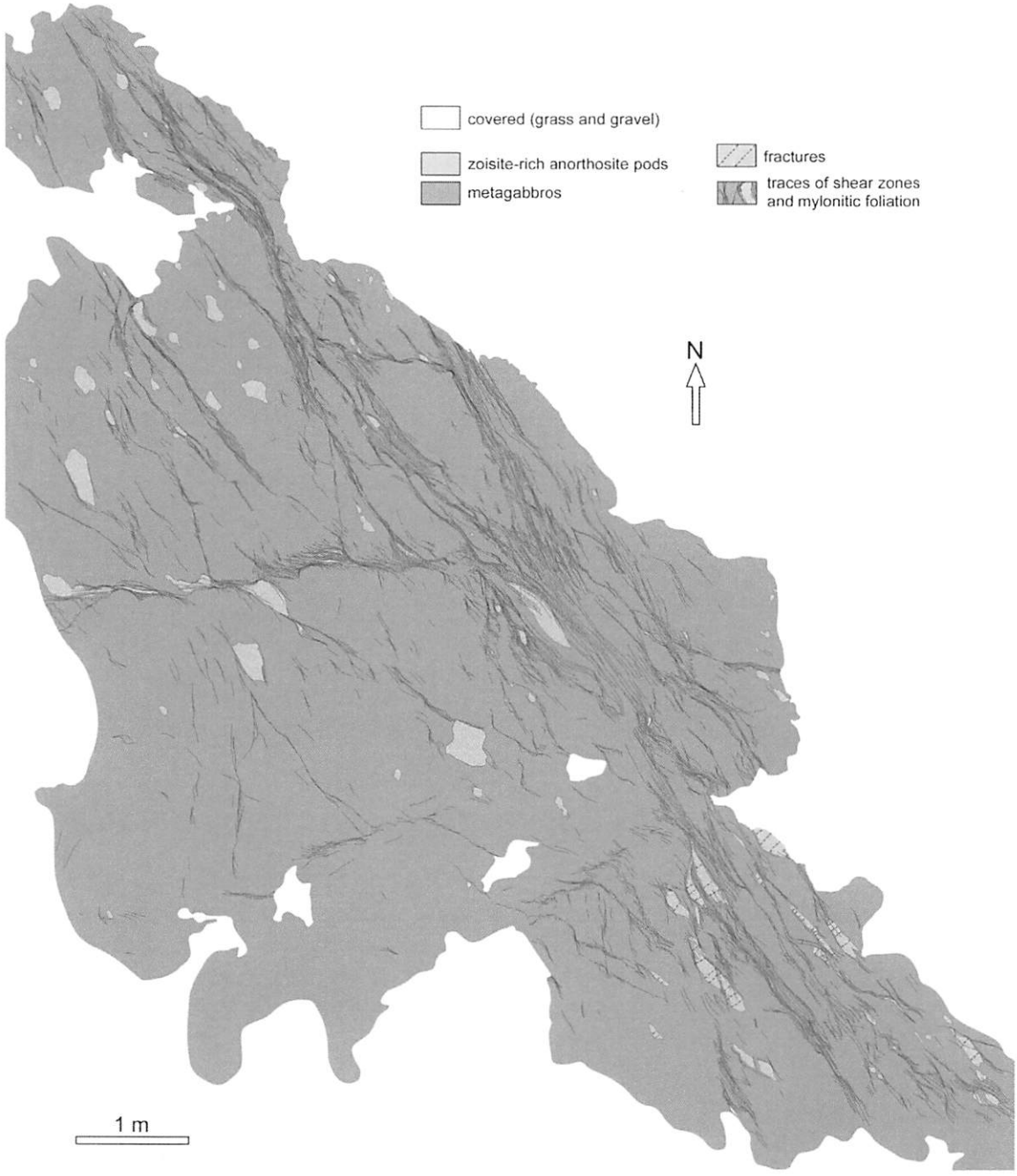

Figure 13. Detailed outcrop map of the shear zones within the Grassy Portage Sill, from Carreras et al. (2010).

region, which is deflected from the typical NE-SW regional strike to a WNW-ESE orientation caused by deflection around the Rice Bay Dome.

Both the gabbros and anorthosites are affected by subsequent small-scale (centimeter to decimeter) shear zones, defined by deflection and intensification of this prevailing foliation, and studied in detail by Carreras et al. (2010) (Fig. 13). These bands are narrow and discrete, with a maximum width of a few centimeters, and define an anastomosed pattern with orientations dominated by NNW-SSE–striking, moderately to steeply dipping strands (Carreras et al., 2010). Inside the shear zones the rocks are well-foliated and fine-grained mylonites. The shear zones are preferentially within the gabbros and commonly localize at the gabbro-pod margins. This prevalence of ductile deformation within the gabbros indicates that the gabbros were less competent than the anorthosites during much of the deformation. However, the shear zones also cut across some pods, where they are defined by mylonitic banding with finer grain size and segregated compositional banding.

Through detailed kinematic analysis, including foliation deflection patterns and relative timing criteria outlined in their paper, Carreras et al. (2010) determined evolution of the shear zones, including the relative timing of initiation and subsequent rotation of the features (Fig. 14). They distinguished two main sets of shear zones, dextral and sinistral, each of which exhibits a range of orientations. The final angular pattern between dextral and sinistral shears is not an original feature. Dextral and sinistral shears formed together at nearly

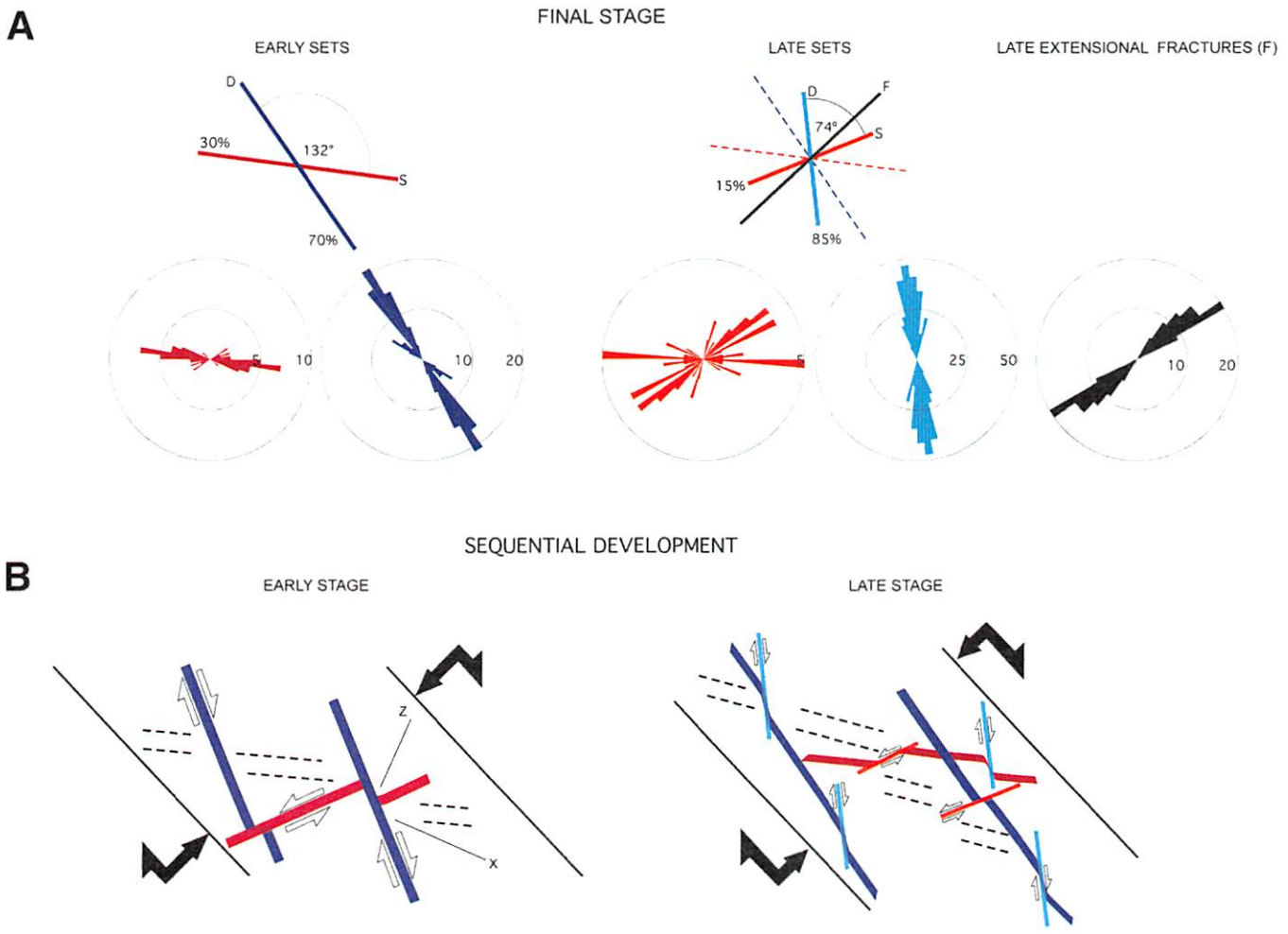

Figure 14. Two-dimensional (horizontal) kinematic model for shear zone set formation from Carreras et al. (2010). (A) Mean orientation of the early and late dextral (D) and sinistral (S) sets of shears and corresponding rose diagrams. The finite bulk shortening direction faces the obtuse angle between the sets. In both stages there are more dextral shears than sinistral ones. The orientation and corresponding rose diagram of the late fractures (F) is also included. (B) Model for the sequential development of shears, drawn on the *XZ* plane with north upward. In addition to shears, the orientation of the bulk *X* and *Z* directions, the assumed shear plane, and the trend of the preexisting foliation (dashed lines) have been drawn. It is assumed that the initial angle that faced the bulk shortening direction between sets was ~90°. As deformation progressed, the two sets rotated in opposite directions, and the angle between them increased. The later development of new dextral and sinistral sets led to complex coalescences and cross-cutting relationships.

right angles, and the angles progressively opened toward the extension direction as a result of increasing strain. The obtuse angles were achieved by the combined effects of continued shearing on newly forming shears and internal deformation of the lozenge-shaped domains of lesser deformed rock. Through time there was an increasing prevalence of dextral shears over sinistral ones. The studied pattern and sequential analysis indicate that bulk deformation was noncoaxial, with a deformation regime evolving from a pure shear-dominated dextral transpression to a higher vorticity dextral transpression (Carreras et al., 2010).

Fractures are the latest structures, cutting both the foliation and shear zones. They are present exclusively in the anorthosite (zoisite) pods and are chiefly oriented transverse to the mylonitic foliation. The regularity of the fracture orientations suggests that they formed in response to the final state of instantaneous strain, because one would expect them only to be subparallel if they had formed without any subsequent rotation. They are interpreted as extensional (Mode I) fractures. The incidence of the fractures exclusively within the pods indicates that the pods were relatively more competent than the surrounding gabbros at this final stage of deformation.

Stop 2-9: Folds and Syntectonic Veins within Mafic Metavolcanics

Return to Highway 502 and drive north 4.2 km (2.6 mi). Outcrop lies along east side of Highway 502. (15U 0496149E, 5401196N)

At this stop, we are in relatively incompetent mafic metavolcanic rocks that are channeled between more competent units: the Black Sturgeon Bay gneiss dome to the northwest, the Rice Bay gneiss dome to the southwest, and the Baseline Bay (Algoman) pluton to the east. The foliation at this outcrop strikes approximately NE-SW in an orientation that is consistent with the foliation in the incompetent units being channeled around the more competent units. Here, the banded mafic metavolcanic rocks are isoclinally folded (F_2). A sequence of leucocratic veins are intruded into the host rock.

The leucocratic veins are syntectonic with D_2 because many such veins that cross-cut F_2 folds are coplanarly folded with them (axial planes are subparallel), although in a more open geometry. This relationship reveals that the host rocks underwent folding prior to vein intrusion, but both vein and host rock underwent additional D_2 folding. Druguet et al. (2008) used veins such as these to estimate two-dimensional strain in metavolcanic and metapelitic host rocks surrounding the competent Rice Bay gneiss dome. This outcrop is in one of the highly strained zones (Figs. 2 and 15).

The veins and their host rocks underwent a competence inversion. When the veins were first intruded, they were less competent than the host rock, but as they cooled they eventually became more competent. Less competent veins, which must have been some of the last to intrude, have cuspate margins and irregular vein boundaries. More competent veins, which must have intruded and cooled during the deformation, are folded.

Return to Fort Frances and hotel.

DAY 3: RAINY LAKE ZONE, ONTARIO (CONTINUED) AND WESTERN LAKE VERMILION, MINNESOTA

Part 1: Rainy Lake Zone (Continued)

Stops are shown in Figure 2. Stops 3-1 through 3-4 are in the Rainy Lake District at the boundary between the Wabigoon and Quetico subprovinces.

Stop 3-1: Folding and Syntectonic Veins in Alternating Pelitic and Psammitic Schists

Return to Highway 11 and drive east 27.3 km (17 mi), immediately to the east of Highway 502 turnoff. Outcrop is along south side of Highway 11. (15U 0495680E, 5396171N)

At this stop we are in relatively incompetent metasedimentary rocks that are channeled between more competent units, the Rice Bay gneiss dome to the northwest and the Grassy Portage gabbroic sill to the east. The foliation at this outcrop is striking approximately NE-SW, parallel with the map expression of this channeled metasedimentary unit. The rock consists of alternating pelitic and psammitic schists with F_2 isoclinal folds easily seen in the metapsammitic layers and early quartz veins.

There are multiple veins ranging from quartz to leucocratic in a variety of orientations. We can see folding and boudins in the veins, depending on their orientation. The folds in the veins have a tighter geometry in the pelitic schists compared with the psammitic schists, owing to the higher competence contrast between the veins and the metapelites (e.g., Ramsay, 1967; Cruikshank and Johnson, 1993). Based on two-dimensional strain analysis of vein deformation with assumed constant volume, this outcrop is in a moderately strained zone with long/short axial strain ratios of ~2:1 and plane strain (Druguet et al., 2008) (Fig. 15).

Stop 3-2: Decimeter-Scale Upright Folds

Drive west on Highway 11 for 200 m. Outcrop is along north side of Highway 11 directly west of Highway 502 turnoff. (15U 0495180E, 5396173N)

The next stop is very near the last, within the layered metasedimentary rocks. Here we can observe decimeter-scale, low-amplitude folds within the sedimentary layers. Note that the F_2 folds plunge eastward and display an asymmetry consistent with the position on the southeast flank of the Rice Bay Dome. Two outcrop localities convincingly demonstrate downward facing in this metasedimentary (metagraywacke) unit: near Pocket Pond (pillow lavas) and Bear Pass Boat Launch (graded beds) (Poulsen et al., 1980). In both cases the metagraywackes are structurally beneath but stratigraphically above the

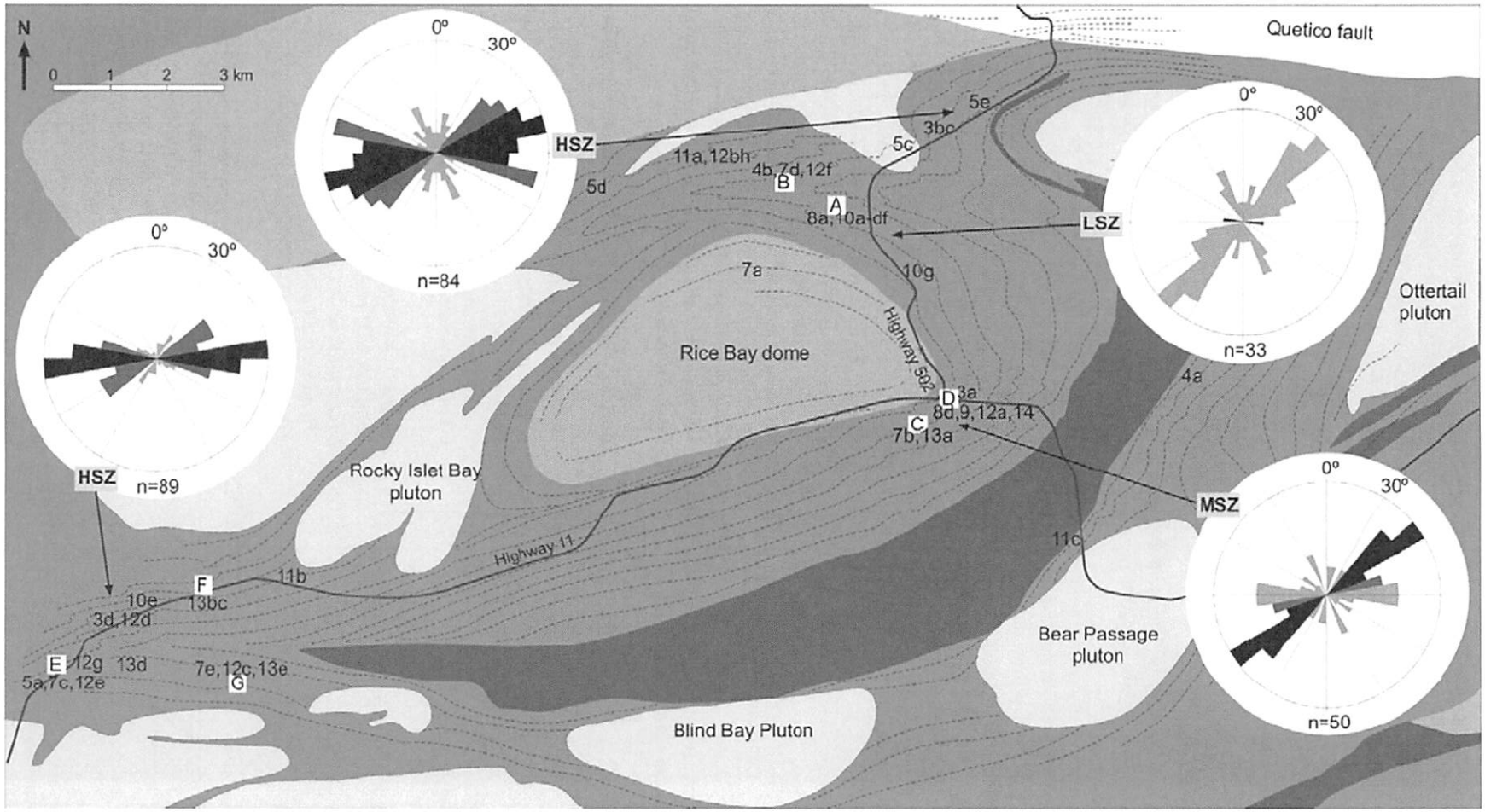

Figure 15. Schematic structural map of the study area with foliations that deflect around competent lithologic units. Modified from Druguet et al. (2008). Strain estimations were performed from deformed dikes in four different areas (diagrams of azimuth distribution of veins shown). Pale gray, shortened veins; black, extended veins; and, where possible, gray, shortened and extended veins. LSZ—low-strain zone; MSZ—moderate-strain zone; HSZ—high-strain zone. Several of the field trip stops were used in part of the strain analysis: Stops 3-1 and 3-2 from a moderately strained zone, and Stops 2-9 and 3-4 from two different high-strained zones.

metavolcanics, a relationship that is supported by zircon ages (Davis et al., 1989). Given that these metasedimentary rocks are younger than both the mafic-ultramafic rocks to the east, and the felsic rocks in the core to the dome to the northwest, there is a problem in interpreting their configuration prior to development of the F_2 "dome." The possible solutions are shown in Figure 16, all resulting in "stacked" tectonostratigraphy. Therefore, in the big-picture view, down-plunge and eastward from this locality is an antiformal syncline.

Stop 3-3: Deformed Pillow Basalts

Drive west along Highway 11 for 11.9 km (7.4 mi). Outcrop is on the N side of the highway. (15U 0484372E, 5392969N)

Here, we can observe metabasalts with prominent pillows in three dimensions. Stretching lineations defined by alignment of mafic minerals and long axes of pillows are near vertical. Strain appears to be constrictional, although detailed strain measurement has not been performed. The pillow rinds have been stretched vertically, forming boudins with quartz-filled necks. Leucocratic intrusions have cuspate structures that preserve magmatic relationships and weak internal fabrics, suggesting syntectonic intrusion.

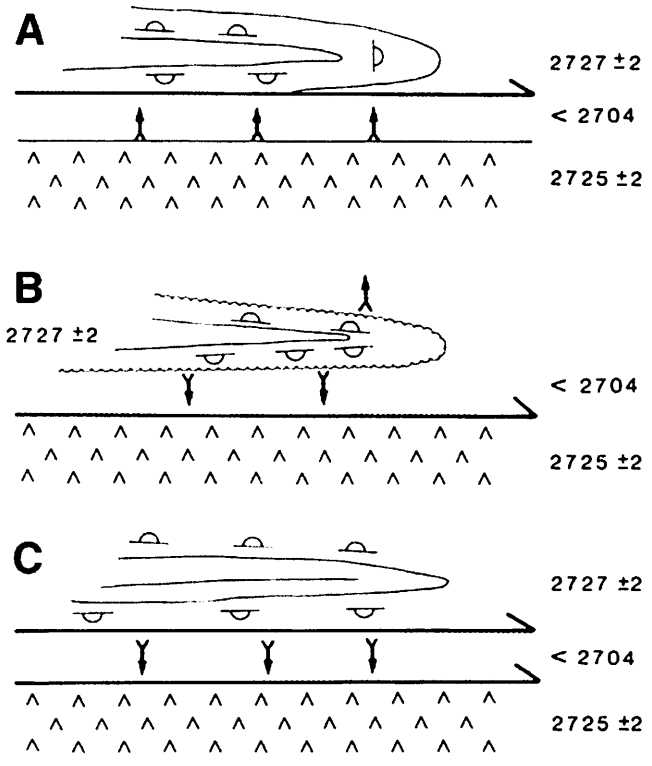

Figure 16. Schematic cross section showing alternative explanations for stacking of tectonic slices in Rice Bay–Bear Pass area. From Davis et al. (1989). Numerals refer to zircon ages.

Stop 3-4: Four Consecutive Sets of Strongly Deformed Leucocratic Veins within a Foliated Metasedimentary Rock

Drive west along Highway 11 for 5.1 km (3.2 mi) to junction with George Armstrong Road. Park on pullout on south side of highway. Outcrop is on the N side of the highway. (15U 0479787E, 5391252N)

This outcrop is a strongly foliated metasedimentary rock of the Quetico Group between various Algoman granitic intrusions to the north and south. Four consecutive sets of strongly deformed leucocratic veins intrude the host rock and are boudinaged and folded depending on orientation. Where veins intruded at angles higher than 30° with respect to the foliation, they were folded. When intruded at lesser angles, they were boudinaged, or folded and then boudinaged. There is an increasing measurable strain in progressively older veins, which indicates multiple synkinematic D_2 intrusions (Druguet et al., 2008). Based on two-dimensional strain analysis of vein deformation with assumed constant volume, this outcrop is in a highly strained zone with long/short axial strain ratios of ~5.5:1 and flattening strain (Druguet et al., 2008) (Fig. 15). In this highly strained zone, the folds are tighter than at outcrops showing lesser deformation. The folds are tight to isoclinal and classified as Ramsay (1967) Class 1C and 2 folds, characterized by relative thickening of the hinge zones, which is compatible with flattening strain. Lastly, the veins are offset by discrete brittle faults, primarily dextral, that presumably occurred during D_3.

Drive back to Fort Frances and then over the U.S. border at International Falls and drive south on Highway 53 to the town of Cook, Minnesota.

Part 2: Wakemup Bay Tonalite and Vermilion Fault

Much of the work in this section is based on the results of R. Bauer and colleagues (Bauer, 1981, 1986; Bauer and Bidwell, 1990) and the Master's thesis of K. Charkoudian (2003).

Stops are shown in Figure 9, and localities are described by UTM coordinates based on NAD 83, UTM Zone 15T.

Stop 3-5: Biotite Schist

From Cook, Minnesota, take Highway 24 north until it becomes adjacent to the western edge of Lake Vermilion. The stop is near "Head of the Lakes" resort. The GPS location for this stop is approximate. (15T 474844E, 5310679N)

The Wakemup block is a lozenge-shaped fault block bounded by the Vermilion fault to the north, and the Haley fault on the south, east, and west (Fig. 9). Three main units within this block, in age order, are the biotite schist, hornblende diorite (appinite) dikes and sills in the schist, the Wakemup Bay pluton, and local veins of granite and pegmatite that are probably late stages of the Lac La Croix Granite. The pluton is surrounded by the biotite schist on all sides and is capped in the center of the pluton by an isolated exposure of flat-lying biotite schist and appinite, which

is topographically higher and structurally overlies the pluton (Fig. 9). This stop highlights the schist.

Bauer (1986) identified three phases of folding adjacent to the Wakemup Bay tonalite in the Vermilion Granitic Complex. The earliest (F_1) folds are most evident as tight to isoclinal folds of quartz veins and thin granitic stringers oriented at a high angle to the approximate bedding-parallel foliation in the biotite schist. On a more regional scale, F_1 folds have also been recognized in downward-facing F_2 folds across the Haley fault (Bauer, 1985) and in the western Vermilion District (Jirsa et al., 1992). The intermediate-age (F_2) folds trend E-W and are regionally pervasive in the biotite schist. The third episode of folding (F_3) produced large easterly plunging F_3 fold axes along the western margin of the Lac La Croix Batholith (Fig. 7). Along the southern margin of the Vermilion Granitic Complex, major F_2 folds were locally refolded about westerly to northwesterly plunging F_3 axes (Fig. 7). Bauer et al. (1992) suggested that late D_2 emplacement of the Lac La Croix Granite and associated satellite plutons reoriented F_2 folds, which were then refolded by large regional F_3 folds during continued regional north-south shortening.

Approximately 2 km to the north, the Vermilion fault extends in a WNW-ESE–oriented direction and crosses Highway 24. Aligned creeks (Hoodoo, Black), elongate lakes (Hoodoo, Black, Wolf), and elongate bays of Lake Vermilion (Black, Norwegian, Wolf) demarcate its position in this area. The lack of any exposures of the Vermilion fault is, unfortunately, a regional phenomenon.

Stop 3-6: Wakemup Bay Tonalite

Turn S on Highway 24 north, returning in the direction of Cook. Approximately 7 km (4.3 mi) S, turn left (E) on Highway 78. Turn left (N) on County Road 478 (Wakely Road); there will be signs for Wakemup campground. Continue past the turnoff for the campground until the intersection with Soderholm Beach Road, and park there. A power line road to the north of the intersection contains a large outcrop of Wakemup Bay tonalite. (15T 468619E, 5305964N)

This stop provides a look directly at the Wakemup Bay tonalite. There is overall a shallowly dipping foliation and preservation of compositional banding. The Wakemup Bay pluton typically contains a weak to moderate foliation, which is parallel to foliation in the surrounding schist (Fig. 9). The foliation is defined by compositional banding of parallel grains of biotite, and less commonly by flattened quartz grains. Some leucocratic veins of granodiorite occur in the pluton and are parallel to foliation within the pluton (Bauer, 1986). At the outer contacts of the pluton, foliations in the biotite schist dip away from the pluton on all sides, and parallel the boundaries of the pluton. In the center of the pluton the foliation is dominantly flat lying. The foliation dips gently to the south near the southern edge of the pluton, and gently to the north near the northern edge of the pluton (Bauer, 1986). Sparse, open warps of S_1, with hinge lines plunging gently to moderately to the east, occur in the schist just east of the pluton contact and represent the only minor F_3 structures observed in the area. The axial planes of these folds, like those of the pluton-cored F_3 structure, are east-west striking and steeply dipping. Along the northern contact the Wakemup Bay tonalite is locally folded with F_2 folds, which suggests that the tonalite was emplaced before or during the late stages of F_2 folding (Bauer, 1986).

Microstructures

The Wakemup Bay pluton records dominantly magmatic microstructures, except along northwestern and western contacts of the stock, where it displays a stronger foliation parallel to schist contact. In thin section, feldspars are euhedral, and quartz grains are sub-equant (Fig. 17). Biotite is aligned, suggesting that magmatic flow occurred. Locally, the Wakemup Bay pluton exhibits evidence for solid-state deformation, mostly by the elongation

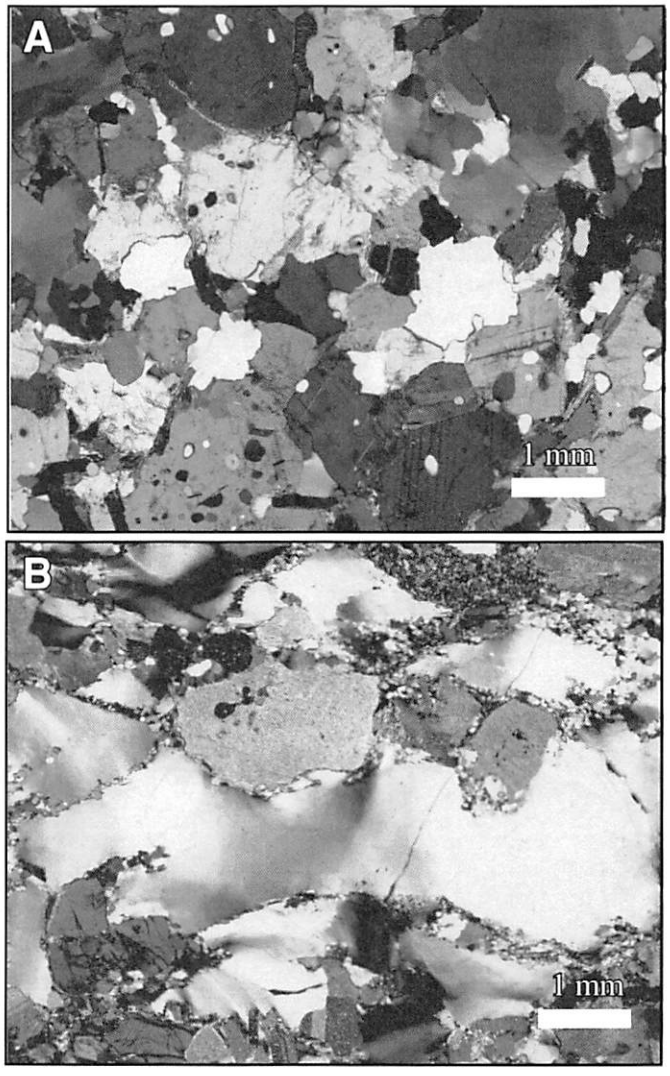

Figure 17. Thin sections/field photos from Wakemup Bay pluton, shown under cross-polarized light. (A) Magmatic fabric, typical of most of the exposures. (B) Crystal-plastic deformation, characterized by elongate quartz but only minor grain-size reduction that occurs locally.

of quartz grains. In map view there is no spatial pattern to the samples that record solid-state deformation (Charkoudian, 2003).

Anisotropy of Magnetic Susceptibility Analysis of the Wakemup Bay Tonalite

The anisotropy of magnetic susceptibility (AMS) technique was used to map fabrics within the Wakemup Bay pluton. The details of the analysis are given in Charkoudian (2003). The Wakemup Bay pluton contains a girdle of oblate fabrics in the center of the pluton and contains prolate fabrics on its east and west ends (Fig. 18). It cores the hinge of a doubly plunging F_3 fold, or a dome structure, and the oblate fabrics occur at the highest part of this dome, where the most flattening is expected to occur. The magnetic foliations (k1–k2 plane) in the pluton dip shallowly (Fig. 18). The magnetic lineations (k1 direction) plunge shallowly E and W and parallel the long axis of the pluton and the F_3 fold hinge (Bauer, 1986). Magnetic fabric and field fabric are compared on equal area, lower hemisphere stereonets (Fig. 18). The maxima of the poles to foliation are vertical for magnetic and field foliations.

Magnetic foliations do not correlate with field foliations in the Wakemup Bay pluton. Magnetite, which controls the orientation of the AMS ellipsoid, crystallizes well before biotite, which locally controls the field foliation. Therefore, the two minerals may record different parts of the emplacement history. Most likely, however, different features were measured for the AMS and field fabrics. The dominant fabric element at the margins of the Wakemup Bay pluton is centimeter-scale compositional layering. Given the present exposure level of the pluton relative to the schist (i.e., the roof is exposed), most of the tonalite outcrops must originally have been near a contact. The foliation defined by compositional layering is not necessarily parallel to the internal fabric within the layer. Unfortunately, as there appears to be no spatial pattern to the AMS data, further speculation for the deviation of the fabrics is unwarranted.

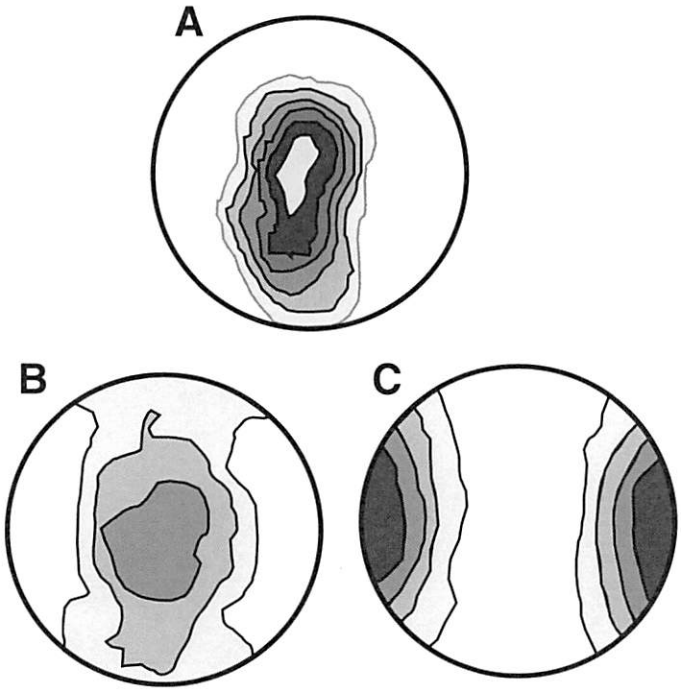

Figure 18. Anisotropy of magnetic susceptibility (AMS) results from the Wakemup Bay pluton, shown in lower hemisphere, equal area stereonet projections. (A) Pole to field foliations. (B) Pole to magnetic foliations, and magnetic lineations.

Stop 3-7: Wakemup Campground

Turn S on County Road 478 (Wakely Road) and follow signs for Wakemup campground. (15T 469270E, 5305442N)

This stop provides an overview of Lake Vermilion and the Wakemup narrows. The parking lot, however, has a variety of tonalite samples from different parts of the intrusion. There is also a small outcrop on the west flank of the hill that contains some campsites; it can be observed (if one "rolls back" the moss). We will discuss the gravity results at this stop, where the topographic features can be observed.

Wakemup Bay Tonalite Gravity Study and Three-Dimensional Shape

A gravity survey was conducted on the Wakemup Bay pluton in 1995. This work was done in collaboration with J.-L. Vigneresse (CREGU–University of Nancy, France); details are reported in Charkoudian (2003). We will focus on just the Bouguer anomaly and three-dimensional inversion of the shape of the Wakemup Bay pluton at depth. It is important to note, because the roof of the pluton is exposed over the center of the intrusion, that the inversion provides a nearly complete three-dimensional picture of the shape of the body.

The Bouguer anomaly map of the Wakemup Bay pluton (Fig. 19) yields –72 to –66 mGal values. The large negative values are indicative of the underlying low-density Wakemup Bay tonalite. The Bouguer anomaly is made up of closed mGal contours, which are concentric and elliptical. The long axis of the elliptical contours trends E-W and parallels the strike of the granite-greenstone belts. A –4 mGal anomaly in the center of the Bouguer map corresponds with the less dense Wakemup Bay pluton. The maximum mGal value, –71 mGal, corresponds with the southeast section of the pluton, and the lowest value, –67 mGal, corresponds with the northern outcrop of the pluton. The small amplitude of the gravity anomaly indicates a shallow and thin pluton, and the steep mGal gradient on the SW side is indicative of root zones.

The Wakemup Bay pluton was modeled, using an iterative inversion technique, with the programs of Vigneresse (1990), based on the Cordell and Henderson (1968) method. Overall, the pluton is a thin, subhorizontal body with a thickness of <0.5 km. There are two deeper zones, apparent from the inversion, which extend to 4 and 2.5 km, respectively. The deepest zone is at the SW part of the pluton and trends NW-SE. At depth, this zone does not lie below the pluton outcrop; rather, it lies below the

biotite schist outcrops. This zone is controlled by low negative values in the Bouguer anomaly map and is not related to the low-density schists. Therefore, we interpret this deeper zone as a true increase in the depth of the pluton. The second deeper zone extends only to 2.5 km in depth but is approximately in the center of the exposed area of the Wakemup Bay tonalite. In map view this gravity anomaly appears centered on the SE corner of the Wakemup Narrows Peninsula (Fig. 19). A cross section of the pluton is shown in Figure 20.

The negative gravity anomaly does not extend to the Haley fault on the southern side of the Vermilion block. On the northern side the gravity anomaly appears truncated by the Vermilion

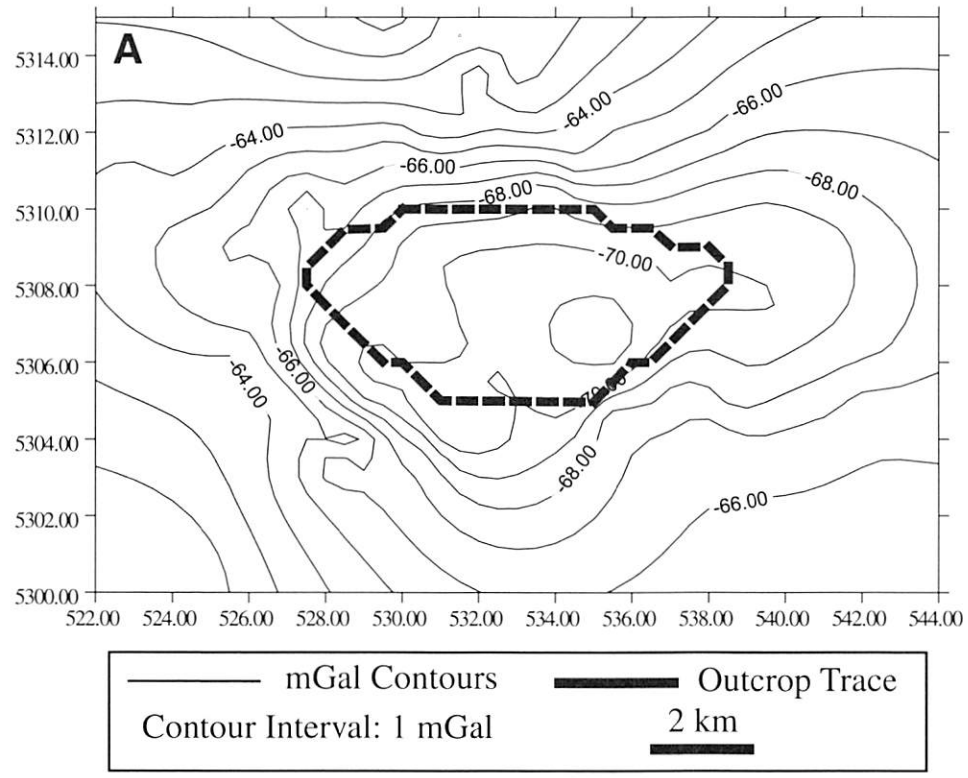

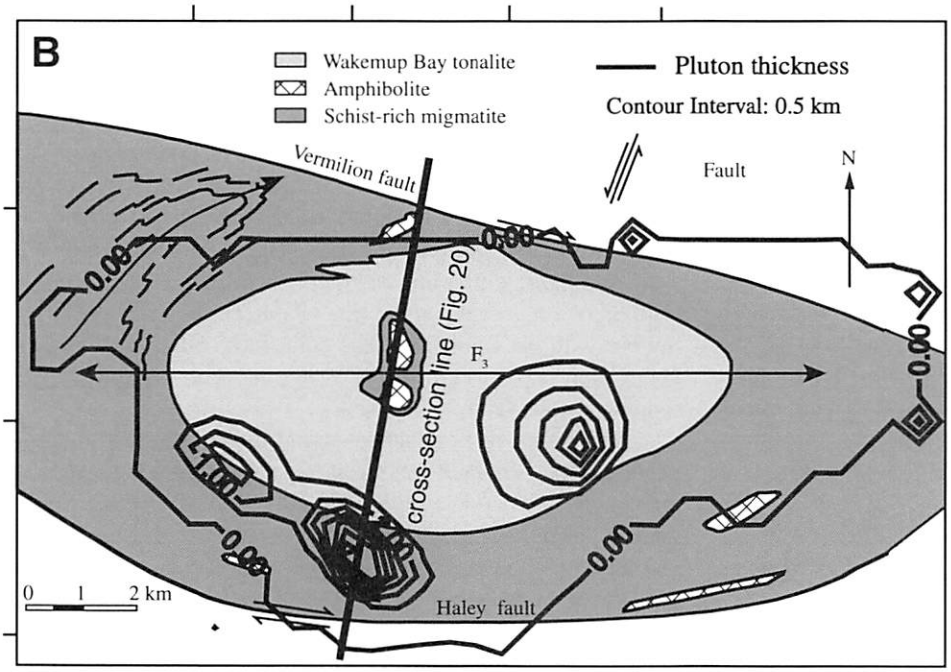

Figure 19. (A) Bouguer anomaly map of the Wakemup Bay pluton, with the outline of the pluton shown in a thick line. (B) Three-dimensional gravity inversion map of the Wakemup Bay pluton, with contours of 0.5 km thickness, overlaid on the geological map. Because the roof is exposed, the gravity inversion shows the approximate true three-dimensional pluton. The thickest part of the pluton extends to ~4 km below the biotite schist just outside the SW margin of the pluton. Another thick root zone is exposed below the Wakemup Peninsula. Although faults were not included as boundary conditions, the gravity inversion indicates that the pluton does not cross the Haley or Vermillion fault.

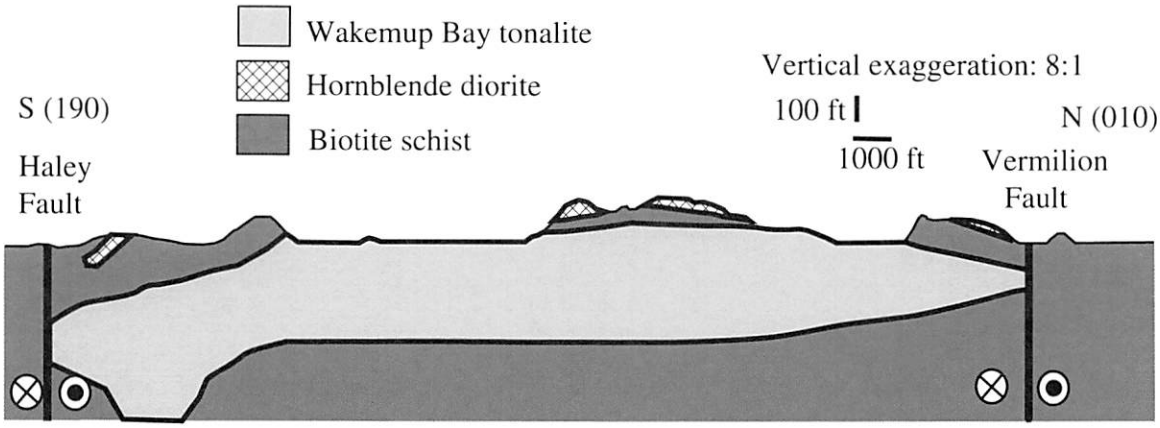

Figure 20. Cross section through the Wakemup Bay pluton, highlighting that the main root zone is below the biotite schist and not the tonalite. Location of line is given in Figure 19. The cross section is oriented 010–190. The position of the appinite (hornblende diorite) sill highlights the relative position of the roof of the Wakemup Bay pluton.

fault, although it does slightly overlap in the NE part of the field area. However, the pluton in this region is so thin (<0.5 km) that its exact extent is not constrained here. Because no assumptions were made about the positions of the faults before undertaking the gravity inversion, we consider that the inversion is consistent with the mapped geology.

Emplacement of Wakemup Bay Pluton

The synthesis of field mapping (Bauer 1986), AMS data, microstructural analysis, and gravity data indicates that the Wakemup Bay pluton was emplaced into the hinge of an F_3 fold (Fig. 9). In addition, along its northern contact the pluton is locally incorporated into F_2 folds. Therefore, field mapping indicates that pluton emplacement was associated with late stage F_2 folding to early F_3 folding. Additionally, the thinness of the body, as determined from the gravity studies, suggests that it intruded into an anticlinal hinge.

Magnetic lineations in the Wakemup Bay pluton obtained from AMS analysis plunge shallowly and parallel the F_3 fold hinge. If the pluton was emplaced after folding, we would expect lineations to trend in a radial manner away from the feeder zones of the pluton. Therefore, the pluton likely intruded during the folding event.

Microstructures are predominantly magmatic, with localized areas of solid-state deformation. If the pluton was emplaced, crystallized, and then folded, a greater extent of solid-state deformation would be expected. Therefore, microstructural studies show that the pluton must have been emplaced either syn-folding or post-folding. In conclusion, by combining AMS data, microstructural analysis, and field mapping, it is evident that the pluton probably was emplaced during a late stage of F_2 folding and an early stage of F_3 folding.

Post-Emplacement Translation of the Wakemup Bay Pluton along the Vermilion Fault

The gravity and microstructural data provide insights into the post-emplacement of the Wakemup Bay pluton as it was affected by the Vermilion fault system. The lack of any cataclastic microstructures as one approaches the Vermilion fault—the northern boundary of the pluton being locally only several hundred meters from the fault—suggests that the pluton was significantly stronger than the surrounding biotite schist. The gravity inversion suggests that the geographic extent of the pluton in outcrop is basically the same as its extent in the subsurface. Thus, on a regional scale the location and extent of the pluton controlled the location and orientation of the fault system. This observation is particularly true for the root zones, extending to 4 km and 2.5 km, which approach the Haley fault. Earlier in the deformation history (through F_2 and F_3 folding) the pluton was a regionally incompetent unit; however, by the time motion commenced on the Vermilion fault the pluton cooled and became a regionally competent unit.

Sims (1976) proposed that the Haley fault was originally a dip-slip fault, bringing up higher grade rocks on the north. Further, he suggested that the Haley fault was possibly once continuous with the Burntside Lake fault.

There are three different options for the apparent juxtaposition of higher grade Vermilion Granitic Complex rocks on the north side of the Haley fault and lower grade rocks on the south side. Sims (1976) proposed that the Haley fault was originally a dip-slip fault, with a minimum of several kilometers of throw. Further, he suggested that the Haley fault was possibly once continuous with the Burntside Lake fault. In this interpretation, the Haley fault could be either a NW-dipping reverse fault or a SE-dipping normal fault.

An alternative explanation is that the Haley fault is dominantly a strike-slip fault that has brought higher grade rocks from the central Quetico (Vermilion Granitic Complex) ESE to their present position. This scenario is consistent with the observation that the same juxtaposition of metamorphic grades occurs along the Vermilion fault away from the Haley and Burntside Lake faults. We propose the following model, assuming that the Vermilion and Haley faults are both dominantly strike-slip faults. When

the Vermilion fault was initially activated, it cut around the Wakemup Bay pluton on its south side, avoiding the thickest and strongest part of the pluton. As a consequence, a promontory consisting of the Wakemup Bay pluton was created in the fault system, with the Vermilion fault cutting N of the Wakemup Bay block. That is, the thickness of the Wakemup Bay pluton locally controlled the geometry and behavior of the Vermilion fault system. The Haley fault continued to act dominantly as a strike-slip fault.

A possible analogous situation to the Wakemup Bay pluton is the currently active Katamaz block, a 100-km, lozenge-shaped, fault-bounded block in western Pakistan (Haq and Davis, 1997). As a result of oblique convergence, the Katawaz block is translating to the northwest along the Chaman fault, the local boundary between the Indian plate and the Eurasian plate. Deformation in the Katawaz block is evident as the Sulaiman Range, which surrounds the Katawaz block. Haq and Davis (1997) modeled the Katawaz block deformation using plexiglass and sand and assumed that the deformation is duplex-style, thin-skinned thrusting, affecting only the upper lithosphere, with no internal deformation. They found that in "simple" oblique convergence, thrusting was normal to the plate margin, resulting in a ridge running parallel to the plate margin. When the fault-bounded block was added, thrust faulting was oblique to the plate margin, and a sand ridge surrounding the plexiglass block was formed (with geometric similarities to the Sulaiman Range). The greater the translation, the greater the deformation resembled the "simple" oblique convergence model (with no fault-bounded block), and a ridge that parallels the plate margin. We use this modeling study to suggest that the Wakemup Bay pluton acted as a regional strength heterogeneity in the Vermillion fault system, thus resulting in the same pattern seen on a larger scale in the Katawaz block of Asia.

Travel from Lake Vermilion area to Ely, Minnesota, for dinner and lodging.

DAY 4: BURNTSIDE LAKE AREA AND VERMILION DISTRICT

Stops on Day 4 examine (1) the boundary between the southern Vermilion Granitic Complex and the central Vermilion District, described by Bauer and Bidwell (1990); (2) the Burntside Lake pluton along the southern margin of the Vermilion Granitic Complex, most recently studied by Charkoudian (2003); (3) folding, shear zone development, and strain in the Vermilion District; and (4) evidence for transpression as the dominant mechanism responsible for the D_2 deformation pattern in the central and western Vermilion District, first elucidated by Hudleston et al. (1988). The effects of transpression extend well south into the Vermilion District from the boundary.

All stops are shown in Figure 8, and localities are described by UTM coordinates based on NAD 83, UTM Zone 15T.

Part 3: Burntside Trondhjemite and Adjacent Areas

Stops 4-1 and 4-2 are in the Vermilion Granitic Complex.

Stop 4-1: Echo Trail Outcrop

Take Highway 88 on the East side of Ely, turning right (N) onto Highway 116 (Echo Trail) in ~3.5 km (2.2 mi). Continue N on Highway 116, past Burntside Lake, until it intersects County Road 803, ~6.9 km (4.3 mi). The outcrop is at the SW corner of that "T" intersection. (15T 418344E, 5312066N)

This outcrop is composed of biotite schist, north of the contact with the Burntside trondhjemite. The schist contains numerous veins of the pluton, forming a complex intrusion migmatite. Numerous kinematic shear sense indicators indicate dextral movement on the horizontal, glacially polished surface. Lineation is steeply plunging within the sub-vertical foliation. Sinistral shear sense indicators do occur (Figs. 21A and 21B), and both the schist and the veins have been folded by probable F_3 folds. Fold axes in the schist plunge gently east and west. A recent article by Erickson (2010) emphasizes that the types of fabrics exposed in this type of shear zone (specifically the Shagawa shear zone) may record a large component of vertical movements. This

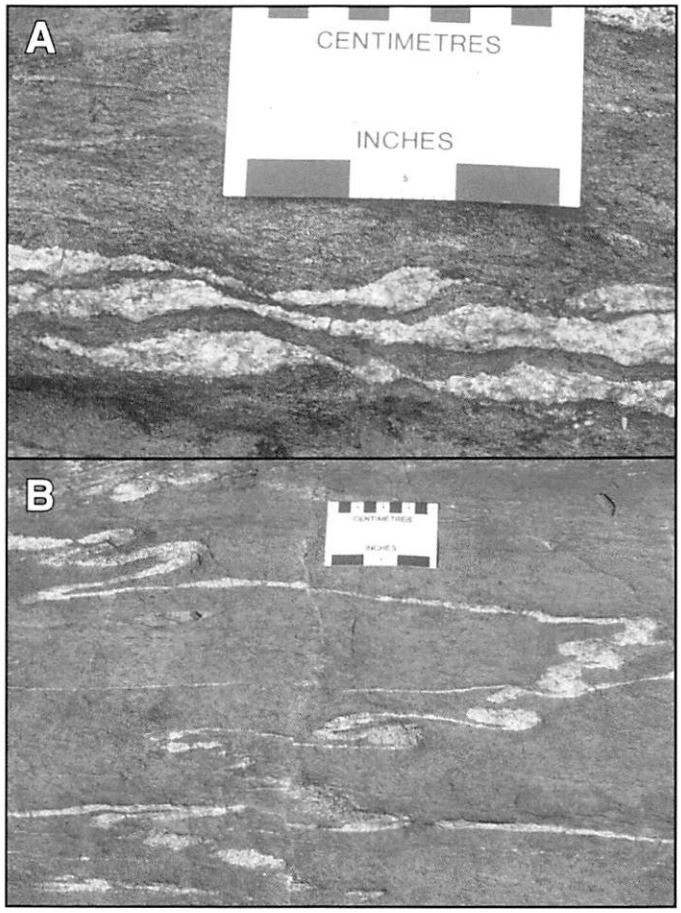

Figure 21. Field photos of Echo Trail outcrop. (A) Asymmetric boudins in granitic veins, indicating dextral shear. (B) Dextral shear folds (upper left) and back-rotated and sheared fold limbs (right central) produced by dextral shear.

interpretation contrasts with the transpression interpretation of Hudleston et al. (1988).

Stop 4-2: Burntside Trondhjemite on Echo Trail

Return S on Highway 116 for 1 km (0.6 mi). There is a large outcrop on the east side of the road, opposite Burntside Lake. (15T 417902E, 5311882N)

The Burntside Lake pluton is a small, lenticular-shaped pluton that is 2 by 11 km in outcrop extent, and outcrops on the islands and shores of Burntside Lake in the southeastern end of the Vermilion Granitic Complex (Fig. 10). Sims and Mudrey (1972) defined the Burntside Lake pluton as a foliated leucocratic granite or trondhjemite. Major minerals in this pluton are plagioclase, quartz, and biotite, with minor chlorite, hornblende, and microcline, zircon, apatite, and magnetite.

The Burntside Lake pluton is intrusive with the biotite schist on the north, west, and east sides, and amphibolite on the south side. Amphibolite occurs in massive and layered forms with local inclusions of metagabbro adjacent to the Burntside Lake pluton. A hornblende lamprophyre cuts the pluton in the south-central part of the pluton. Along the contact of the pluton the trondhjemite intertongues repeatedly with the biotite schist and amphibolite and cross-cuts these rocks.

Deformation in the Eastern Burntside Lake Area

Foliation in the Burntside Lake pluton is defined by alignment of biotite grains, and in some areas by stretched quartz. Foliations dip steeply and are parallel to the north and south boundaries of the pluton (Figs. 10 and 22). Along its periphery, foliations in the biotite schist are parallel to the borders of the Burntside Lake pluton, which locally contains a linear fabric (Fig. 22).

In addition, the long axis of the Burntside Lake pluton is parallel to the hinge of the Twin Lakes synform, which is a major F_3 fold 4 km north of the Burntside Lake pluton (Bauer et al., 1992). The Twin Lakes synform is cored by amphibolite and was probably formed during emplacement of the Lac La Croix Batholith (Bauer and Bidwell, 1990). In addition to the Twin Lakes synform, folding is pervasive throughout the area. Near the SW end of the Burntside Lake pluton, major F_2 folds and refolded fold hinges are oriented to the NNE. Locally, F_2 folds are incorporated into the Burntside trondhjemite, which indicates that the trondhjemite was emplaced prior to, or during, F_2 folding. F_2 folds that were initially plunging to the west were refolded at the SW margin of the Burntside Lake pluton, to plunge NE. Bauer and Bidwell (1990) suggest that during regional contraction the pluton acted as a rigid body, and that this local deviation in kinematics caused the refolding. The latest deformational event is pervasive NNE-trending sinistral faulting and some dextral WNW faulting, both with minor offsets (Fig. 10).

Microstructures

Microstructures were characterized in the Burntside Lake pluton, and are shown in Figure 23. Microstructures were classified into magmatic (Fig. 23A), crystal-plastic (Fig. 23B), severe crystal-plastic (Fig. 23C), and low-temperature cataclasis (Fig. 23D). On the western half, magmatic fabric is evident where quartz has lobate boundaries and plagioclase has planar boundaries. Deformation is more extensive on the eastern half of the Burntside Lake pluton, where severe crystal-plastic deformation is common.

Solid-state deformation is probably (1) a result of late-stage, NW-trending sinistral faults that cross-cut the Burntside Lake pluton (Fig. 10); or (2) a result of right-lateral deformation associated with the Vermilion fault. Both events presumably occurred during the latest movement on the Archean fault system. If the pluton intruded prior to folding, then solid-state deformation would be pervasive throughout the pluton. Because solid-state deformation is localized on the east side, microstructural analysis indicates that the pluton probably intruded syn-folding, or post-folding. Therefore, the Burntside Lake pluton probably intruded during late-stage F_2 folding, and perhaps during early stage F_3 folding.

AMS of Burntside Lake Pluton

AMS analysis was conducted for the Burntside Lake pluton and is reported in Charkoudian (2003). For our purposes, we will only report the orientation of fabrics that are derived from this study. Magnetic foliations trend ENE, dip steeply, and are oriented parallel to the pluton-schist contact. Magnetic lineations plunge shallowly and trend parallel to the long axis of the

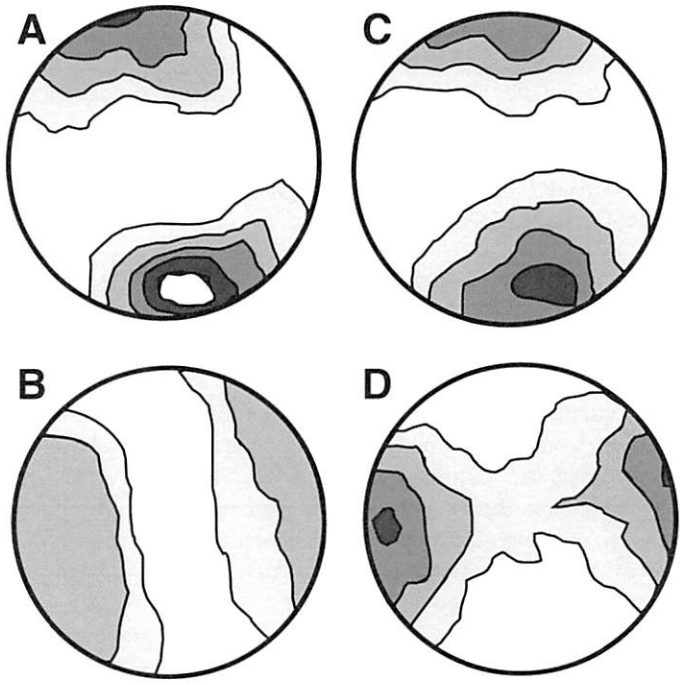

Figure 22. AMS results from the Burntside Lake pluton, shown in hemisphere, equal-area stereonet projections. (A) Pole to field foliations (n = 102). (B) Field lineations (n = 6). (C) Pole to magnetic foliation (n = 39). (D) Magnetic lineation (n = 39).

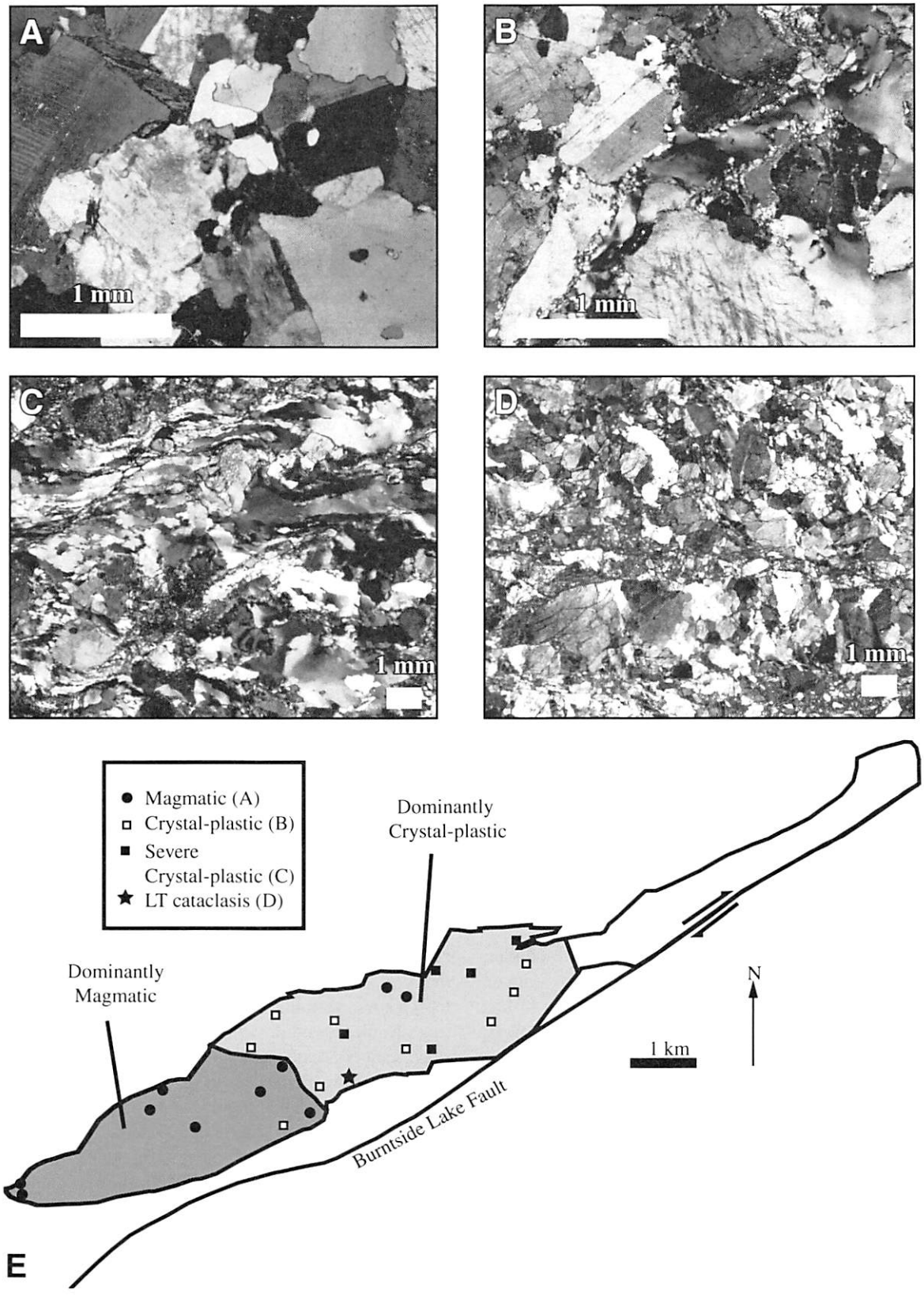

Figure 23. Photomicrographs of thin sections from the Burntside Lake pluton, taken under cross-polarized light and with a 1-mm scale bar. (A) Magmatic fabric as illustrated by large, equant grains and high-angle grain boundaries. (B–D) Crystal-plastic deformation, showing increasingly low-temperature (LT) deformation. (E) Map view of the distribution of microstructures.

Burntside Lake pluton (Fig. 22). Figure 22 shows magnetic fabrics and field fabrics plotted on lower-hemisphere, equal-area stereonet projections. Poles to field foliation and poles to magnetic foliation both dip shallowly NNW and SSE (Fig. 22). Both field lineations and magnetic lineations plunge shallowly to moderately to the ENE and WSW.

In summary, the AMS fabrics in the Burntside Lake pluton are consistent with the field measurements and are much better developed than AMS fabrics in the Wakemup Bay pluton. The steeply dipping foliations and subhorizontal lineations that are recorded in the parts of the pluton where magmatic fabrics dominate are parallel to the solid-state deformation fabrics to the SE, suggesting syntectonic intrusion.

Burntside Lake Pluton Gravity Study and Dip of the Archean Subprovince Boundaries

A gravity study was conducted on the Burntside Lake pluton across the Burntside Lake fault and is reported in Charkoudian (2003). We report here only on the Bouguer anomaly and how it constrains the geometry of the subprovince boundary.

The mGal values in the Bouguer anomaly map of the Burntside Lake pluton (Fig. 24A) range from −71 to −51 mGal. A steep, northeast-southwest–trending mGal gradient is the most significant gravity anomaly, extending throughout the gravity survey, and corresponding to a 1 mGal change over 0.1 km from 68 mGal to 60 mGal. This 10 mGal gradient corresponds to the density contrast across the Burntside Lake fault. This fault juxtaposes the −71 to −66 mGal Quetico schists to the north with the −64 to −51 mGal Wawa greenstone to the south. On the south side of the fault, contours are parallel to its trend. Contours become more negative to the south, with a gentle gradient, which corresponds to the meta-sediments of the Newton Lake Formation. To the north of the steep gradient, the mGal contours are normal to the fault trend and increase in value to the northeast.

Although it was intended to determine the three-dimensional shape of the Burntside Lake pluton, the gravity data are much more useful for determining the dip of the fault. In fact, the Burntside Lake pluton appears to have a minimal gravity signal (~1 mGal). This situation arises because there are very dense rocks on the south side of the Burntside Lake fault and the generally lower density Burntside Lake pluton on the north side. Charkoudian (2003) used a geophysical interpretation software program (WinGLink) to model the Burntside Lake pluton and the geometry of the Burntside Lake fault with a forward model. The locations and densities of the fault and pluton were held constant, and the two-dimensional geometries at depth were manipulated. The granite schist of the Vermilion Granitic Complex, with a density of 2.76 g/cm^3 was input as the surrounding rock. The location of the fault at the surface was held constant, and the greenstone was modeled with a density of 2.85 g/cm^3 to a 6 km depth. Finally, fault angles were manipulated for a best fit.

Forward gravity models were constructed on the transect shown in Figure 24A. The data are best matched by a steeply north-dipping Burntside Lake fault with a 2–3-km-thick Burntside Lake pluton (Fig. 24B). Charkoudian (2003) used an additional transect and found the same result. On the basis of her study, it appears that (1) the Burntside Lake pluton is ~2 km deep, and (2) the Burntside Lake fault is vertical to steeply north dipping (~70°) adjacent to the Burntside Lake pluton.

Emplacement of the Burntside Lake Pluton

In the Burntside Lake pluton, solid-state deformation is pervasive on the east side, and magmatic deformation is pervasive on the west side. If the pluton intruded prior to folding, solid-state deformation would be pervasive throughout the pluton, which is not observed. Rather, solid-state deformation is localized on the east side, but with fabrics forming in magmatic foliation that are parallel to the solid-state foliation. We interpret that the Burntside Lake pluton probably intruded during late stage F_2 folding and perhaps during early stage F_3 folding.

It is possible to speculate that the Wakemup Bay and Burntside Lake plutons are, in fact, the same body that has been offset along the Vermilion fault. Charkoudian (2003) investigated this possibility specifically, documenting chemical variations in the minerals, and found ambiguous results. Neither the biotite nor the plagioclase compositions overlapped in value; thus, it is probably best to consider them separate plutons.

Movement on the Burntside Lake Fault

Sims (1976) suggested that the Burntside Lake fault was initially active as a dip-slip fault in order to explain the exhumation of the amphibolite facies rocks on the north side relative to the greenschist facies rocks on the south side. The fault is often assumed to be a normal fault, although this interpretation requires a south-dipping fault. The gravity analysis, in contrast, indicates that the boundary is vertical to steeply north dipping. Thus, assuming dip-slip motion, it is more likely that the Burntside Lake fault is a reverse fault, which makes more sense for both the Burntside Lake and Haley faults, particularly considering that the Quetico-Vermillion boundary is dominantly transpressional (e.g., Hudleston et al., 1988) and includes no other evidence of significant N-S extension.

Alternatively, the Burntside Lake fault could be a dominantly strike-slip fault, albeit steeply dipping, in the overall Vermilion transpressional fault zone system. The San Andreas fault in southern California may be a useful analogue for this alternative. The overall deformation along the San Andreas fault system is dextral transpressional (e.g., Teyssier and Tikoff, 1998), with different types of kinematic partitioning occurring along strike. Sylvester (1988) describes deformation in the Salton Trough area, where volcanic rocks are bounded to the northeast by the Painted Canyon fault, and to the southwest by the Skeleton Canyon fault, which dips 60°–70°. This volcanic block was uplifted and juxtaposed with sedimentary basin fill. In this locality, basement rocks were differentially uplifted in response to dominantly

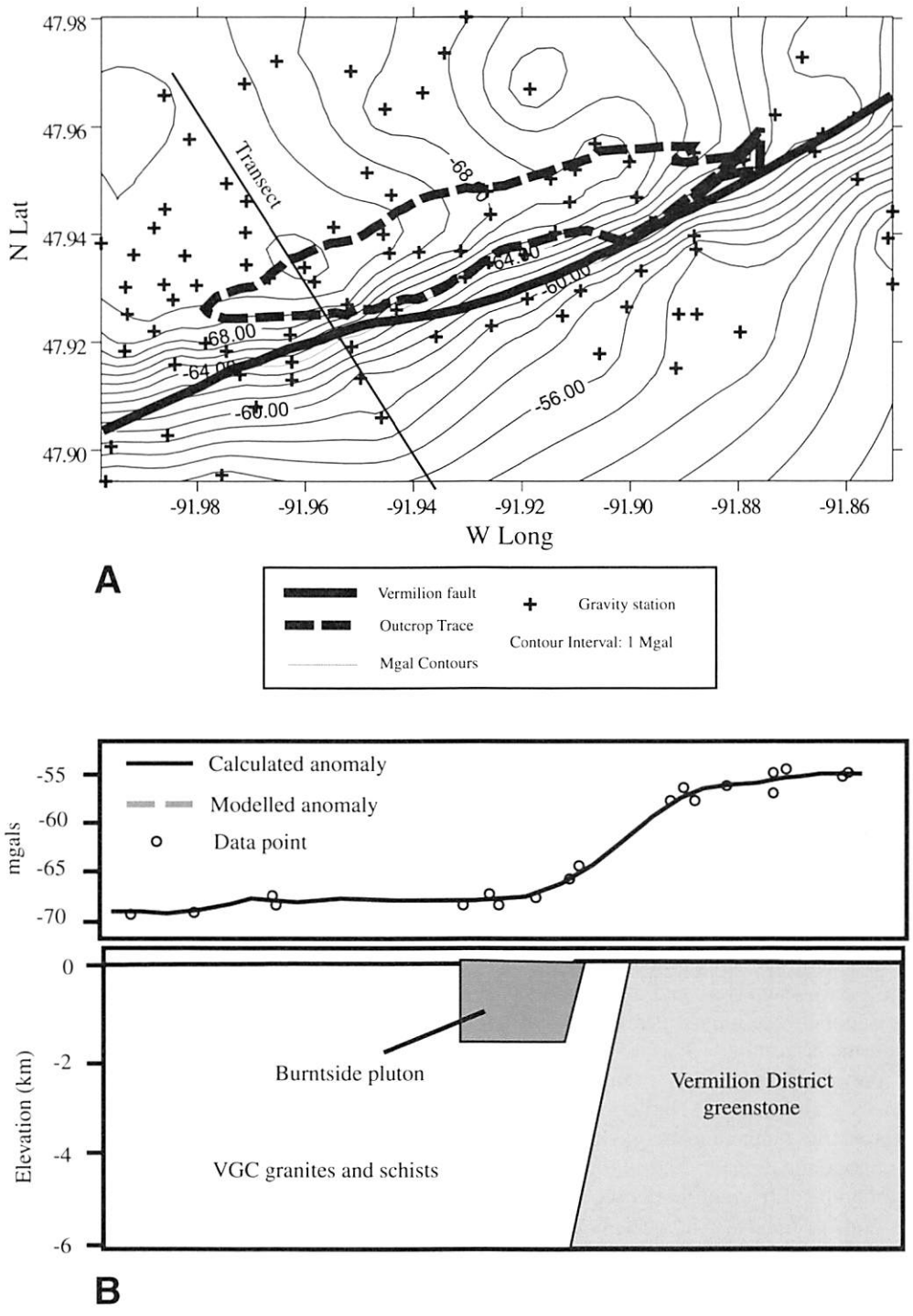

Figure 24. Gravity results from the Burntside Lake pluton. (A) Bouguer anomaly map, showing stations as plus signs, the Burntside Lake fault as a dark line, the surface extent of the Burntside Lake pluton as a dashed line, and the location of the transect used for B as a solid line. (B) The result of forward gravity modeling. The best-fitting model utilizes a N-dipping contact between the Vermilion Granitic Complex (VGC) and the Vermilion District, with a ~2-km-thick (lower density) Burntside Lake pluton.

right-lateral motion on dipping faults. Thus, differential exhumation occurs in dextral transpressional regimes along steeply dipping strike-slip faults.

Part 4: Deformation in the Central and Western Vermilion District

Stops 4-3 through 4-7 are in the Vermilion District (Fig. 9). Several of these outcrops are also described in Jirsa et al. (2004).

The central Vermilion District (Fig. 8), in the vicinity of the town of Ely, includes the narrowest extent of the supracrustal sequence in the district, where it is confined between the faulted contact with the southern Vermilion Granitic Complex to the north and the intrusive contact with the Giants Range Batholith to the south. The supracrustal sequence is complex stratigraphically and structurally (in terms of competence contrast) owing to the interlayering of the rigid volcanic flows of the Ely Greenstone and the Newton Lake Formation with less competent iron formation and volcaniclastic metasediments. To the west the western Vermilion District widens into exposures of the deformed metagraywacke of the Lake Vermilion Formation as the contact with the Giants Range Batholith trends to the southwest. The supracrustal rocks in both parts of the Vermilion District have a complex geometry and deformation history produced by two periods of folding and numerous E-W–trending dextral shear zones that anastomose through the region. The rocks of the central Vermilion District dip steeply either side of vertical and strike to the east-northeast over most of the region. Stratigraphic younging, to the north in the overall rock sequence, varies locally as a result of both F_1 and F_2 folding. Structural facing in the axial surfaces of the F_2 folds is mostly W on horizontal outcrop surfaces, but locally E owing to F_1 folds.

Dextral transpression-induced strains across the Vermilion District have produced strong flattening strains with a generally steeply plunging *X*-axis (Stop 4-3) and a preponderance of *Z*-symmetry folds and cleavage almost parallel to, but left of bedding, in the volcaniclastic units (Stop 4-7). Away from the Vermilion fault toward the south, the strain in the Vermilion District becomes constrictional (Hudleston, 1976). A retro-deformation, geometric finite-element model that uses measured strains in contiguous domains across the Vermilion District can account for both north-south shortening and dextral shear and flattening strains that increase in intensity toward the Vermilion fault (Schultz-Ela and Hudleston, 1991). The strong competence contrast among the units in the central Vermilion District has resulted in the localization of transpression-induced shear zones within the less competent volcaniclastic sedimentary units and locally along the margins of the volcanic flows. S-C, C′, and S′ fabrics indicating dextral shear are locally well developed in the shear zones (Fig. 24). The shear zones are not easily accessible, however, except for the Mud Creek shear zone (Stop 4-4). Sheath folds produced by shearing in an unlithified state during F_1 and modified by F_2 are recognized locally (Stop 4-5), and are distinguished from typical F_1-F_2 interference patterns that are spectacularly illustrated in the Soudan Iron Formation (Stop 4-6).

Stop 4-3: Deformed Pillow Basalts of the Ely Greenstone

Drive west out of Ely on Highway 169 for ~0.4 km (~0.25 mi) to where the road bends to the right. The outcrop is the high road cut on the north side of the road. (15T 583836E, 5305847N)

Outcrops showing more than a two-dimensional view of pillowed greenstone are rare in the flat terrain of northern Minnesota. One sees deformed pillows in three dimensions in this exposure and can get a sense of the bulk strain that the rock has undergone. The pillows are flattened in the plane of cleavage (essentially the main face of the cut); the *Z*-direction is normal to cleavage, and the *X*- and *Y*-axes lie in the cleavage and are sub-equal in length. Thus these rocks occupy a zone of flattening strain. Cleavage strikes northeast and dips steeply south; the *X*-axes of deformed pillows and a weak to pronounced mineral lineation both plunge steeply northeast.

Stop 4-4: Mud Creek Shear Zone; Outcrops near the Crossing of Mud Creek Road over Mud Creek

Continue west on Highway 169 ~16.9 km (~10.5 mi) to Mud Creek Road. Turn north (right) on the Mud Creek Road and follow it for ~6.1 km (~3.8 mi) to Mud Creek. (15T 564207E, 5302806N)

Several small outcrops in the valley of Mud Creek illustrate various small-scale structures and fabrics characteristic of rocks that have undergone intense shear strain, all attributed to D_2. The best exposures are in scrub just north of the creek and within ~100 m of the road on the east side. The best example of local S_2' and F_2 development in a lens of otherwise uniform S_2 is here (see Fig. 24). In general, S_2 is subparallel to the margins of the Mud Creek shear zone (N 70° E). Locally, S_2 has been perturbed and rotated clockwise ~40° to form folds with a secondary crenulation cleavage (S_2') developed parallel to the axial plane. Both cleavages can be traced from within the perturbed zone outward to merge into a single planar fabric, S_2', in the surrounding rock. Good examples of en echelon tension veins can also be found in nearby outcrops.

On the outside of the first bend in the road north of the creek is a road cut in a pinkish quartz sericite schist, a rock produced by intense shear (Fig. 25). Nice shear bands (or C′ planes) are developed in this rock, which is rendered friable by the closely spaced and intersecting S and C planes. Farther along the road, after it has run some 500 m in a more or less westward direction, it turns to the north and begins to climb onto the ridge overlooking Mud Creek. There is a small quarry off to the right in which a highly fissile chlorite schist or mylonite is exposed, which is presumably derived from pillow basalt. Several features of these outcrops provide indicators of sense of shear, and these are consistently dextral. They include shear bands (or C′ planes, local development of S_2' where S_2 has been perturbed and rotated clockwise,

and formation of Z-folds (most commonly in association with S_2') (Fig. 24).

Although well developed in highly sheared rocks, such as at Mud Creek, similar features can be found through much of the Vermilion District, increasing in intensity of development as the Vermilion fault is approached. The Mud Creek shear zone is flanked on the north by pillowed greenstone (upper member of the Ely Greenstone) that is moderately deformed except in narrow shear zones, and on the south by assorted felsic tuff, tuff-breccia, block breccia, and their reworked sedimentary equivalents (tuffaceous member of the Lake Vermilion Formation). Sims and Southwick (1985) interpreted the highly schistose

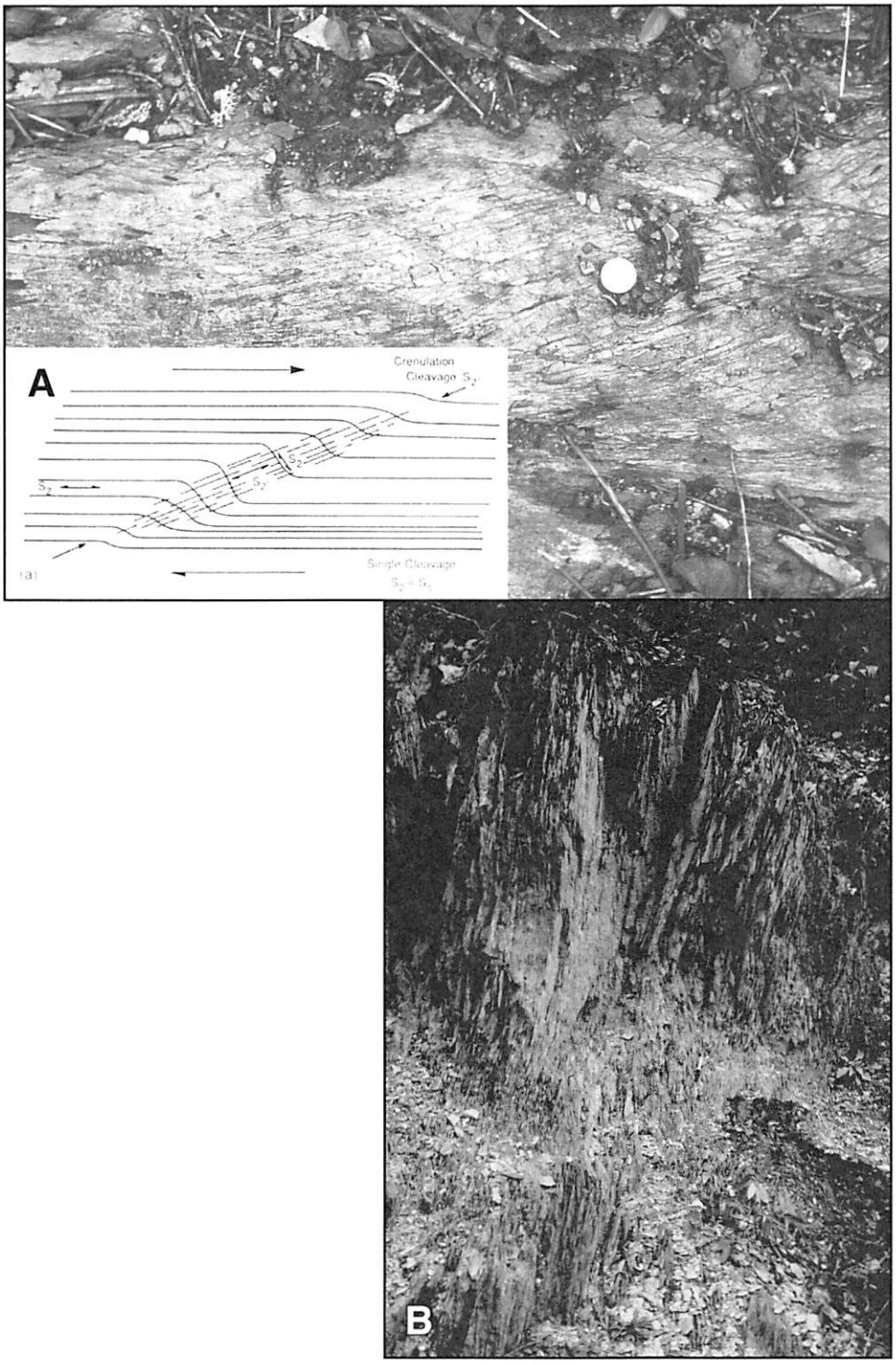

Figure 25. Photographs of rocks and fabric in the Mud Lake shear zone at Stop 4-4. (A) Intense dextral shear produced a strong planar fabric, S_2, that locally became folded, and a new foliation, crenulation cleavage S_2', developed axially planar to these folds that merges with S_2 outside the perturbed zone, as shown in the inset (after Hudleston et al., 1988). (B) Road cut in intensely deformed fault rock of steeply north-dipping quartz-sericite-chlorite schist or phyllonite.

material within the shear zone to have been derived chiefly from fine-grained felsic to intermediate tuff belonging to the Lake Vermilion sequence. It is now recognized that shear zones of this magnitude commonly contain the sheared equivalent of many different rock types, all reduced to a more or less common "fault rock" composed chiefly of quartz, sericite, and chlorite (Fig. 25). The phyllonitic rocks of the Mud Creek shear zone are similar to the "fault rocks" in other strike-slip fault zones elsewhere in the Superior Province. The westward extent of the Mud Creek shear zone beneath Lake Vermilion has not been established.

Stop 4-5: Soudan Mine Folds

Return to Highway 169 and travel west to the town of Soudan. Follow signs to the right toward Soudan State Park for ~0.5 km

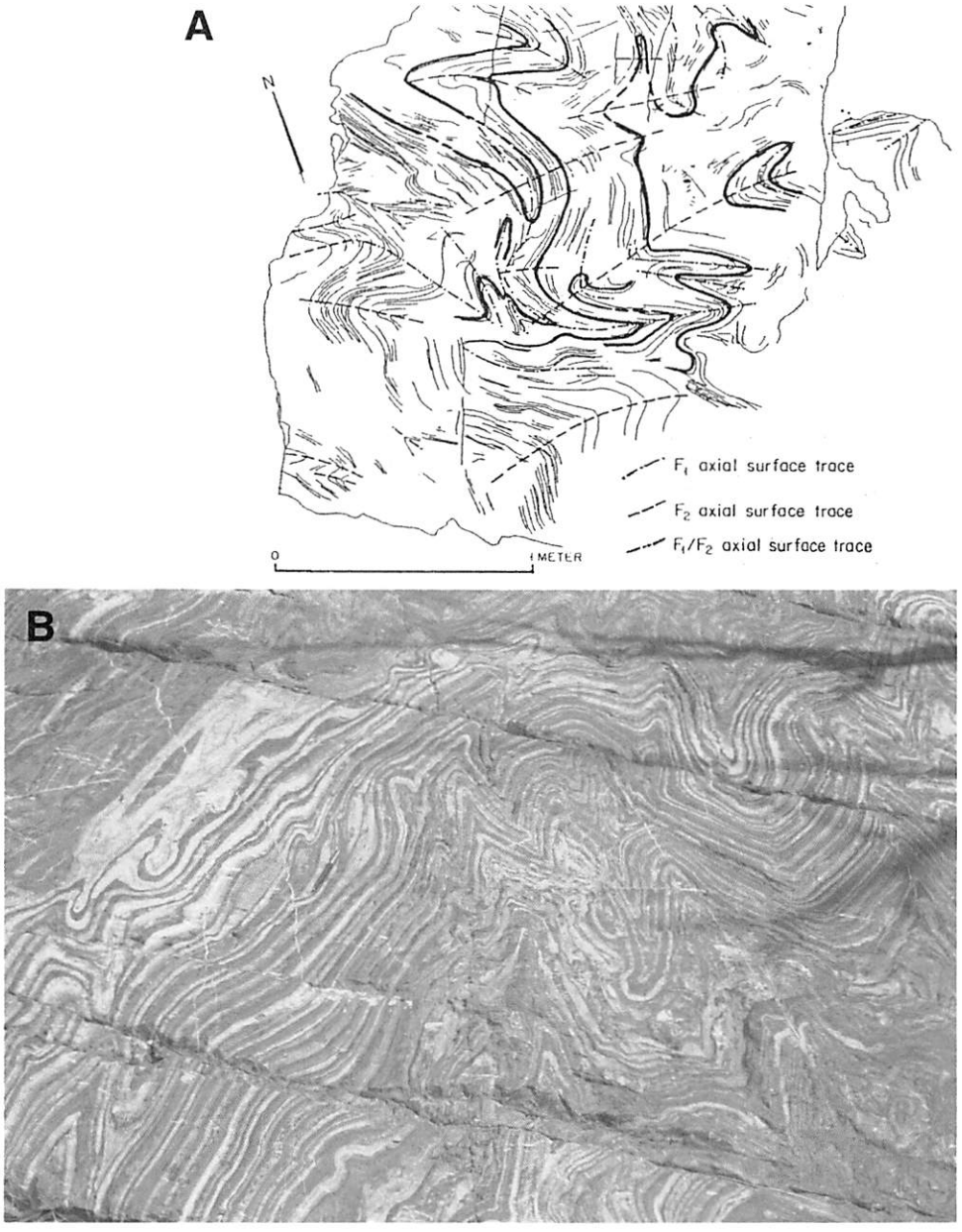

Figure 26. Classic outcrop of Soudan Iron Formation exposed at Stop 4-5. (A) Map showing F_1/F_2 fold interference, with selected horizons emphasized and axial surface traces shown (after Lundy, 1985). (B) Photograph of the outcrop.

(~0.3 mi): At this point do not follow State Park signs that indicate a turn to the left, but continue on the road, turning toward the right, and follow the road to the junction ~0.6 km (~0.4 mi) to the east. Turn left and drive for ~0.8 km (~0.5 mi), past the Soudan Fire Station and up the hill toward the back side of the Park and Stuntz Bay. Park at the mine buildings and walk ~150 ft north and uphill on the Stuntz Bay road to the glaciated surface outcrop on the right. (15T 557124E, 5296657N)

This classic exposure of the Soudan iron-formation member of the Ely Greenstone lies on the north limb of the Tower-Soudan Anticline, and at the stratigraphic top of the volcanic sequences that constitute the Lower member of the Ely Greenstone. It displays two generations of close folding in delicate laminations of chert (creamy white), chert-hematite (red), and magnetite-chert (black). The second-generation folds are of tectonic origin; their subvertical axial surfaces trend east-west, their axes plunge steeply east, and they are dominantly of *Z*-symmetry. The first-generation folds have been sharply refolded by the second generation, resulting in fold interference patterns of several types (Figs. 26A and 26B). Some geologists (e.g., Hooper and Ojakangas, 1971) have interpreted the first folds to be of tectonic origin; others (e.g., Hudleston, 1976) have suggested that they may have formed by soft-sediment processes. Small faults and kink bands of brittle origin cut across the folds.

Lundy (1985) studied the folding in this outcrop in considerable detail (cf. Fig. 26A) and concluded that some of the first-generation folds are sheath folds and thus appear as interference patterns without the involvement of F_2 (see discussion for Stop 4-6). Moreover, he found that the F_1 structures exhibit a wide variety of style and orientation, and are predominantly intrafolial. These observations suggest a high component of shear strain during D_1 and are consistent with layer-parallel, soft-sediment slumping as a probable mechanism to account for the F_1 structures.

Numerous late-stage, small-displacement strike-slip faults, trending nearly N-S, cut all earlier structures at this outcrop. Most of these faults show left-lateral displacement, but about one-fourth show right-lateral displacement (Craddock and Moshoian, 1995). Unlike the fracture zones of similar orientation seen at Stop 4-7, these structures do not have bands of cataclasis and arrays of secondary fractures associated with them. See Stop 4-7 for more information about the origin and timing of these structures.

The deep open pits a few meters north of the outcrop are early workings of the Soudan iron mine, the first iron mine in Minnesota. The mine produced ~16 million tons of high-grade hematite lump ore between 1884 and 1962, when high mining costs and changes in steel-making technology forced it to close. The early open-cut method of mining was replaced by underground operations in ca. 1900, and most of the historic production has come from underground mining. The mine was deeded to the state of Minnesota in 1962 and is now operated as a tourist facility featuring guided underground tours. Since 1999 the University of Minnesota has operated a high-energy physics laboratory in a space excavated half a mile down in the mine to minimize cosmic radiation. The main purpose of this lab has been to detect neutrinos and cryogenic dark matter.

Stop 4-6: Sheath Folds

Return to Highway 169 and turn right (west). Drive through the town of Tower and continue ~4.8 km (~3 mi) to just east of the junction of 169 and Pike Bay Drive (County Road 526). The outcrops are the glaciated surfaces on the south side of the road. (15T 550024E, 5293979N)

This outcrop of the Lake Vermilion Formation was revealed during highway realignment and power line construction ~40 yr ago, and it has become a field-trip classic. It clearly shows the superposition of two generations of folds in thin-bedded, well-graded turbidite (Fig. 27A). The second folds (F_2) are clearly tectonic, inasmuch as they are associated with regional axial-plane

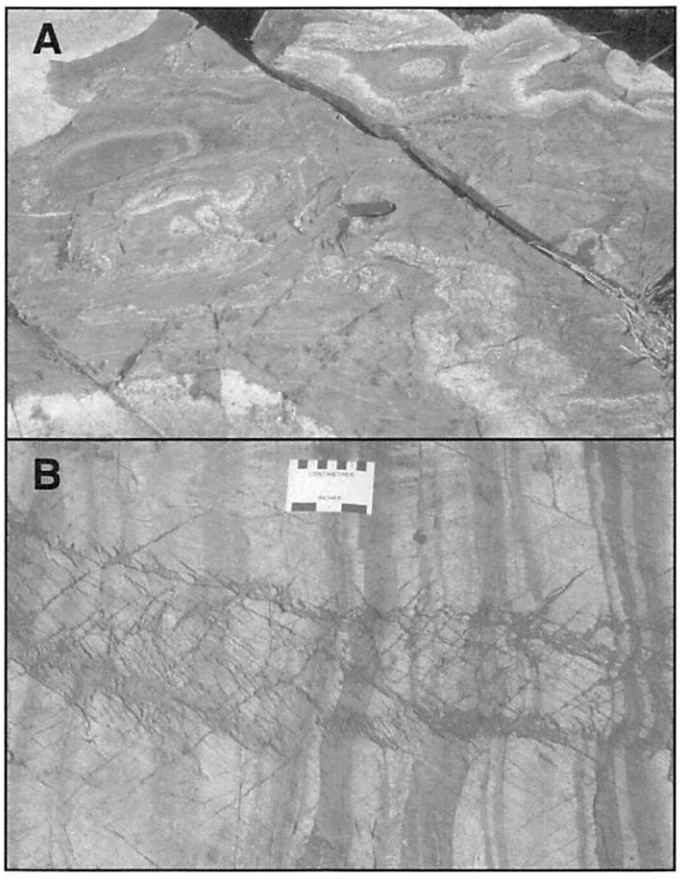

Figure 27. Photographs of turbidites of the Lake Vermilion Formation. (A) Planar and subhorizontal outcrop surface at Stop 4-6, displaying F_1 sheath folds outlined in graded graywacke beds and modified by D_2 deformation and F_2 folds. The F_1 structures are drawn out in an E-W direction by D_2. (B) Unfolded vertical beds of turbidite cut by late-stage brittle fracture zones, with Riedel and tension fractures of both left-lateral and right-lateral sense of movement. Exposed in subhorizontal glaciated outcrop at Stop 4-7.

cleavage in which sedimentary clasts are visibly flattened. The earlier folds (F_1) have no associated cleavage or observable clast strain, and tend toward concentric, cuspate, and bulbous morphologies in more competent layers. They include isoclinal folds and sheath folds. These characteristics are consistent with a soft-sediment or partially lithified origin for the F_1 structures (Hudleston, 1976), an interpretation the present leadership endorses. This position has not been accepted universally, however (Hooper and Ojakangas, 1971; Ojakangas et al., 1978).

The evidence for fold superposition includes interference patterns of several sorts ("eye" and "mushroom" forms are well represented) and the transection of F_1 folds by cleavage related to F_2 folding. Most of the "eye" interference structures, however, are wholly of D_1 age (Fig. 27A). They represent sheath folds associated with large shear strains. Removing the effects of D_2 strain and F_2 folds would not remove these structures. The magnitude of the D_2 strain is not nearly enough here to produce sheath folds; shear strains of about $\gamma = 10$ would be needed for this (Cobbold and Quinquis, 1980). One can find numerous examples of antiformal synclines and synformal anticlines, indicating local stratigraphic inversion prior to the second folding. As at Stop 4-7, the linear component of the metamorphic fabric is stronger than the planar, and the strain is constrictional. The S_2 cleavage is nearly vertical, with an east-west strike, and L_2 plunges at 40°–50° to the east.

Stop 4-7: Pike River Dam Outcrop

Continue west on Highway 169 for ~3.2 km (~2 mi) Turn right (north) on County Road 77. Drive ~0.8 km (~0.5 mi) and stop just past the bridge over the Pike River, with a dam visible on the left. (15T 547265E, 5293361N)

This outcrop of graded, thin-bedded, south-topping metagraywacke and slate of the Lake Vermilion Formation contains a good cleavage (left of bedding) and lineation (which is hard to appreciate on this flat outcrop), but, in contrast to the previous stops, no F_2 folds are present. Graded bedding and other structures characteristic of turbidites are exceptionally well preserved. Of the 201 graywacke beds in this outcrop, 64% are graded, and 9% of the 100 silt beds are graded (Ojakangas, 1972). The thin bedding displayed in this outcrop (~0.1 m) is relatively local; graywacke beds as thick as 3 m occur a short distance to the south, and nearly massive dacite tuff and reworked tuff occur just up the hill to the north. The graded graywacke beds in this thin-bedded section are composed of the same sand-size materials—volcanic quartz, plagioclase, and fine-grained dacitic rock fragments—as the more massively bedded tuffaceous and agglomeratic rocks.

Although F_2 folds are lacking in this outcrop, the relationships among bedding, cleavage, and stratigraphic younging directions are entirely consistent with the D_2 structural geometry of the previous two stops. They imply westward structural facing in the cleavage, and a position on the south limb of a large, south-overturned regional F_1 structure. Strain is still constrictional.

The prominent, mostly north-trending kink bands and shear zones traversing this outcrop (Fig. 27B) are the result of the youngest deformation, D_3, to affect the Vermilion District. These zones contain small-scale features indicative of progressive shear deformation in the brittle and brittle-ductile regime, and are uncommonly photogenic. Good examples of Riedel shears and en echelon extensional fractures can be seen. The fracture zones are in an orientation that is conjugate to a regional northeast-trending left-lateral fault, which follows the south side of the Pike River between the bridge and the dam. The dominant sense of displacement on the structures is right lateral and thus is consistent with the fracture zones and adjacent fault being conjugate structures, although it is clear that many of the individual fracture zones have undergone both left-lateral and right-lateral displacement, indicating that the history of late brittle deformation is not straightforward (Zahasky and Hudleston, 2010).

Based on the parallelism between the fracture zones and dikes of the 2.2 Ga Kenora-Kabetogama mafic dike swarm, Craddock and Moshoian (1995) interpret the fracture zones as being of Proterozoic age. However, the faults and fracture zones formed under a different stress regime than the dikes, and it is at least as likely that the dikes were emplaced along an older set of fractures, which we interpret as having been late stage in the amalgamation of the terranes of the Superior Province.

End of field trip.

ACKNOWLEDGMENTS

The authors wish to thank J. Craddock and M. Jirsa for reviews that allowed significant improvement to this guide. DMC acknowledges work by graduate students D. Fissler and T. Anderson on the Seine conglomerates, E. Thalhamer on the gabbroic shear zones, and L.M. Castaño (UAB) on the dikes; postdoctoral work by E. Horsman on the Seine conglomerates; previous field trip colleagues P. Fralick and K. H. Poulsen; and research colleagues J. Carreras and E. Druguet. PJH thanks P.K. Sims for introducing him to the joys of Archean geology many decades ago. BT wishes to thank J.L. Vigneresse for working on the gravity data collection and subsequent inversion for the Wakemup Bay pluton. The field mapping, microstructural analysis, and AMS data for the Wakemup Bay and Burntside Lake plutons, in addition to the gravity data for the Burntside Lake pluton, were collected by K. Charkoudian for her Master's thesis at the University of Wisconsin–Madison.

REFERENCES CITED

Bauer, R.L., 1981, The petrology and structural geology of the Western Lake Vermilion area, Northeastern Minnesota [Ph.D. thesis]: Minneapolis, University of Minnesota, 204 p.

Bauer, R.L., 1985, Correlation of early recumbent and younger upright folding across the boundary between an Archean gneiss belt and greenstone terrane, northeastern Minnesota: Geology, v.13, p. 657–660, doi:10.1130/0091-7613(1985)13<657:COERAY>2.0.CO;2.

Bauer, R.L., 1986, Multiple folding and pluton emplacement in Archean migmatites of the southern Vermilion granitic complex, northeastern

Minnesota: Canadian Journal of Earth Sciences, v. 23, p. 1753–1764, doi:10.1139/e86-161.

Bauer, R.L., and Bidwell, M.E., 1990, Contrasts in the response to dextral transpression across the Quetico-Wawa subprovince boundary in northeastern Minnesota: Canadian Journal of Earth Sciences, v. 27, p. 1521–1535, doi:10.1139/e90-162.

Bauer, R.L., and Tabor, J.R., 1990, Syntectonic, intermediate-pressure regional metamorphism along the northern margin of the Quetico belt in northeastern Minnesota: Contrasts with adjacent areas: Institute on Lake Superior Geology, Annual Meeting, 36th, Proceedings, v. 36, p. 2–4.

Bauer, R.L., Hudleston, P.J., and Southwick, D.L., 1992, Deformation across the western Quetico subprovince and adjacent boundary regions in Minnesota: Canadian Journal of Earth Sciences, v. 29, p. 2087–2103, doi:10.1139/e92-166.

Blackburn, C.E., Johns, G.W., Ayer, J., and Davis, D.W., 1991, Wabigoon subprovince, *in* Thurston, P.C., Williams, H.R., Sutcliffe, R.H., and Stott, G.M., eds., Geology of Ontario: Ontario Geological Survey Special Volume 4, pt. 1, p. 303–381.

Boerboom, T.J., and Zartman, R.E., 1993, Geology, geochemistry, and geochronology of the central Giants Range batholith, northeastern Minnesota: Canadian Journal of Earth Sciences, v. 30, p. 2510–2522, doi:10.1139/e93-217.

Bons, P.D., and Druguet, E., 2007, Some misleading boudin-like structures: Geogaceta, v. 41, p. 31–34.

Bons, P.D., Druguet, E., Hamann, I., Carreras, J., and Passchier, C.W., 2004, Apparent boudinage in dykes: Journal of Structural Geology, v. 26, p. 625–636, doi:10.1016/j.jsg.2003.11.009.

Borradaile, G.J., 1982, Comparison of Archean structural styles in two belts of the Canadian Superior Province: Precambrian Research, v. 19, p. 179–189, doi:10.1016/0301-9268(82)90058-4.

Borradaile, G.J., 1988, Magnetic susceptibility, petrofabrics and strain—A review: Tectonophysics, v. 156, p. 1–20, doi:10.1016/0040-1951(88)90279-X.

Borradaile, G.J., and Dehls, J.F., 1993, Regional kinematics inferred from magnetic subfabrics in Archean rocks of northern Ontario, Canada: Journal of Structural Geology, v. 15, p. 887–894, doi:10.1016/0191-8141(93)90182-A.

Borradaile, G.J., and Henry, B., 1997, Tectonic applications of magnetic susceptibility and its anisotropy: Earth-Science Reviews, v. 42, p. 49–93, doi:10.1016/S0012-8252(96)00044-X.

Borradaile, G.J., Werner, T., Dehls, J.F., and Spark, R.N., 1993, Archean regional transpression and paleomagnetism in northwestern Ontario, Canada: Tectonophysics, v. 220, p. 117–125, doi:10.1016/0040-1951(93)90226-A.

Card, K.D., 1990, A review of the Superior Province of the Canadian Shield, a product of Archean accretion: Precambrian Research, v. 48, p. 99–156, doi:10.1016/0301-9268(90)90059-Y.

Card, K.D., and Ciesielski, A., 1986, DNAG Subdivisions of the Superior Province of the Canadian Shield: Geoscience Canada, v. 13, p. 5–13.

Carreras, J., Czeck, D.M., Druguet, E., and Hudleston, P.J., 2010, Structure and development of an anastomosing network of ductile shear zones: Journal of Structural Geology, v. 32, p. 656–666, doi:10.1016/j.jsg.2010.03.013.

Castaño, L.M., 2007, Análisis estructural de venas y diques sintectónicos en Rainy Lake Wrench Zone, Superior Province (Ontario, Canadá) [M.S. thesis]: Universitat Autònoma de Barcelona, Spain, 148 p.

Chandler, V.W., 1991, Shaded-relief aeromagnetic anomaly maps of Minnesota: Minnesota Geological Survey State Map Series S-17, scale, 1:500,000, 1 sheet.

Chandler, V.W., and Lively, R.S., 2007, Revised aeromagnetic data for Minnesota: Minnesota Geological Survey Open File Report OFR_07_06, http://www.geo.umn.edu/mgs/magnetics.htm.

Charkoudian, K., 2003, A tale of two plutons: Pluton emplacement and strike slip deformation, Vermilion granitic complex, northern Minnesota [M.S. thesis]: University of Wisconsin–Madison, 216 p.

Cobbold, P.R., and Quinquis, H., 1980, Development of sheath folds in shear regimes: Journal of Structural Geology, v. 2, p. 119–126, doi:10.1016/0191-8141(80)90041-3.

Corcoran, P.L., and Mueller, W.U., 2007, Time-transgressive Archean unconformities underlying molasse basin-fill successions of dissected oceanic arcs, Superior Province, Canada: Journal of Geology, v. 115, p. 655–674, doi:10.1086/521609.

Cordell, L., and Henderson, R.G., 1968, Iterative three dimensional solution of gravity anomaly using a digital computer: Geophysics, v. 33, p. 596–601, doi:10.1190/1.1439955.

Craddock, J.P., and Moshoian, A., 1995, Continuous strike-slip fault–en echelon fracture arrays in deformed Archean rocks: Implications for fault propagation mechanics, *in* Ojakangas, R.W., Dickas, A.B. and Green, J.C., Basement Tectonics, v. 10, p. 379–407.

Cruikshank, K.M., and Johnson, A.M., 1993, High-amplitude folding of linear-viscous multilayers: Journal of Structural Geology, v. 15, p. 79–94, doi:10.1016/0191-8141(93)90080-T.

Czeck, D.M., 2001, Strain analysis, rheological constraints, and tectonic model for an Archean polymictic conglomerate: Superior Province, Ontario, Canada [Ph.D. thesis]: Minneapolis, University of Minnesota, 245 p.

Czeck, D.M., and Fralick, P., 2002, Field trip 3: Structure and sedimentology of the Seine Conglomerate, Mine Centre area, Ontario: Institute on Lake Superior Geology, Proceedings and Abstracts, v. 48, pt. 2, p. 37–67.

Czeck, D.M., and Hudleston, P.J., 2003, Testing models for obliquely plunging lineations in transpression: A natural example and theoretical discussion: Journal of Structural Geology, v. 25, p. 959–982, doi:10.1016/S0191-8141(02)00079-2.

Czeck, D.M., and Hudleston, P.J., 2004, Physical experiment of vertical transpression with localized nonvertical extrusion: Journal of Structural Geology, v. 26, p. 573–581, doi:10.1016/j.jsg.2003.07.002.

Czeck, D.M., and Poulsen, K.H., 2010, Field trip guide: Deformation in the Rainy Lake Region: A fabulous display of structures controlled by rheological contrasts: International Falls, Minnesota, Institute on Lake Superior Geology, Annual Meeting, 56th, pt. 2, p. 47–75.

Czeck, D.M., Maes, S.M., Sturm, C.L., and Fein, E.M., 2006, Assessment of the relationship between emplacement of the Algoman plutons and regional deformation in the Rainy Lake region, Ontario: Canadian Journal of Earth Sciences, v. 43, p. 1653–1671, doi:10.1139/e06-061.

Czeck, D.M., Fissler, D.A., Horsman, E., and Tikoff, B., 2009, Strain analysis and rheology contrasts in polymictic conglomerates: An example from the Seine metaconglomerates, Superior Province, Canada: Journal of Structural Geology, v. 31, p. 1365–1376, doi:10.1016/j.jsg.2009.08.004.

Davis, D.W., Poulsen, K.H., and Kamo, S.L., 1989, New insights into Archean crustal development from geochronology in the Rainy Lake area, Superior Province, Canada: Journal of Geology, v. 97, p. 379–398, doi:10.1086/629318.

Day, W.C., Southwick, D.L., Schultz, K.J., and Klein, T.L., 1990, Bedrock Geologic Map of the International Falls 1° × 2° Quadrangle, Minnesota, United States, and Ontario, Canada: Minnesota Geological Survey Miscellaneous Investigations Series Map I-1965-B, scale 1:250,000, 1 sheet.

Druguet, E., Czeck, D.M., Carreras, J., and Castaño, L.M., 2008, Emplacement and deformation features of syntectonic leucocratic veins from Rainy Lake zone (Western Superior Province, Canada): Precambrian Research, v. 163, p. 384–400, doi:10.1016/j.precamres.2008.02.001.

Dunnet, D., 1969, A technique of finite strain analysis using elliptical particles: Tectonophysics, v. 7, p. 117–136, doi:10.1016/0040-1951(69)90002-X.

Dutton, B.J., 1997, Finite strains in transpression zones with no boundary slip: Journal of Structural Geology, v. 19, p. 1189–1200, doi:10.1016/S0191-8141(97)00043-6.

Erickson, E.J., 2010, Structural and kinematic analysis of the Shagawa Lake shear zone, Superior Province, northern Minnesota: Implications for the role of vertical versus horizontal tectonics in the Archean: Canadian Journal of Earth Sciences, v. 47, p. 1463–1479, doi:10.1139/E10-054.

Fissler, D.A., 2006, A quantitative analysis of strain in the Seine River metaconglomerates, Rainy Lake region, Northwestern Ontario, Canada [M.S. thesis]: University of Wisconsin–Milwaukee, 100 p.

Fossen, H., and Tikoff, B., 1993, The deformation matrix for simultaneous simple shearing, pure shearing and volume change, and its application to transpression-transtension tectonics: Journal of Structural Geology, v. 15, p. 413–422, doi:10.1016/0191-8141(93)90137-Y.

Fralick, P., and Davis, D., 1999, The Seine-Coutchiching problem revisited: Sedimentology, geochronology and geochemistry of sedimentary units in the Rainy Lake and Sioux Lookout Areas: University of British Columbia, Western Superior Transect, Annual Workshop, 5th, Lithoprobe Secretariat, p. 66–75.

Frantes, J.R., 1987, Petrology and sedimentation of the Archean Seine Group conglomerate and sandstone, Western Wabigoon Belt, Northern Minnesota and Western Ontario [M.S. thesis]: Duluth, Minnesota, University of Minnesota–Duluth, 148 p.

Green, J.C., and Schulz, K.J., 1982, Geologic Map of the Ely Quadrangle, St. Louis and Lake Counties, Minnesota: Minnesota Geological Survey Miscellaneous Map Series M-50, scale 1:24,000, 1 sheet.

Grégoire, V., Darrozes, J., Gaillot, P., Nédélec, A., and Launeau, P., 1998, Magnetite grain shape fabric and distribution anisotropy vs. rock magnetic

fabric: A three dimensional case study: Journal of Structural Geology, v. 20, p. 937–944, doi:10.1016/S0191-8141(98)00022-4.

Haq, S.S., and Davis, D.M., 1997, Oblique convergence and the lobate mountain belts of western Pakistan: Geology, v. 25, p. 23–26, doi:10.1130/0091-7613(1997)025<0023:OCATLM>2.3.CO;2.

Harland, W.B., 1971, Tectonic transpression in Caledonian Spitsbergen: Geological Magazine, v. 108, p. 27–42, doi:10.1017/S0016756800050937.

Hoffman, P.F., 1989, Precambrian geology and tectonic history of North America, *in* Bally, A.W., and Palmer, A.R., eds., The Geology of North America: An Overview: Boulder, Colorado, Geological Society of America, Geology of North America, v. A, p. 447–512.

Hoffman, P.F., 1990, On accretion of granite-greenstone terrane, *in* Greenstone Gold and Crustal Evolution; NUNA Conference Volume: St. John's, Newfoundland, Geological Association of Canada, p. 32–45.

Hooper, P., and Ojakangas, R.W., 1971, Multiple deformation in the Vermilion district, Minnesota: Canadian Journal of Earth Sciences, v. 8, p. 423–434, doi:10.1139/e71-044.

Hudleston, P.J., 1976, Early deformational history of Archean rocks in the Vermilion district, northeastern Minnesota: Canadian Journal of Earth Sciences, v. 13, p. 579–592, doi:10.1139/e76-061.

Hudleston, P.J., Schultz-Ela, D., and Southwick, D.L., 1987, Transpression in an Archean greenstone belt, northern Minnesota: Canadian Journal of Earth Sciences, v. 25, p. 1060–1068.

Hudleston, P.J., Bauer, R.L., Southwick, D.L., Schultz-Ela, D.D., and Bidwell, M.E., 1987, Structural geology of the boundary between Archean terranes of low-grade and high-grade rocks, Northern Minnesota, *in* Balaban, N.H., ed., Field Trip Guidebook for Selected Areas in Precambrian Geology of Northeastern Minnesota: Minnesota Geological Survey Guidebook Series 17, p. 1–42.

Hudleston, P.J., and Schwerdtner, W.M., 1997, Strain, *in* De Wit, M.J., and Ashwal, L.D., eds., Greenstone Belts: Oxford, UK, Oxford Monographs on Geology and Geophysics v. 35, p. 296–308.

Jiang, D., and Williams, P.F., 1998, High-strain zones: A unified model: Journal of Structural Geology, v. 20, p. 1105–1120, doi:10.1016/S0191-8141(98)00025-X.

Jirsa, M.A., Southwick, D.L., and Boerboom, T.J., 1992, Structural evolution of Archean rocks in the western Wawa subprovince, Minnesota: Refolding of precleavage nappes during D_2 transpression: Canadian Journal of Earth Sciences, v. 29, p. 2146–2155, doi:10.1139/e92-170.

Jirsa, M.A., Boerboom, T.J., Green, J.C., Miller, J.D., Morey, G.B., Ojakangas, R.W., and Peterson, D.M., 2004, Classic outcrops of northeastern Minnesota: Institute on Lake Superior Geology, Field Trip Guide, p. 129–169.

Jirsa, M.A., Boerboom, T.J., Chandler, V.W., Mossler, J.H., Runkel, A.C., and Setterholm, D.R., 2011, Geologic Map of Minnesota—Bedrock Geology: Minnesota Geological Survey State Map Series S-21, http://purl.umn.edu/101466.

Jones, R.R., and Holdsworth, R.E., 1998, Oblique simple shear in transpression zones, *in* Holdsworth, R.E., Strachran, R.A., and Dewey, J.F., eds., Continental Transpressional and Transtensional Tectonics: Geological Society [London] Special Publication 135, p. 35–40.

Kennedy, M.C., 1984, The Quetico Fault in the Superior Province of the southern Canadian Shield [M.S. thesis]: Ontario, Canada, Lakehead University.

Langford, F.F., and Morin, J.A., 1976, The development of the Superior Province of northwestern Ontario by merging island arcs: American Journal of Science, v. 276, p. 1023–1034, doi:10.2475/ajs.276.9.1023.

Launeau, P., and Robin, P.-Y.F., 2003, Ellipsoid 2003, http://www.sciences.univ-nantes.fr/geol/UMR6112/SPO/.

Launeau, P., Robin, P.-Y.F., 2005, Determination of fabric and strain ellipsoids from measured sectional ellipses—Implementation and applications: Journal of Structural Geology, v. 27, p. 2223–2233.

Lawson, A.C., 1913, The Archaean Geology of Rainy Lake Re-studied: Geological Survey of Canada Memoir 40, 115 p.

Lin, S., Jiang, D., and Williams, P.F., 1998, Transpression (or transtension) zones of triclinic symmetry: Natural example and theoretical modeling, *in* Holdsworth, R.E., Strachran, R.A., and Dewey, J.F., eds., Continental Transpressional and Transtensional Tectonics: Geological Society [London] Special Publication 135, p. 41–57.

Lisle, R.J., 1985, Geological Strain Analysis: A Manual for the Rf/ϕ Method: Oxford, UK, Pergamon Press, 99 p.

Lundy, J.R., 1985, Clues to structural history in the minor folds of the Soudan Iron Formation, NE Minnesota [M.S. thesis]: Minneapolis, University of Minnesota, 144 p.

McNaught, M.A., 2002, Estimating uncertainty in normalized Fry plots using a bootstrap approach: Journal of Structural Geology, v. 24, p. 311–322, doi:10.1016/S0191-8141(01)00067-0.

Mulchrone, K.F., 2005, An analytical error for the mean radial length method of strain analysis: Journal of Structural Geology, v. 27, p. 1658–1665, doi:10.1016/j.jsg.2005.05.009.

Ojakangas, R.W., 1972, Rainy Lake area, *in* Sims, P. K. and Morey, G. B., eds., Geology of Minnesota: A Centennial Volume in honor of George M. Schwartz: Minnesota Geological Survey, p. 163–171.

Ojakangas, R.W., Sims, P.K., and Hooper, P.R., 1978, Geologic Map of the Tower Quadrangle, St. Louis County, Minnesota: U.S. Geological Survey Geologic Quadrangle Map GQ-1457, scale 1:24,000, 1 sheet.

Pattison, D.R.M., Spear, F.S., and Cheney, J.T., 1999, Polymetamorphic evolution of muscovite + cordierite + staurolite + biotite assemblages: Implications for the metapelitic petrogenetic grid and for P-T paths: Journal of Metamorphic Geology, v. 17, p. 685–703, doi:10.1046/j.1525-1314.1999.00225.x.

Pattison, D.R.M., Spear, F.S., DeBuhr, C.L., Cheney, J.T., and Guidotti, C.V., 2002, Thermodynamic modeling of the reaction Muscovite + Cordierite = Al_2SiO_5 + Biotite + Quartz + H_2O: Constraints from natural assemblages and implications for the metapelitic petrogenetic grid: Journal of Metamorphic Geology, v. 20, p. 99–118, doi:10.1046/j.0263-4929.2001.356.356.x.

Percival, J.A., 1989, A regional perspective of the Quetico metasedimentary belt, Superior Province, Canada: Canadian Journal of Earth Sciences, v. 26, p. 677–693, doi:10.1139/e89-058.

Percival, J.A., and Helmstaedt, H., 2006, The Western Superior Province Lithoprobe and NATMAP transects: Introduction and summary: Canadian Journal of Earth Sciences, v. 43, p. 743–747, doi:10.1139/e06-063.

Percival, J.A., and Williams, H.R., 1989, Late Archean Quetico accretionary complex, Superior province, Canada: Geology, v. 17, p. 23–25, doi:10.1130/0091-7613(1989)017<0023:LAQACS>2.3.CO;2.

Percival, J.A., Sanborn-Barrie, M., Skulski, T., Stott, G.M., Helmstaedt, H., and White, D.J., 2006, Tectonic evolution of the western Superior Province from NATMAP and Lithoprobe studies: Canadian Journal of Earth Sciences, v. 43, p. 1085–1117, doi:10.1139/e06-062.

Peterman, Z., and Day, W.C., 1989, Early Proterozoic activity on Archean faults in the western Superior province—Evidence from pseudotachylite: Geology, v. 17, p. 1089–1092, doi:10.1130/0091-7613(1989)017<1089:EPAOAF>2.3.CO;2.

Pettijohn, F.J., 1943, Archean sedimentation: Geological Society of America Bulletin, v. 54, p. 925–972.

Poulsen, K.H., 1986, Rainy Lake Wrench Zone: An example of an Archean Subprovince boundary in Northwestern Ontario, *in* Tectonic Evolution of Greenstone Belts: Houston, Lunar and Planetary Institute Technical Report, p. 177–179.

Poulsen, K.H., 2000a, Archean Metallogeny of the Mine Centre–Fort Frances Area: Ontario Geological Survey Report 266, 121 p.

Poulsen, K.H., 2000b, Geological Setting of Mineralization in the Mine Centre–Fort Frances Area: Ontario Geological Survey Mineral Deposits Circular 29, 78 p.

Poulsen, K.H., 2000c, Precambrian Geology and Mineral Occurrences, Mine Centre–Fort Frances Area: Map, scale 1:50,000, 1 sheet.

Poulsen, K.H., Borradaile, G.J., and Kehlenbeck, M.M., 1980, An inverted Archean succession at Rainy Lake, Ontario: Canadian Journal of Earth Sciences, v. 17, p. 1358–1369, doi:10.1139/e80-143.

Ramsay, J.G., 1967, Folding and Fracturing of Rocks: New York, McGraw-Hill, 568 p.

Ramsay, J.G., and Graham, R.H., 1970, Strain variation in shear belts: Canadian Journal of Earth Sciences, v. 7, p. 786–813, doi:10.1139/e70-078.

Robin, P.-Y., and Cruden, A.R., 1994, Strain and vorticity patterns in ideally ductile transpression zones: Journal of Structural Geology, v. 16, p. 447–466, doi:10.1016/0191-8141(94)90090-6.

Sanderson, D.J., and Marchini, W.R.D., 1984, Transpression: Journal of Structural Geology, v. 6, p. 449–458, doi:10.1016/0191-8141(84)90058-0.

Schmitz, M.D., Bowring, S.A., Southwick, D.L., Boerboom, T.J., and Wirth, K.R., 2006, High-precision U-Pb geochronology in the Minnesota River Valley subprovince and its bearing on the Neoarchean to Paleoproterozoic evolution of the southern Superior Province: Geological Society of America Bulletin, v. 118, p. 82–93, doi:10.1130/B25725.1.

Schultz-Ela, D., 1988, Strain patterns and deformation history of the Vermilion district, northeastern Minnesota [Ph.D. thesis]: Minneapolis, University of Minnesota, 373 p.

Schultz-Ela, D.D., and Hudleston, P.J., 1991, Strain in an Archean greenstone belt of Minnesota: Tectonophysics, v. 190, p. 233–268, doi:10.1016/0040-1951(91)90432-R.

Schulz, K.J., and Cannon, W.F., 2007, The Penokean orogeny in the Lake Superior region: Precambrian Research, v. 157, p. 4–25, doi:10.1016/j.precamres.2007.02.022.

Sims, P.K., 1972, Vermilion district and adjacent areas, *in* Sims, P.K., and Morey, G.B., eds., Geology of Minnesota: A Centennial Volume: Minnesota Geological Survey, p. 49–62.

Sims, P.K., 1976, Early Precambrian tectonic-igneous evolution in the Vermilion district, northeastern Minnesota: Geological Society of America Bulletin, v. 87, p. 379–389, doi:10.1130/0016-7606(1976)87<379:EPTEIT>2.0.CO;2.

Sims, P.K., and Mudrey, M.G., 1972, Burntside granite gneiss, Vermilion District, *in* Sims, P.K., and Morey, G.B., eds., Geology of Minnesota: A Centennial Volume: Minnesota Geological Survey, p. 98–101.

Sims, P.K., and Southwick, D.L., 1985, Geologic Map of Archean Rocks, Western Vermilion District, Northern Minnesota: U.S. Geological Survey Miscellaneous Investigation Series Map I-1527, scale 1:48,000, 1 sheet.

Southwick, D.L., 1972, Vermilion granite-migmatite massif, *in* Sims, P.K., and Morey, G.B., eds., Geology of Minnesota: A Centennial Volume: Minnesota Geological Survey, p. 49–62.

Southwick, D.L., and Ojakangas, R.J., 1979, Geologic Map of Minnesota, International Falls Sheet, Bedrock Geology: Minnesota Geological Survey, scale 1:250,000, 1 sheet.

Southwick, D.L., and Sims, P.K., 1980, The Vermilion Granitic Complex—A New Name for Old Rocks in Minnesota: U.S. Geological Survey Professional Paper 1124-A, 11 p.

Stockwell, C.H., 1982, Proposals for Time Classification and Correlation of Precambrian Rocks and Events in Canada and Adjacent Areas of the Canadian Shield. Part 1: Time Classification of Precambrian Rocks and Events: Geological Survey of Canada Paper 80–90, 135 p.

Stone, D., Hallé, J., and Murphy, R., 1997a, Precambrian Geology, Mine Centre Area: Ontario Geological Survey Preliminary Map P. 3372, scale 1:50,000, 1 sheet.

Stone, D., Hallé, J., and Murphy, R., 1997b, Precambrian Geology, Mine Centre Area: Ontario Geological Survey Preliminary Map P. 3373, scale 1:50,000, 1 sheet.

Sylvester, A.G., 1988, Strike-slip faults: Geological Society of America Bulletin, v. 100, p. 1666–1703, doi:10.1130/0016-7606(1988)100<1666:SSF>2.3.CO;2.

Tabor, J.R., 1988, Deformational and metamorphic history of Archean rocks in the Rainy Lake District, Northern Minnesota, [Ph.D. thesis]: Minneapolis, University of Minnesota, 224 p.

Tabor, J.R., and Hudleston, P.J., 1991, Deformation at an Archean subprovince boundary, northern Minnesota: Canadian Journal of Earth Sciences, v. 28, p. 292–307, doi:10.1139/e91-028.

Teyssier, C., and Tikoff, B., 1998, Strike-slip partitioned transpression of the San Andreas fault system: A lithospheric scale approach, *in* Holdsworth, R.E., Strachan, R.A., and Dewey, J.F., eds., Continental Transpression and Transtension Tectonics: Geological Society [London] Special Publication 135, p. 143–158.

Tikoff, B., and Teyssier, C., 1992, Crustal-scale, en-echelon "P-shear" tensional bridges: A possible solution to the batholithic room problem: Geology, v. 20, p. 927–930, doi:10.1130/0091-7613(1992)020<0927:CSEEPS>2.3.CO;2.

Treagus, S.H., and Treagus, J.E., 2002, Studies of strain and rheology of conglomerates: Journal of Structural Geology, v. 24, p. 1541–1567, doi:10.1016/S0191-8141(01)00162-6.

Vigneresse, J.L., 1990, Use and misuse of geophysical data to determine the shape at depth of granitic intrusions: Geological Journal, v. 25, p. 249–260, doi:10.1002/gj.3350250308.

Williams, H.R., 1991, Quetico subprovince, *in* Thurston, P.C., Williams, H.R., Sutcliffe, R.H., and Stott, G.M., eds., Geology of Ontario: Ontario Geological Survey Special Volume 4, pt. 1, p. 383–403.

Wood, J., 1980, Epiclastic sedimentation and stratigraphy in the North Spirit Lake and Rainy Lake areas; a comparison: Precambrian Research, v. 12, p. 227–255, doi:10.1016/0301-9268(80)90030-3.

Wood, J., Dekker, J., Jansen, J.G., Keay, J.P., and Panagapko, D., 1980a, Mine Centre Area (Eastern Half), District of Rainy River: Ontario Geological Survey Preliminary Map P. 2202, scale 1:15,840, 1 sheet.

Wood, J., Dekker, J., Jansen, J.G., Keay, J.P., and Panagapko, D., 1980b, Mine Centre Area (Western Half), District of Rainy River: Ontario Geological Survey Preliminary Map P. 2201, scale 1:15,840, 1 sheet.

Yonkee, A., 2005, Strain patterns within part of the Willard thrust sheet, Idaho-Utah-Wyoming thrust belt: Journal of Structural Geology, v. 27, p. 1315–1343, doi:10.1016/j.jsg.2004.06.014.

Zahasky, C., and Hudleston, P., 2010, The role of fabric and shear inversion on the development of fractures in brittle shear zones: Geological Society of America Abstracts with Programs, v. 42, no. 5, p. 263.

Manuscript Accepted by the Society 28 June 2011

Printed in the USA